
GAZİ ÜNİVERSİTESİ
Gazi
1926

DEVELOPMENT OF METHOD FOR THE DETERMINATION OF DINOBUTON FUNGICIDE BY SQUARE WAVE VOLTAMMETRY

A THESIS SUBMITTED TO
THE GRADUATE SCHOOL OF NATURAL AND APPLIED SCIENCES
OF
GAZİ UNIVERSITY

BY
Zeynep MURATHAN

IN PARTIAL FULFILLMENT OF THE REQUIREMENTS
FOR
THE DEGREE OF MASTER OF SCIENCE
IN
CHEMISTRY

SEPTEMBER 2022

ETHICAL STATEMENT

I hereby declare that in this thesis study I prepared in accordance with thesis writing rules of Gazi University Graduate School of Natural and Applied Sciences;

- All data, information and documents presented in this thesis have been obtained within the scope of academic rules and ethical conduct,
- All information, documents, assessments and results have been presented in accordance with scientific ethical conduct and moral rules,
- All material used in this thesis that are not original to this work have been fully cited and referenced,
- No change has been made in the data used,
- The work presented in this thesis is original,

or else, I admit all loss of rights to be incurred against me.

Zeynep MURATHAN

14/09/2022

DEVELOPMENT OF METHOD FOR THE DETERMINATION OF DINOBUTON FUNGICIDE BY SQUARE WAVE VOLTAMMETRY

(M.Sc. Thesis)

Zeynep MURATHAN

GAZİ UNIVERSITY

GRADUATE SCHOOL OF NATURAL AND APPLIED SCIENCES

September 2022

ABSTRACT

Fungicides are used to protect agricultural products from fungis and their spores, insects and other harmful environmental effects. Dinobuton is a fungicide which is a dintrophenol group of pesticide. Electrochemical behavior of dinobuton was investigated by using multi-walled carbon nano tube paste electrode (MWCNTPE) by square wave stripping voltammetry (SWSV) and cyclic voltammetry(CV). In this study, first of all, optimum parameters such as pH, step potential, frequency, amplitude, deposition time and deposition potential were specified by using SWSV. In the negative potential scans, it was evaluated that the first peak obtained was not well defined and the second peak could be used for analytical purposes to a large extent. The second sharp peak appeared at -760 mV (vs Ag/AgCl) was used in analytical purposes. Linear operating range was found to be within 3.74 μM and 25.8 μM. The limit of detection(LOD) and the limit of quantification(LOQ) values were found to be 0.73 μM and 2.43 μM respectively. Then interference study was conducted in the presence of triasulfuron, azinphos-methyl, bromoxynil-octanoate, dialifos, fipronil, vinclozoline, iprodione, procymidone pesticides and some selected metal ions. The method was also applied to apple juice, tap water and grape juice and percent recoveries (%) were detected as 105.9±4.3; 98.3±0.9; 103.7±2.5% with a relative standart deviations of 4.0, 1.0 and 2.4%, respectively. On the other hand, percent relative errors were calculated as 5.90; –1.65 and 3.74%, respectively. High recovery and low relative standart deviations indicate the applicability of the proposed method in both matrix and real samples.

Science code : 20102
Keywords : Pesticide, dinobuton, voltammetry, determination
Page number : 129
Advisor : Prof. Dr. Recai İNAM

KARE DALGA VOLTAMETRİSİYLE DİNOBUTON FUNGİSİTİNİN TAYİNİ İÇİN YÖNTEM GELİŞTİRİLMESİ

(Yüksek Lisans Tezi)

Zeynep MURATHAN

GAZİ ÜNİVERSİTESİ

FEN BİLİMLERİ ENSTİTÜSÜ

Eylül 2022

ÖZET

Mantar ilaçları, tarım ürünlerini mantarlardan ve bunların sporlarından, böceklerden ve diğer zararlı çevresel etkilerden korumak için kullanılır. Dinobuton, bir dintrofenol grubu pestisit olan bir fungisittir. Dinobutonun elektrokimyasal davranışı, kare dalga sıyırma voltametrisi (SWSV) ve dönüşümlü voltametri (CV) ile çok duvarlı karbon nano tüp pasta elektrot (MWCNTPE) kullanılarak incelendi. Bu çalışmada öncelikle kare dalga sıyırma voltametrisi (SWSV) kullanılarak pH, basamak potansiyeli, frekans, genlik, biriktirme süresi ve biriktirme potansiyeli gibi optimum parametreler belirlenmiştir. Negatif yöndeki potansiyel taramalarında, elde edilen birinci pikin iyi tanımlanamadığı ve ikinci pikin ise önemli ölçüde analitik amaçlı olarak kullanılabileceği değerlendirildi. -760 mV'de (Ag/AgCl'ye karşı) ortaya çıkan ikinci keskin pik analitik amaçlarla kullanıldı. Lineer çalışma aralığı 3,74 µM ve 25,8 µM aralığında bulundu. Gözlenebilirlik sınırı (LOD) ve tayin sınırı (LOQ) değerleri sırasıyla 0,73 µM ve 2,43 µM olarak bulundu. Daha sonra triasülfuron, azinfos-metil, bromoksinil-oktanoat, dialifos, fipronil, vinklozolin, iprodione, procymidon pestisitleri ve bazı seçilmiş metal iyonlarının varlığında girişim etkileri çalışması yapılmıştır. Yöntem ayrıca elma suyu, musluk suyu ve üzüm suyuna da uygulanmış ve geri kazanım yüzdeleri sırasıyla %4,0, %1,0 ve %2,4 bağıl standart sapmalarla 105.9±4.3; 98.3±0.9; 103.7±2.5% bulunmuştur. Öte yandan yüzde bağıl hatalar ise sırasıyla 5.90; –1.65 ve 3.74%, olarak hesaplanmıştır. Yüksek geri kazanım ve düşük bağıl standart sapmalar, önerilen yöntemin hem matris hem de gerçek numunelerde uygulanabilirliğini göstermektedir.

Bilim Kodu : 20102
Anahtar Kelimeler : Pestisit, dinobuton, voltametri, tayin
Sayfa Adedi : 129
Danışman : Prof. Dr. Recai İNAM

ACKNOWLEDGEMENT

First and firemost I would like to express my gratitudes to Prof. Recai İNAM for sharing his scientific professionalism all the time and supporting me all the time during master education.

I wish to express my appreciation to Assoc. Prof. Ersin DEMİR for sharing me his perfect scientist point of view and teaching me being patient during the experiments.

Last but not least, my deepest thanks go to my family, my mother Latife MURATHAN, my father Fuat MURATHAN and my sister Gül Murathan DURAN for their support all the time and making me feel confident.

TABLE OF CONTENTS

Page

Page

Page

LIST OF TABLES

Table **Page**

Table **Page**

LIST OF FIGURES

Figure **Page**

Figure **Page**

Figure **Page**

Figure **Page**

LIST OF IMAGES

SYMBOLS AND ABBREVIATIONS

The symbols and abbreviations used in this study, presented below together with instructions.

Symbols	Definitions
α	Transfer coefficient
A	Surface area of electrode
C	Concentration of analyte (M)
C_A	Elektrot yüzeyi derişimi
C_A^0	Ana çözelti derişimi
D	Diffusion coefficient (cm^2 /s)
D_A	Diffusion coefficient (cm^2/s)
E	Potential (mV, V)
E_{acc}	Accumulation potential
E_{cell}	Cell potential (mV)
E_{ind}	Potential of indicator electrode (mV, V)
E_p	Peak potential (mV, V)
E_{ref}	Potential of reference electrode (mV, V)
E_j	Junction potential (mV, V)
F	Faraday constant (C/s)
f_x	Add function in Excel
ΔE	Amplitude potential (mV, V)
ΔE_s	Step potential (mV, V)
E_{work}	Potential of working electrode (mV, V)
f	Frequency (Hertz)
I	Current (A)
I_p	Peak current (μA, A, mA)
m	Slope
n	Number of moles of electrons
R	Universal gas constant (J mol^{-1} K^{-1})
R^2	Coefficient of regression
S_b	Standard deviation of cut-off point

Symbols	Definitions
S_r	Standard deviation of regression
S_y	Standard deviation of y-axis
δ	Distance from electrode
T	Temperature (Kelvin)
t_{acc}	Accumulation time
ν	scan rate (mV/s)
µA	microamper
µL	microliter
µM	micromolar

Abbreviations	Definitions
ASV	Anodic stripping voltammetry
AdSV	Adsorptive stripping voltammetry
BR	Britton-Robinson buffer
CPE	Carbon paste electrode
CPE	Controlled potential electrolysis
CSV	Cathodic stripping voltammetry
CV	Cyclic voltammetry
DME	Dropping mercury electrode
DPP	Differential pulse polarography
DPASV	Different pulse anodic stripping voltammetry
DPCAdSV	Differential pulse cathodic adsorptive stripping voltammetry
DPV	Differential pulse voltammetry
DPP	Differential pulse polarography
GCE	Glassy carbon electrode
HDV	Hydrodynamic voltammetry
HMDE	Hanging mercury drop electrode
HPLC-DAD	High performance liquid chromatoghraphy-diode-array detector
LOD	Limit of detection

Abbreviations	Definitions
LOQ	Limit of quantification
LSV	Linear scanning voltammetry
MFE	Mercury film electrode
MW	Molecular weight
MWCNT	Multi-walled carbon nano tube
MWCNTPE	Multi-walled carbon nano tube paste electrode
RE	Relative error
RSD	Relative standard deviation
SWCAdSV	Square-wave cathodic adsorptive stripping voltammetry
SWP	Square wave polarography
SWSV	Square wave stripping voltammetry
SWV	Square wave voltammetry

1. INTRODUCTION

Having a diet including vegetables and fruits reduces the risk of high blood pressure, heart disease, diabetes, stroke, many cancers and other chronic disease. That is to say, benefitting from vegetables and fruits in maximum efficiency plays a very important role in our lives. Higher efficiency of agricultural products leads to a healthier population. At that point, using pesticides effectively is one of the important factors resulting maximum efficiency for agricultural products (Aktar, Sengupta and Chowdhury, 2009).

There are some kind of organisms that harms farm products like insects, fungis etc. Pesticides have a role that prevent these harmful organisms from damaging them. In this way, product efficiency is increased. However, pesticides have harmful effects on environment as well as benefits (Kumar, Yadav, Saxena, Paul and Tomar, 2021). Therefore, highest efficiency with lowest concentration of pesticides in crops may decrease the damage on environment. At that point, quantification of pesticides at very low concentrations creates need for sensitive and efficient methods.

To date, different kinds of methods have been developed for determination of pesticides including conventional and new ones. Chromatographic methods provide sensitive results but have some disadvantages like time consuming preparation steps, expensive instruments and high use of organic solvents. To date, many new methods have been developed with voltammetric techniques (Samsidar, Siddiquee and Shaarani, 2018).

Voltammetry is a group of electroanalytical methods that measures current as a function of applied potential under polarized conditions. The working electrodes have generally very small surface area to provide polarization (Skoog, West, Holler and Crouch, 2004: 665).

Voltammetry is widely used by chemists for the following basic studies:

- To investigate oxidation and reduction behaviors of molecules in different media,
- To investigate adsorption behaviors of surfaces,
- To enlighten electron transfer mechanism of electrode surfaces (Skoog and et al., 2004: 665).

According to waveform, voltammetry is classified into four groups (Skoog, Holler and Crouch, 2014:717).

- Linear scan → Hydrodynamic voltammetry (HDV)
- Differential pulse → Differential pulse voltammetry (DPV)
- Square wave → Square-wave voltammetry (SWV)
- Triangular → Cyclic voltammetry (CV)

There are many studies related to electrochemical determination of pesticides in the literature. Some examples are: Demir ve İnam, 2018; Uslu and Özkan, 2002; Kumaravel and Murugananthan, 2021; Oliveira-Brett, Piedade, Silva and Diculescu, 2004; Goyal and Singh, 2006; Goyal, Gupta, Sangal and Bachheti, 2005; Sanghavi and Srivastava, 2010; Fotouhi, Fatollahzadeh and Heravi, 2012; Ni, Wang and Kokot, 2001; Lu and Compton, 2013; Purushothama, Nayaka, Vinay, Manjunatha, Yathisha and Basavarajappa; 2018; Movaghgharnezhad and Mirabi; 2019.

In the present work, dinobuton pesticide was analysed by square wave stripping voltammetry (SWSV) and CV. Dinobuton ((2-butan-2-yl-4,6-dinitrophenyl) propan-2-yl carbonate) is fungicide as a subtype of pesticides. It has a dinitrophenol content and accordingly is included in the dinitrophenol class of pesticides. Dinobuton is bio-activated fungicide/acaricides group of dinitrophenyl group of pesticide (Aktar, Sengupta and Chowdury, 2009).

Sreedhar, Samatha and Sujatha (2000) studied dinobuton pesticide by polarography, cyclic voltammetry, differential pulse polarography (DPP), controlled potential electrolysis (CPE) and millicoulometry. They tried different techniques in different solvents with different pH values and some parameters were optimised. Linear dynamic range was determined to be $3.01x10^{-9}$ - $1.2x10^{-5}$ M**.** The developed DPP method for determination of dinobuton was also applied in agricultural formulations and spiked water and % recovery and % standart deviation were found to be around 99% and within 0.012 - 0.021% respectively, in the agricultural formulations. On the other hand, percentage recovery and percentage standart deviation were found to be within 93.50 - 97.50 % and 0.012 - 0.021% respectively, in spiked distilled water.

Aruna, Prasad, Reddy and Srredhar (2018) proposed an electrochemical determination of dinobuton pesticide by using Fe_2O_3–ZnO modified glassy carbon electrode (GCE). DPV and CV thecniques were used as electrochemical methods and parameters were optimized. Limit of detection (LOD), limit of quantificaiton (LOQ) and linear working range were determined for the validation of the proposed method. LOD and LOQ were determined to be 0.01200 and 0.03636 μg/mL, respectively. Linear working range was determined to be 0.05 - 30.00 μg/mL. The developed method was applied to environmental samples. The percentage recoveries were found to be 97.8 and 99.8 % in water and soil samples respectively.

Gebrehiwot, Erkmen and Uslu (2020) analysed different pesticides including buprofezin, dinobuton and chlorothalonil by using HPLC-DAD (high performance liquid chromatoghraphy-diode-array-detector) method in urine, serum, tomatoe, soil and commercial dosage form and water samples. LOD and LOQ values were determined for dinobuton at between 0.09-0.17 μg/mL and 0.28-0.51 μg/mL respectively. Linear operating range was determined to be 1-200 μg/mL. Percentage recoveries were found to be within 92.3 - 109.74% in samples studied.

In the present work, the electrochemical reduction behavior of dinobuton was investigated by using square wave stripping voltammetry. There is no work on the determination of dinobuton pesticide so far by using square wave stripping voltammetric method. Therefore, this study will be the first one for the respect. Multi-walled carbon nano tube (MWCNT) paste electrode was used as working electrode, Ag/AgCl (in 3M NaCl) eletrode was the reference electrode and platinum electrode was counter electrode. First, optimum parameters were determined. After determining optimum pH value, step potential, frequency, amplitude, deposition time and deposition potentials were optimized. Cyclic voltammetry was applied as well as SWSV. Different scan rates were used for observation of the change of voltammograms at different scan rates. The reaction was characterized whether it was diffusion or adsorption controlled.

Electrochemical behavior of dinobuton was investigated in the presence of different metal ions and other pesticides to observe interference effects. There was no significant change in the presence of different co-existing pesticides. Dinobuton can also be quantified analytically even in the presence of other species in the same environment.

As a result, the validity of method was showed by using square wave stripping voltammetric method in natural samples. Dinobuton is used as a pesticide in different vegetables and fruits such as apples, tomatoes, cucumber, vine, aubergine. Therefore, it was analysed in spiked apple juice, tap water and grape juice. Recoveries, relative standart deviations (RSD) and relative errors (RE) were also determined. High percent recovery value and low relative standart devations indicated that the method was accurate and precise.

2. AN OVERVIEW OF PESTICIDES AND ELECTROCHEMISTRY

2.1. Pesticides

Pesticides are defined by United States Environmental Protection Agency as:

- Any substance preventing the damages of pests.
- Any substance used for plant, farm crop regulator.
- Any nitrogen stabilizer

Pesticides are generally organic compounds including plant based and synthetic (Kaur and others, 2019).

2.1.1. The history of pesticides

The first pesticides in history were some mineral compounds and extracts of some plants like tobacco. After use of earliest pesticides, new compounds were developed such as the mixture of copper sulphate and calcium hydroxide. Then different metals with different mixtures and some other organic and inorganic compounds were developed especially to prevent outbreaks caused by a lack of fungicide (Bertomeu-Sánchez, 2019).

The discovery of DDT is a big development in science World. It was discovered as a pesticide by Paul Hermann Müller in 1939. Followingly, the discovery of new pesticides increased (Jarman and Ballschmiter, 2012). New equipments were also improved for the application of pesticides on farm products such as atomizers, dusters, sprayers etc.

Pests not only damaged agricultural products and prevented crop efficiency; but also human. On the other hand, damaged agriculture leads to growing unhealthy persons (Bertomeu-Sánchez, 2019).

As well as benefits, pesticides have some risks and harms. As the pesticide use increases, some risks developed following their discovery and development. These problems were categorised into three groups in the literature. Exposure to toxins, residuum in natural sources and loss of natural fauna and environment. Some accidents happened during the

preparation of pesticides. To prevent negative effects of pesticides, some protection guideliness were applied and farmers were informed about that (Bertomeu-Sánchez, 2019). At that point, the limited use of pesiticides play a critical role for taking maximum efficiency without damage to crops and environment. Very low concentration of pesticides may be useful for undamaged agricultural products. That is to say, trace amount of pesticide use is better for efficiency without harmful effects. At that point, determination of trace amount of pesticide gains importance. If pesticide use is controlled and small amount of them is being used, determination of them at very low concentrations should be main purpose in developing new analytical methods.

2.1.2. Classification of pesticides

Drum suggested three method for pesticide classification: based on mode of entry, function and organisms they kill chemical composition (Drum, 1980).

Table 2.1. Classification of pesticides

BASED ON MODE OF ENTRY	BASED ON PESTICIDE FUNCTION AND PEST ORGANISM THEY KILL		BASED ON CHEMICAL COMPOSITION
-Systemic pesticides, -Non-systematic pesticides, -Stomach poisons, -Fumigants, -Repellents.	-Insecticides, -Fungicides, -Bactericides, -Herbicides, -Acaricides, -Rodenticides, -Algaecides, -Larvicides, -Repellents, -Desiccants,	-Ovicides, -Virucides, Molluscicides, -Nematicides, -Avicides, -Moth balls, -Lampricides, -Piscicides, -Silvicides, -Termiticides.	-Organochlorines, -Organophosphates, -Carbamates, -Synthetic pyrethroids,

Kaur, Mavi, Raghav and Khan (2019) has also classified pesticides according to their chemical combination and the molecular structure of their active ingredients (organochlorines, organophosphorus, carbamates, pyrethrin and pyrethroids). They described this classification as most useful classification. This classification gives an idea about physical and chemical properties of related pesticides. These properties are important to know for the way of application and taking precautions.

2.1.3. Pesticide use

The use of pesticides have risks as well as benefits. The short and long-term effects of pesticides on farmers had been a critical concern. Therefore, the awareness about the controlled use of pesticides were developed for cultural perception. The government campaigns, mass media, courses about agriculture etc. played an important role to inform people about conscious use of pesticides (Bertomeu-Sánchez, 2019).

During the years, pesticides have been cumulated in the ecosystem. Most of them has seriously toxic effect on human and environment. The leakage of pesticides stored in the unsuitable conditions contaminate the water sources. The Food and Agriculture Organization of the United Nations has applied a program to provide the sufficient tools for controlled use of pesticides. The management and effective control of pesticides includes storage methods, the controlled release to the environment, public information and regulations and restrictions. Because most of pesticides are not biodegradable, they simply diffuse to plant organs and human metabolism by food chain (Terziev and Petkova-Georgieva, 2019).

After the harmful effects of pesticides on human health was noticed, the pharmaceutical industry aimed to produce drug forms keeping the effective drug level and reducing the side effects to minimum. It was purposed that whereas increasing the crop protection, the amount of pesticides was reduced at the same time. One of the studies performed with that purpose, was encapsulating the pesticides or keeping them in a polymer membrane (Muro-Suñé, Gani, Bell and Shirley, 2005).

Many other differents methods have been developed for only one purpose: To protect human healt and environment. Human medicines are authorised by health authorities when their benefits outweigh their risks. Pesticides actually have same procedure that when their risks make decreased and benefits are dominant over risks, they can be used as approved by food authorities.

2.1.4. Dinobuton

Dinobuton ((2-Butan-2-yl-4,6-Dinitrophenyl) Propan-2-yl Carbonate) is fungicide as a subtype of pesticides. It has a dinitrophenol content and accordingly is included in the dinitrophenol class of pesticides. Dinobuton ((2-Butan-2-yl-4,6-Dinitrophenyl) Propan-2-yl Carbonate) is bio-activated fungicide/acaricides group of dinitrophenyl group of pesticide. (Aktar, Sengupta and Chowdury, 2009). Dinobuton is a non-systematic acaricide and fungicide. It has been used against mites resistant to organophosphorus compounds on fruits, vegetables, tomatoes and cotton (Sreedhar, Samatha and Sujatha, 2000). Molecular structure of dinobuton is shown in Figure 2.1.

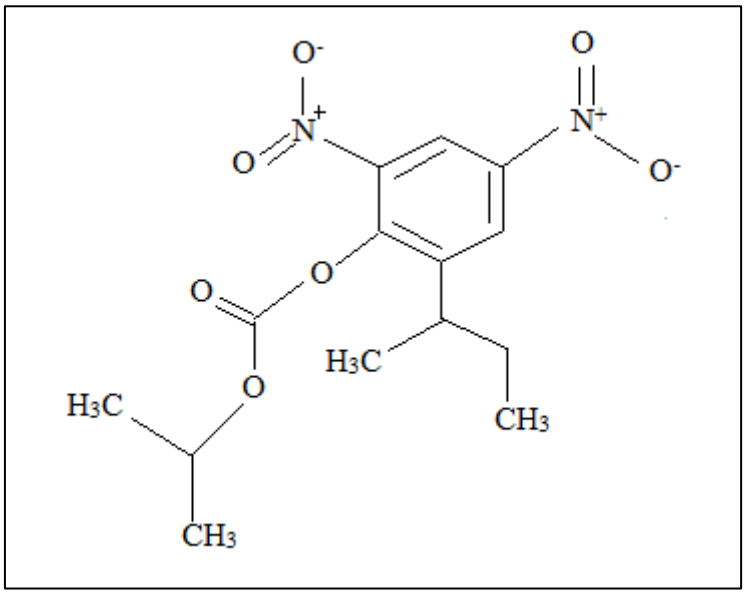

Figure 2.1. Molecular structure of dinobuton

Since there are two nitro groups, it is convenient to determine the dinobuton by voltammetric techniques. H+ atoms from the environment join the oxygen atoms in the nitro groups and cause the reduction of the molecule. Electron transfer follows H^+ atom transfer and electron transfer can be detected if there is a sensing material such as an electrode in the environment. The reaction can be initiated by applying potential to the medium. The molecular structure of dinobuton and dinobuton-like molecules with nitro groups in their structures is suitable for electrochemical analysis.

The hydrolytic cleavage of the carbonate is the major metabolic pathways of dinitrophenol compounds and the corresponding phenols are produced as biologically active component.

The degradation of dinobuton in soils, plants and animals involves the reduction of nitro group to produce amino group, N-acetylation, deamination and carboxylation of sec-butyl group.

The metabolic pathways of dinobuton in plants and animals:

- Hydrolytic cleavage of the carbonate-dinitrophenyl linkage.
- Dinoseb is produced with hydrolytic cleavage of the carbonate-dinitrophenyl linkage.
- Reduction of nitro groups of dinoseb.
- Production of monoamino and diamino analogues.
- Acetylation and deamination (via hydroxylation/elimination).
- Oxidation of the sec-butyl moiety.
- N-Conjugation and O-Conjugation as glucosides and glucuronides (Roberts, Hutson, Jewess, Lee and Nicholls, 1999: 1189-1192).

2.2. Basics of Electroanalytical Chemistry

Electroanalytical methods are related to interplay between electrical quantities like potential, current, electrical charge and chemical parameters. Electrochemical reactions take place at the electrode-solution interface (Wang, 2006: 1).

Electroanalytical chemistry includes qualitative and quantitative determination of analyte. It is carried out in an electrochemical cell. Potentiometric and potentiostatic techniques are two essential types of electroanalytical measurements which require at least two electrodes and an electrolyte solution in the electrochemical cell (Wang, 2006: 1). Electroanalytical methods provide low detection limit and information about electrochemically accessible systems such as rate of interfacial charge transfer, the rate of mass transfer, absorption properties (Skoog and et al., 2004: 628).

Electroanalytical methods have some advantages over other type of methods. Whereas most analytical methods are specific for an oxidation state of an element, electrochemical methods

could be used for determination for different oxidation states of same element. Another advantage of electrochemical methods is, instrumentation is cheap. In addition to these advantages, long pre-treatment time is not necessary for electrochemical works and recording of experiment results are obtained in a short time (Skoog and et al., 2004: 628).

Jaroslav Heyrovsky, Czech chemist, took first step for electrochemistry by discovering polaroghraphy in 1922. He used a dropping mercury electrode. He observed electron flow between two electrodes by trying different voltage values. Then he obtained first current-voltage curves, which were the basis of polaroghraphy. The polarographic cell is shown in Figure 2.2.

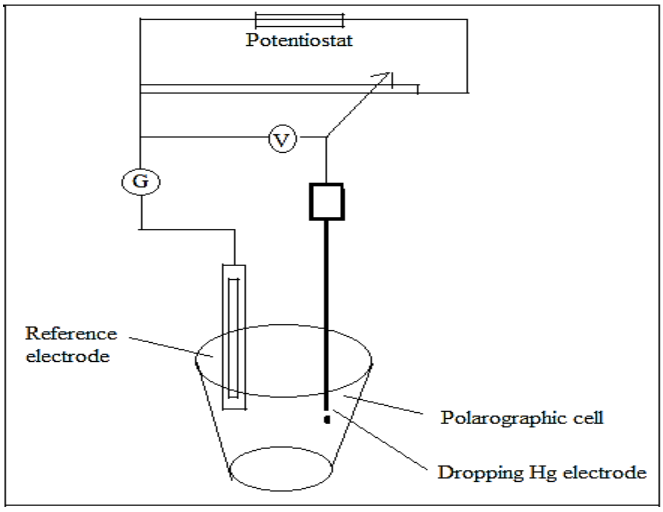

Figure 2.2. A Polarographic cell.

There are number of studies using electrochemical methods in the literature. Scientists prefer these techniques for their ability to get good results in a short time. As the sensitivity of working electrode increases, the sensitivity of results increases. Therefore, scientists try to develop new sensors for sensitive measurements.

An electrochemical system composes of cell in which all reactions happen, supporting electrolyte, reference electrode, working electrode and counter electrode. In general, pH of the solution should stay same after standart additions of stock analyte solution. Therefore, buffer solutions are necessary to use because they are resistant to pH change. Britton-Robinson buffer solution is a universal buffer and widely used in electrochemical experiments.

2.2.1. Electrochemical methods

Electrochemical methods were cataogarized into potentiometry, electrogravimetry and culometry and voltammetry in “Fundamentals of Analytical Chemistry” book (Skoog et al. 2004).

Potentiometry

Potentiometric studies are based on measurement of electrode potential when current is zero. Ion-selective membrane electrodes are used in some new methods. Their potentials are measured and concentrations of ions are determined (Skoog et al., 2004;588). Potentiometric methods are used in many fields. For example, measurement of concentration of blood gases in clinical laboratories to follow how diseases continue with the time. Another example is: concentration of carbon dioxide in water is measured and quantified by marines,

Alternatively, pH of wastewaters are measured regularly. Equipments used in potentiometry is cheap and simple (Skoog et al., 2004; 589).

- Reference electrode,
- Working electrode,
- Potential measuring system.

The potential of the cell in the presence of analyte is calculated:

$$E_{cell} = E_{ind} - E_{ref} - E_j \quad (2.1)$$

Reference electrodes are the one keeps its potential unchanged. For example, reference electrode, Ag/AgCl (in 3 M NaCl). Indicator or working electrodes contrary to reference electrodes are very sensitive to detect relatively low concentrations. Metallic indicator electrodes, membrane electrodes and glassy electrodes are some examples of indicator electrodes.

Electrogravimetry and coulometry

Two methods (electrogravimetry and coulometry) are both based on electrolysis to obtain a product whose concentration is known. Analyte was collected on the surface of electrode and weighed in electrogravimetry. Concentration is calculated form charge carried in coulometry (Skoog et al., 2004; 633).

There are many studies in the literature with regard to electrogravimetric and coulometric analyzes. In 2018 Musa, Sha'Ato, Eneji and Itodo analysed Cu (copper) by using electrogravimetric method. In 2007, Sharma, Bhardwaj, Jain and Aggarwal studied on controlled potential coulometric determination of Ga (gallium) in sodium perchlorate and sodium thiocyanate.

Voltammetry

The development of voltammetry was based on the discovery of polaroghraphy by Jaroslav Heyrovsky in the 1920 (Skoog et al., 2004; 665). Voltammetry is a different kind of polaroghraphic technique.The analyte is determined with voltammetry by measuring current according to applied potential. Polarization of working electrode is necessary in voltammetric methods.

2.2.2. Voltammetric methods

Voltammetric methods are based on potential difference between reference electrode and working electrode. Redox reaction occurs on electrode surface. When potential reaches a value at which species in the solution is induced to oxidize or reduce, current increases sharply (F. Rouessac and A. Rouessac, 2007: 453, 465).

Voltammogram takes shape after voltammetric scan, which is the graph of current vs potential. According to voltammograms, determination and measurement of concentrations of species in the analyte solution can be performed (F. Rouessac and A. Rouessac, 2007: 453, 466). A typical voltammogram is shown in Figure 2.3.

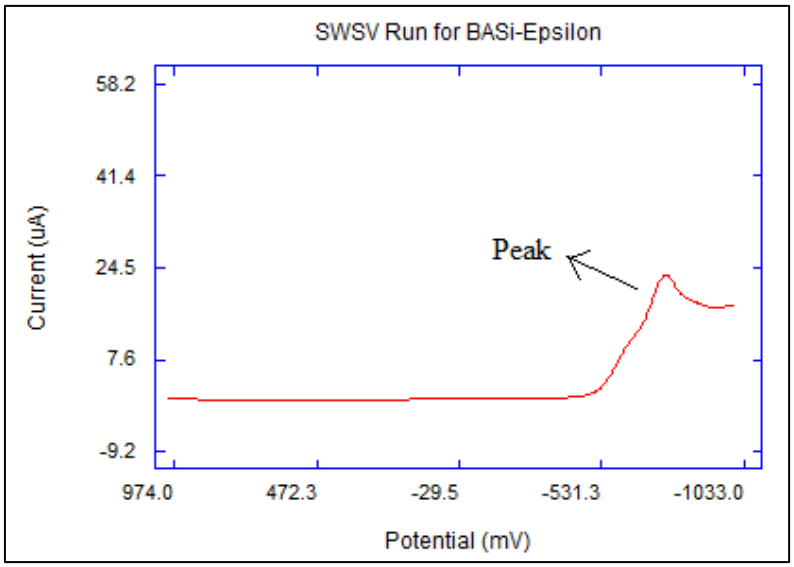

Figure 2.3. A typical voltammogram.

A typical voltammetric cell consists of reference electrode, working electrode and counter electrode. Potential is measured versus to the reference electrodes. Working electrode is the one, which all measurements are based on this electrode and counter electrode is an auxiliary electrode. Ag/AgCl (in *x* M NaCl or KCl) is used generally as reference electrode and platinum electrode is generally used as counter electrode. As working electrode, different kinds of electrodes are used. Besides, many studies have been developed for more sensitive working electrodes. That is to say, voltammetric analyzes are based on sensitivity and selectivity of working electrode.

Simple working electrodes are modified with different nanomaterials, polymers or inorganic substances. These modified electrodes were tried in different studies in the literature to determine the most sensitive working electrode for electrochemical determination of analytes. There are also studies comparing different working electrodes according to their signal detected. These studies are very valuable because unknown analyte determination helps to diagnose some diseases, to enlighten some criminal issues, to solve environmetal problems etc.

Boumya, Taofuik, Achak and Barka in 2021 investigated developments of new modified electrodes for quantification of paracetamol. İnnovative properties were also developed by nanotechnology for more sensitive determination of paracetamol. The modified electrodes with nanomaterials are more sensitive compared to other conventional electrodes.

Conventional electrodes lost their popularity with showing up modified electrodes as new trend. Modified electrodes work according to signals resulting from analyte reactions. More explicit signals are detected by using modified electrodes, due to their effective surface kinetics. For this reason, researchers make an effort to contribute to science world by discovering new modified electrodes (Baig, Sajid and Saleh, 2019).

The simplest voltammetry is linear scanning voltammetry (LSV) that potential increases or decreases linearly (Skoog et al., 2004; 667). Measurements are performed on voltammograms, which is a graph of current *vs* potential. Peaks on this graphs helps us to comment on the properties of analyte. According to peak currents which is observed as a peak height (μA), different parameters and values can be estimated. By comparing each voltammogram, most apparent and highest peak taken into consideration compared to other peaks observed and optimum parameters are determined. Qualification and quantification of analyte is carried out by just making different calculations with changing parameters. There are some equations, which are based on the peak currents. These are very valuable findings, which lights the way for analytical calculations.

Analyte solution is mixed with different methods to provide ongoing movement in analyte solution in hydrodynamic voltammetry. The purpose is to carry analyte into electrode surface. There are three methods for analyte move to electrode surface (Skoog et al., 2004; 673):

1. Migration
2. Convection
3. Diffusion

Mass transfer methods are shown in Figure 2.4. Convection can be applied by mixing solution with stirrer such as magnetic strirrer (İnam and Acer, 2019). Migration occurs with effect of electric field and diffusion occurs with concentration difference. Convection accelerates transfer speed of analyte towards electrode surface (Skoog et al., 2004; 673).

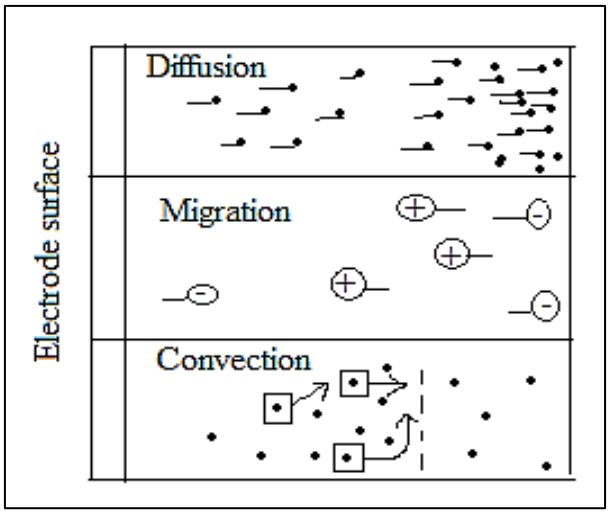

Figure 2.4. Mass transfer to the electrode surface.

Voltammetric currents

$A + ne^- \rightarrow P$ shows an electrolytic reduction in solution A. The current can be stated as in Equation 2.2 for a planary electrode. In this equation *i* indicates current in amper, *n*, number of moles of electrons per mol of analyte; *F*, Faraday constant; A, surface area of electrode in cm^2; D_A is diffusion coefficient in cm^2s^{-1}; C_A is concentration of A on electrode surface in $molxcm^{-3}$; C_A^0 is concentration of A in bulk solution in $molxcm^{-3}$.

$$i = \frac{n.F.A.DA}{\delta}(c_A - c_A^0) \qquad (2.2)$$

i= current (A)
n = number of moles of electrons
F= Faraday constant
A= electrode surface area (cm^2)
D_A= Diffusion coefficient (cm^2/s)
c_A = Concentration of A at the electrode surface
c_A^0 = Concentration of A in the bulk solution
δ= Distance from electrode

This equation shows us relationship between current and other parameters on the bulk solution and electrode surface (Skoog et al., 2004; 677).

Hydrodynamic voltammetry is widely used in identification and determination of oxidizable and reducable compounds or ions in hydrodynamic conditions. An example of hydrodynamic voltammetric system is shown in Figure 2.5. (Skoog and et al., 2004; 681).

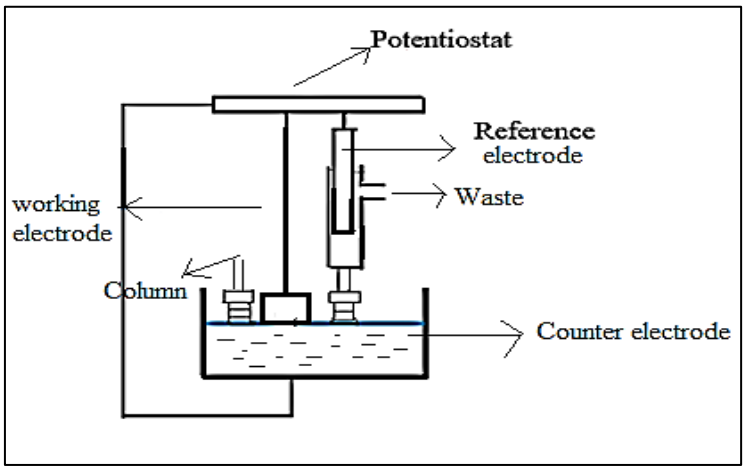

Figure 2.5. Hydrodynamic voltammetric system.

Polarographic methods of analysis

Polarographic methods differ from voltammetric methods in terms of working electrode. Static mercury drop electrode shown in Image 2.1, can be used as working electrode.

Image 2.1. Static mercury drop electrode

Pulse polarography is widely used within polarographic techniques. Differential pulse and square wave polarographic methods are the most widely used in polarographic techniques. Differential pulse polarography is shown in Figure 2.6.

A pulse is applied during a period to the working electrode for every consecutive drops of mercury. First measurement is made immediately before pulse and second measurement is made immediately before drop falls. In this manner, two measurements are made on same drop (F. Rouessac and A. Rouessac, 2007: 470, 471).

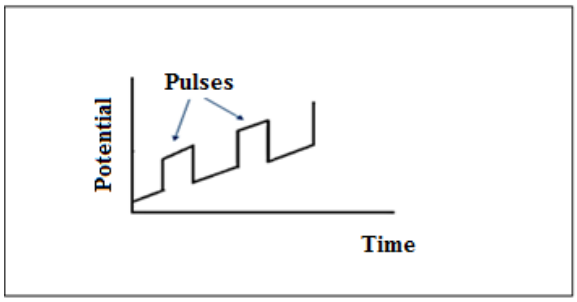

Figure 2.6. Differential pulse polarography potential-time graph

Square waves are observed in square wave polarography (SWP) which is shown in Figure 2.7.

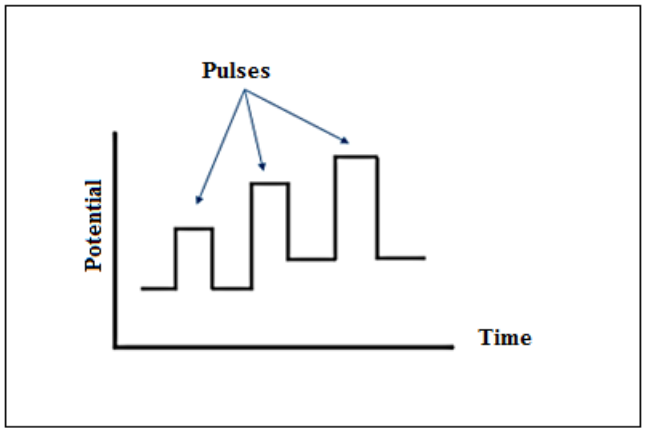

Figure 2.7. SW application and potential-time graph.

Cyclic voltammetry

Cyclic voltammetry (CV) is widely used in voltammetric methods. It is generally used to obtain qualitative information about electrochemical processes. Cyclic voltammetry provides information about thermodynamics of electrode reactions and kinetics of electron transfers (Wang, 2006: 29).

It is applied in some selected scan rate as mV/s. There are initial potentials, switching potentials and final potentials. Scanning is carried out firstly from initial potential to switching potential and then from switching potential to final potential. Switching potential means the potential from which turning back to initial potential applied. Cyclic voltammetry is good method for qualification and quantification of analyte. Randles-Sevcik equation is used for the determination of diffusion coefficient (Ang, Lee, Yu, Uy, Soriano and Dugos, 2020).

$$\dot{I}_p = 0.496 \text{ x } (\alpha n)^{1/2} \text{x nFAC x } (FD\nu/RT)^{1/2} \quad (2.3)$$

$\dot{I}_p$ = Peak current (A)
α = Transfer coefficient
n = Number of moles in the reaction
F = Faraday constant (C/s)
D= Diffusion coefficient (cm^2 /s)
C = Concentration of analyte (M)
T = Temperature (Kelvin)
ν = Scan rate (mV/s)
R = Universal gas constant ($Jmol^{-1}K^{-1}$)

Reversibility of the reaction can also be estimated by using CV, which can be reversible, non-reversible or quasi-reversible. Different waveforms of reversible, quasi-reversible and non-reversible reactions in cyclic voltammogram are shown in Figure 2.8.

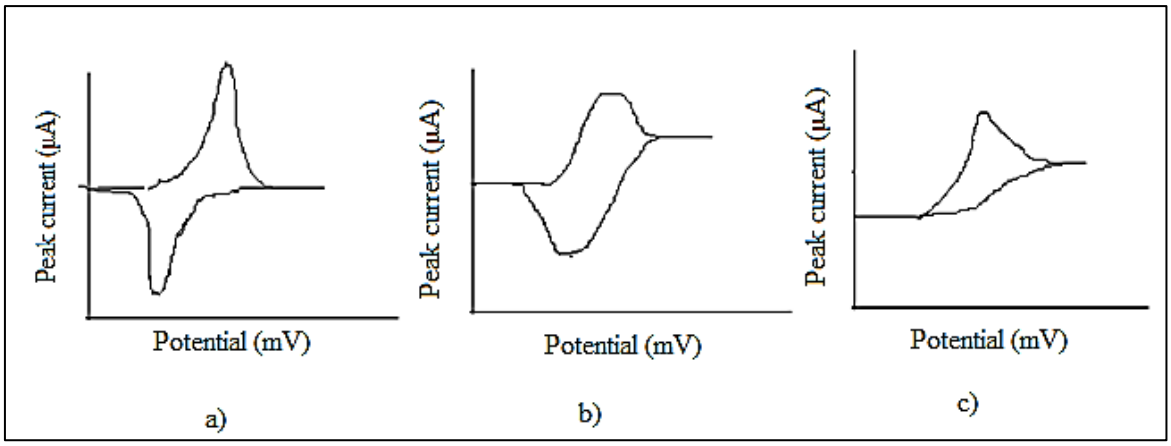

Figure 2.8. Waveforms in cyclic voltammetry a) reversible, b) quasi-reversible, c) ireversible

If peaks are located on opposite sides of voltammogram baseline and have almost same heights, electrode reaction is reversible. If peaks are located on opposite sides of voltammogram baseline but have different heights, reaction is quasi-reversible. If one single peak is observed that means reaction is irreversible. According to reversibility of reaction, oxidation or reduction behaviors of reactions can be estimated.

Scan rate is a characteristic for CV. Scan rate is potential change as a function of time (dE/dt) (Harnisch and Freguia, 2012). It can be calculated from the slope of the curve shown in Figure 2.9. It shows potential vs time graph of CV.

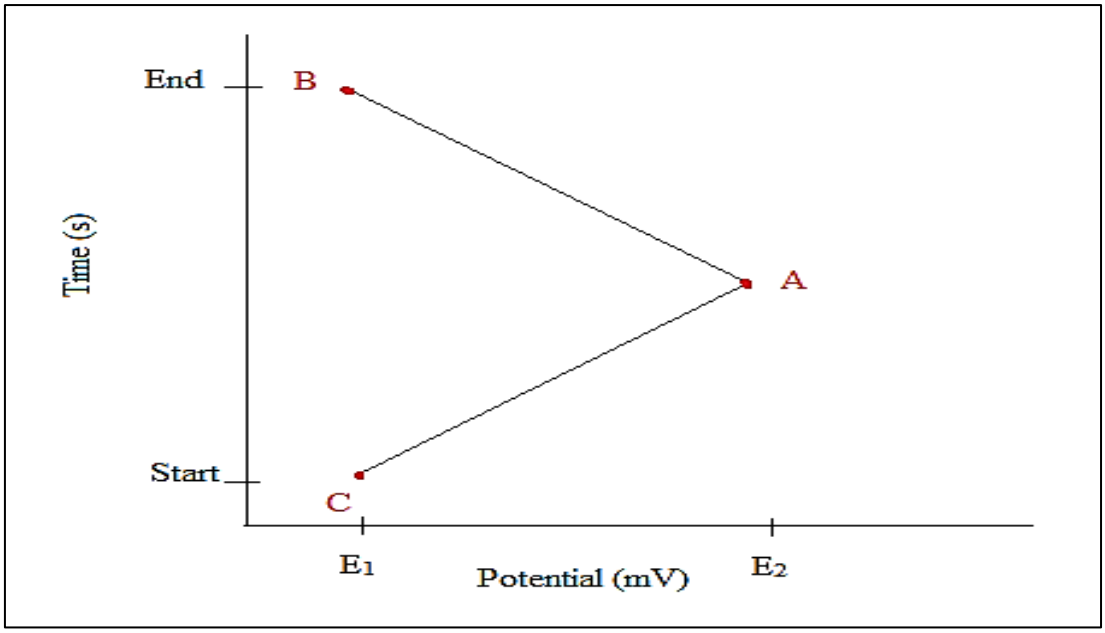

Figure 2.9. Triangular wave in cyclic voltammetry.

Cyclic voltammogric scan begins from E_1 potential which is initial potential and reaches to E_2 potential which is switching potential. This potential scan goes back to initial potential (Elgrishi et al, 2017). Whereas in diffusion-controlled process, a linear relationship is observed between peak current and square root of scan rate, in surface-controlled process, linear relationship is observed between peak current and scan rate (Harnisch and Freguia, 2012). Harnisch and Freguia observed diffusion controlled and surface controlled processes by using Fe^{2+}/Fe^{3+} redox couple in 2012. The oxidation reaction is given below.

$Fe^{2+} \rightarrow Fe^{3+} + e^-$

Stripping voltammetric methods

Stripping voltammetric methods especially anodic and cathodic stripping methods are used for the determination of trace amount of metals. Two steps are defined in stripping methods.

1-Preconcentration step. The step in which analyte is deposited on electrode surface.

2-Redissolving step. After deposition of analyte on electrode surface, analyte in reverse reaction is redissolved into solution. Reverse reaction means oxidation or reduction reaction which is reverse occurred in deposition time. That is to say, if reduction is observed in preconcentration step, oxidation is observed in re-dissolivng step. If oxidation is observed in preconcentration step, reduction is observed in re-dissolving step (F. Rouessac and A. Rouessac, 2007: 478, 479).

In voltammetric analyzes, analyte solution is generally mixed for transfer of analyte to electrode surface. It is carried out during deposition time. After deposition on electrode surface, voltammetric measurements are recorded. This is a key step for detection of electrode reaction occurring on electrode surface. After analyte is moved to electrode surface by hydrodynamic condition, it slowly diffuses to solution from electrode surface. This is called stripping. Three thecniques for stripping are:

1. Anodic stripping voltammetry (ASV)
2. Cathodic stripping voltammetry (CSV)
3. Adsorptive stripping voltammetry (AdSV)

In deposition time, analyte is moved to electrode surface and usually reduced. After deposition, the reduced analyte is dissolved into solution by electro-oxidation, working electrode acts as a surface. This is called anodic stripping voltammetry (ASV). In deposition time, analyte is moved to electrode surface and it can be oxidized. After deposition, when oxidized analyte is dissolved into solution by reduction, working electrode acts as a surface. This is called cathodic stripping voltammetric(CSV) method. Deposition of analyte on electrode surface is employed with physical adsorption. HMDE could be used in adsorptive stripping methods (Skoog and others, 2004: 702).

Alispahic, Krivohlavek and Galic (2021) analysed arsenic molecule by using stripping voltammetry method. They defined ASV method as sensitive and appropriate for inorganic molecules like arsenic and differential pulse anodic stripping voltammetry (DPASV) is highly cost-effective compared to spectroscopic methods and a good way for determination of trace amount of inorganic species like arsenic (Alispahić et al, 2021).

In stripping methods, a strirrer is used such as magnetic stirrer which is very appropriate for stripping voltammetric methods. Because it is small and effective for moving of analyte to electrode surface. Absorbable analytes stay on electrode surface longer time compared to others and leads to decrease of sensitivity of electrodes. That is to say, working electrode detects reaction of analyte more difficult. Besides, it may not detect at all. This is one of reasons for undetected signals. To overcome this, working electrode should be cleaned regularly if absorbable analytes are tried to be determined.

In stripping thecnique, there is a deposition time parameter. It can be adjusted according to peak heights. After trying different deposition times, optimum deposition time value can be determined. Whereas short deposition time like 10 seconds is best for some voltammetric analyzes, longer deposition time like 100 seconds may not be enough to detect highest peaks.

Types of electrodes

There are three types of electrodes in an electrochemical cell.

1. Reference electrode
2. Working electrode
3. Counter electrode

Reference electrode

Reference electrode provides a stable and repeatable potential to the system. Potential of working electrode is measured against to potential of reference electrode. Stable potential is provided by a constant composition of its redox couple like Ag/AgCl and Hg/Hg_2Cl_2. In general, Ag/AgCl/(KCl lor NaCl) electrode is used. It is made of a silver coated with AgCl immersed into KCl lor NaCl solution (F. Rouessac and A. Rouessac, 2007: 466). Reference

electrode is not affected by analyte solution. Because it is insulated from analyte solution by means of intermediate bridge (Wang, 2006: 115, 116). Recations for Ag/AgCl and Hg/Hg_2Cl_2 electrodes given in below.

$AgCl\ (s) + e^- \leftrightarrow Ag\ (s) + Cl^-$
$Hg_2Cl_2\ (s) + 2\ e^- \leftrightarrow 2Hg\ (s) + 2\ Cl^-$

Potential of electrochemical cell is measured by substracting potential of reference electrode and potential of other factors like junction potential from potential of working electrode.

Working electrode

The electrode which is used for measurement and pervious to analyte solution is called working electrode (F. Rouessac and A. Rouessac, 2007: 453, 454).

Electro-oxidation or reduction reactions occur on the surface of working electrodes. They are designed to be sensitive to perceive electrode reactions happening on surface. Some external and internal factors may effect sensitivity of working electrodes. For example, a contaminated surface of working electrode makes detection of signals more dificult.

There are some types of working electrodes (Wang, 2006: 123):

1. Mercury electrodes
2. Solid electrodes
3. Chemically modified electrodes
4. Microelectrodes

Mercury electrodes

These electrodes are preferable for electrochemical analyzes due to the high reproducibility and renewability. They also have some disadvantages like toxicity and low anodic range because of oxidation of mercury. Anodic range here means oxidation window of electrochemical reaction.

There are types of mercury electrodes (Wang, 2006: 124):

1. Dropping mercury electrode (DME)
2. Hanging mercury drop electrode (HMDE)
3. Mercury film electrode (MFE)

Solid electrodes

Low dynamic working range may limit the use of mercury electrodes. Becuase of oxidation of mercury, mercury electrodes may not perceive oxidation of analyte. Therefore, solid electrodes may be preferred due to high anodic working range compared to mercury electrodes. Many solid materials can be used for solid electrodes such as carbon, platinum, gold and silver (Wang, 2006: 127).

Surface of solid electrodes is main factor for electrochemical process. Pretreatment of electrode surface can be made by polishing by microfiber cloth or electrochemical cleaning. Cleaning of electrode surface is very important in terms of perception of reaction, sensitivity and selectivity.

In electroanalysis, carbon electrodes have a wide use among solid electrodes. They have advantages like wide potential window, low background window, cost-efficiency. Glassy carbon electrode (GCE), carbon paste electrode (CPE), carbon fiber electrodes are some examples of carbon electrodes. CPE is shown in Image 2.2. There is a little active space in tip of CPE. Paste-like materials are filled to tip of carbon paste electrode. These paste-like materials can be graphit powder-mineral oil mixture or carbon nano tube-mineral oil mixture.

Image 2.2. Carbon paste electrode.

Chemically modified electrodes

Modification on eletrode surface contributes to electrochemical process in the way of acceleration of electron transfer reactions, sufficient accumulation and good permeability. Polymerfilm coating is one of the most used methods for chemical modification. A solution including polymer film is prepared firstly. Then the solution is dripped into electrode surface and solution is evaporated. Electropolymerization can be used for electrochemical modification as well as physical coating of polymerfilm (Wang, 2006: 136).

Microelectrodes

There is a trend in analytical chemistry which is miniaturazition. Microelectrode means that electrodes whose one dimension at least in electrode is not larger than 25 μm (Wang, 2006: 149).Microelectrodes have capability to detect very low concentrations of analytes. This is an advantage for trace analyzes of some molecules.

Counter electrode

They are auxiliary electrodes which helps to complete circuit of electrochemical cell. Platinum wire electrode is generally used as counter electrode. Counter electrode helps to complete curent circuit together with working electrode. Reference electrode, working electrode and counter electrode is shown in Image 2.3.

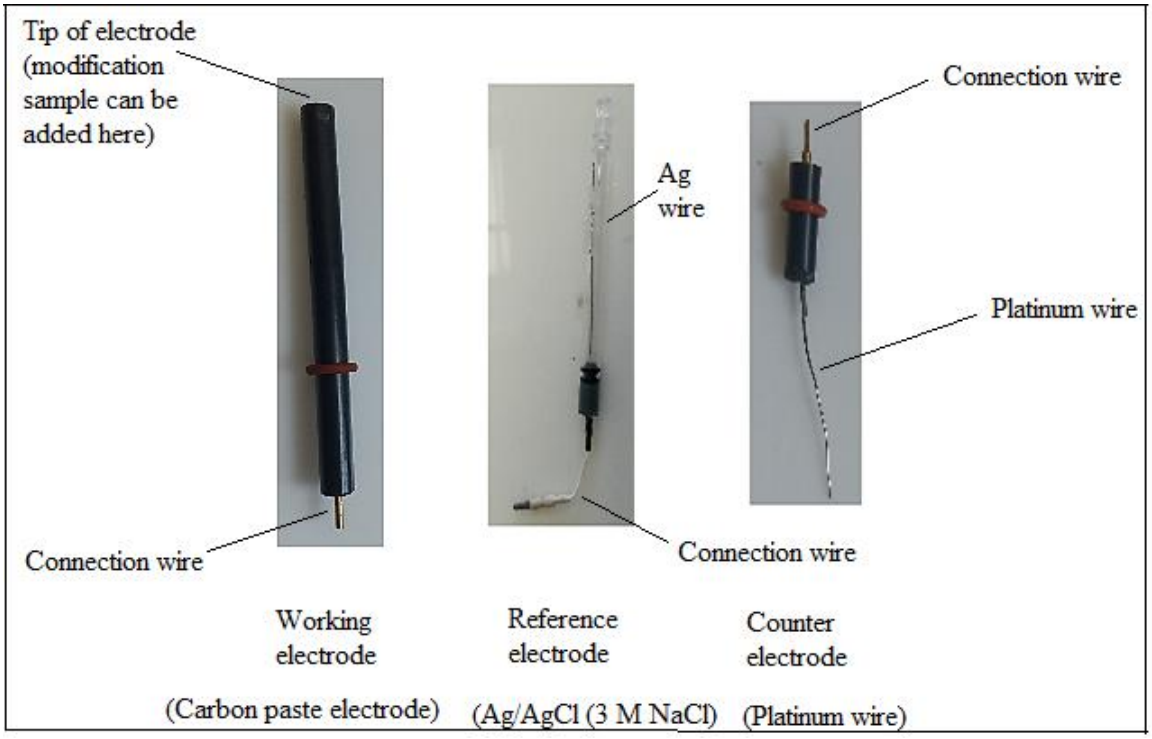

Image 2.3. Working electrode, reference electrode (Ag/AgCl in 3M NaCl) and counter electrode (platinum electrode).

2.2.3. Voltammetric determination of pesticides and pharmaceuticals in literature

To date, many voltammetric measurements were performed with pesticides or in human drugs, veterinary drugs, inorganic molecules etc. Deffo, Temgoua, Mbokou, Njanja, Tonlé and Ngameni (2021) analysed Alizarin Red S by CV and DPV. Molecular structure of Alizarin Red S is shown in Figure 2.10. GCE was used as working electrode. Parameters related to CV and DPV were optimised. Calibration curve was plotted versus peak heights within 0.01 μM and 0.1 μM and detection limit was 3.8 nM.

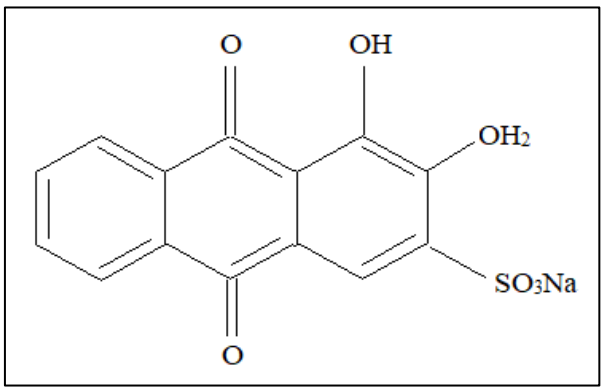

Figure 2.10. Molecular structure of Alizarin Red S

Jakubczyk, Michalkiewicz, Skorupa and Slefarska (2021) studied voltammetric determination of isopropylmethylphenols (thymol and carvacrol) in herbal spices. Molecular structure of thymol (THY) and carvacrol (CAR) are shown in Figure 2.11. DPV was used and linear working range was determined to be between 0.39 and 1105; 0.47 and 640 µg/mL. Detection limit was 0.04 and 0.05 µg/mL, respectively. Multiple standart addition was used for detections.

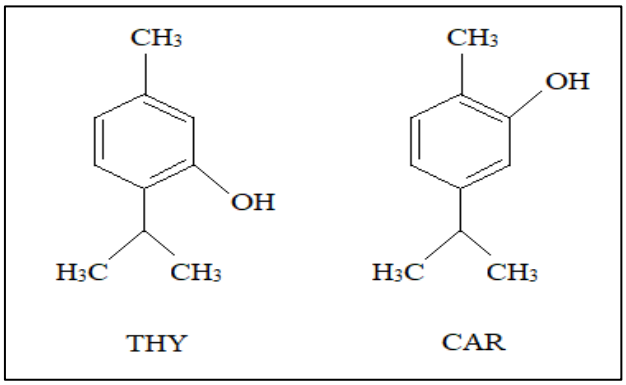

Figure 2.11. Molecular structure of thymol and carvacrol.

Pınar, Allahverdiyeva, Yardım and Şentürk (2020) studied voltammetric determination of dinoterb on cathodically pretreated boron-doped diamond electrode. ASV was used for quantitavive work and CV was recorded for investigation of electro-oxidation or reduction mechanism of dinoteb. Molecular structure of dinoterb is shown in Figure 2.12. Experimental settings were determined by SWV. Single oxidation peak was observed at 1.22 V in BR buffer solution at pH 7. Cetyl-trimethylammonium bromide was included in the solution as cation surfactant. Concentration range was determined between 0.0075 to 0.75 µg ml^{-1}. Square wave stripping voltammograms with increasing concentrations of dinoterb was used for calibration graph shown in Figure 2.21. Detection limit was found to be 0.0022 µg ml^{-1}. Recovery values were obtained by applying method to river water and soil matrices.

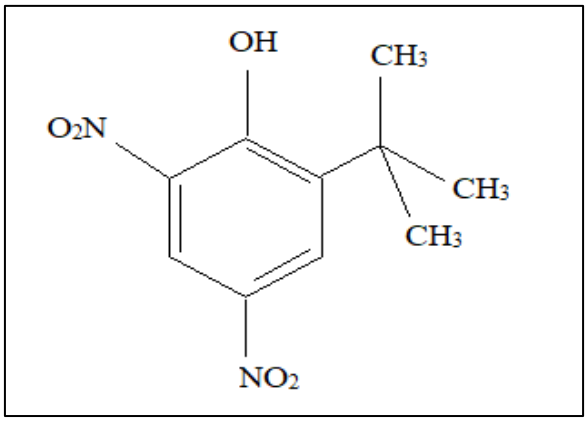

Figure 2.12. Molecular structure of dinoterb.

Gajdár, Barek and Fischer (2019) studied voltammetric determination of difenzoquat (DFQ) pesticide by using electrochemical microcell based on silver solid amalgam electrode. Molecular structure of difenzoquat is shown in Figure 2.13. Single cathodic peak was observed at around -1.4 V (vs Ag/AgCl/3 M KCl). Optimum pH was determined to be 12. DPV method was used for determination of difenzoquat in BR buffer solution at pH 12 and the method was applied to river water samples. LOQ was 0.41 µmol L^{-1} and 0.45 µmol L^{-1}, respectively.

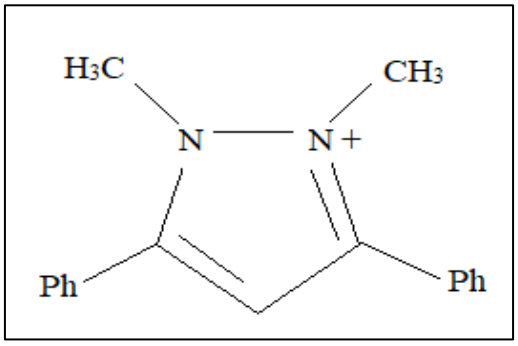

Figure 2.13. Molecular structure of difenzoquat.

Demir and İnam (2018) analysed phenmedipham herbicide by using SWV method. Phenmedipham molecule is shown in Figure 2.14. They used MWCNT as working electrode and determined an oxidation peak at +1320 mV (vs Ag/AgCl). Linear working range was 0.02 and 2.0 mg/L with a regression coefficient 0.9989. LOD and LOQ were detected as 6.96 µg/mL and 23.2 µg/mL respectively on the calibration graph. The interference study was performed with different pesticides to observe electrocehmical behavior of phenmedipham in presence of co-existing species. Then method was applied to natural

samples and phenmedipham was spiked to sugar solution and percent relative error and % relative standart deviation values were determined to be 5% and 3.16 %, respectively.

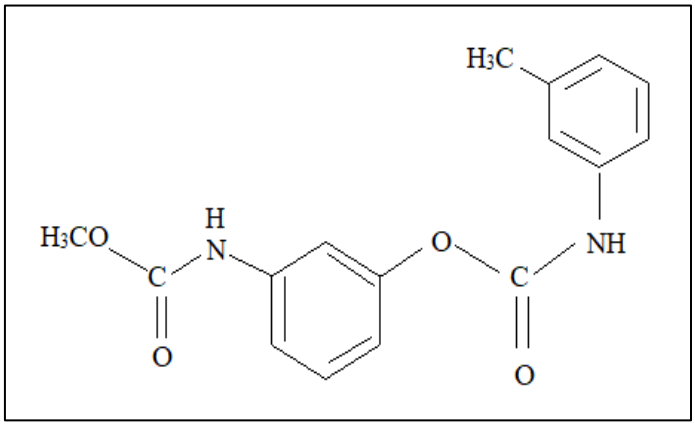

Figure 2.14. Molecular structure of phenmedipham

Demir and İnam (2014) analyzed rimsulfuron herbicide by SWSV. Molecular structure of rimsulfuron is shown in Figure 2.15. Static HMDE was used and the peak was observed at -600 mV (vs Ag/AgCl). The optimum pH value was determined to be 3. Other parameters optimized were accumulation potential (E_{acc}), accumulation time (t_{acc}), frequency (*f*), pulse amplitude (ΔE) and step potential (ΔE_s). Linear working range was determined between 4.4 µg/L and 134.4 µg/L. LOD was 1.3 µg/L. The validity of method was evaluated in natural samples like lake water and tomato juice. Then method was also applied to agrochemical formulation of Doncep (commercial formulation).

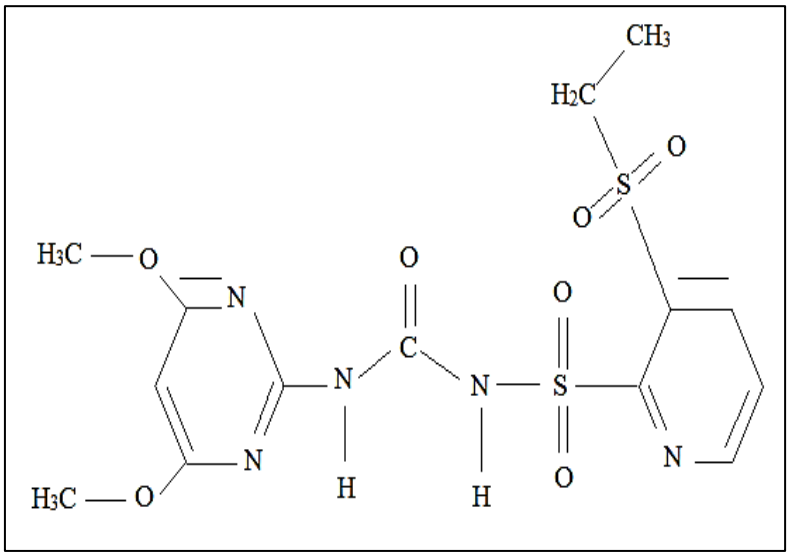

Figure 2.15. Molecular structure of rimsulfuron.

Jain, Gupta, Jadon and Radhapyari (2010) studied the voltammetric determination of cefixime by CV, differential pulse cathodic adsorptive stripping voltammetry (DPCAdSV) and square-wave cathodic adsorptive stripping voltammetry (SWCAdSV) at HMDE. Molecular structure of cefixime is shown in Figure 2.16. The optimum parameters were determined. Linear operating range was determined to be within the range of 50 ng/mL to 25.6 µg/mL. LOD and LOQ were determined to be 3.99 and 13.3 ng/mL by SWCAdSV and 7.98 and 26.6 ng/mL by DPCAdSV, respectively. The method was applied to the drug in tablets and urine samples. Minimum detectability was 12.6 ng/mL by SWCAdSV and 58.4 ng/mL by DPCAdSV in urine sample.

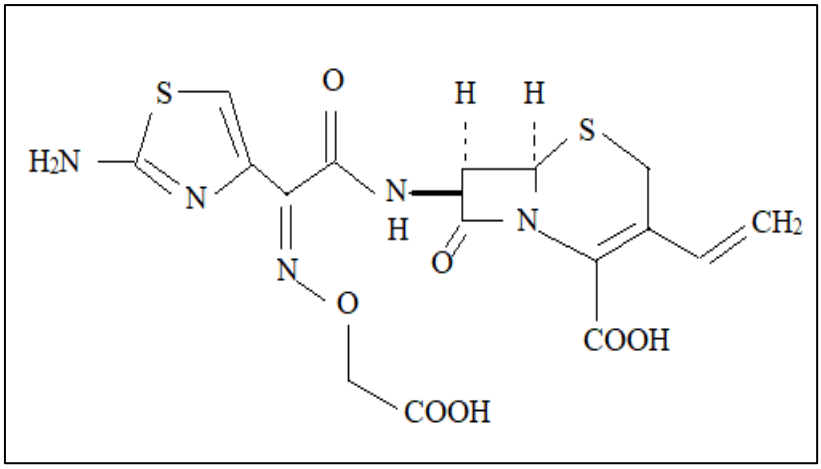

Figure 2.16. Molecular structure of cefixime.

2.2.4. Literature for dinobuton and dinitrophenyl group pesticides

To the best of our acquaintance, there is no study of SWSV of dinobuton on MWCNT electrode. The electrochemical studies based on determination of dinobuton and dinitrophenylic pesticides were performed. Comparison of studies for determination of dinobuton in literature is shown in Table 2.2. Comparison of studies for determination of dinobuton in literature in natural samples is shown in Table 2.3. Methods for the determination of dinitrophenyl pesticides in literature and their comparison with the present work is shown in Table 2.4. Finally, comparison of studies for determination of dinitrophenylic pesticides in literature in natural samples and this study is shown in Table 2.5.

Table 2.2. Comparison of studies for determination of dinobuton in literature.

Sensing Material	Method	LOD(μg/mL)	LOQ(μg/mL)	Linear Operating Range (μg/mL)	References
DME	DC polarography CV DPP CPE Millicoulometry	-	-	$9.82x10^{-4}$-3.91	Sreedhar, Samatha and Sujatha, 2000
Nanostructured Fe_2O_3-ZnO modified GCE	DPV and CV	0.01200	0.03636	0.05-30.00	Aruna and et al., 2018
Stopped-flow pneumatic system	Semiautomatic Method	0.40	-	-	Espinosa-Mansilla, Madera and Salinas, 1999
MWCNT	SWSV CV	0.238	0.793	1.22-8.42	This study

CV: Cyclic voltammetry, CPE: Controlled potential electrolysis, DC: Direct current, DME: Dropping mercury electrode, DPP: Differential pulse polarography, DPV: Differential pulse voltammetry, GCE: Glasssy carbon electrode, SWSV: Square wave stripping voltammetry, MWCNT: Multi-walled carbon nano tube.

Sreedhar *et al* (2000) studied electrochemical behavior of dinobuton by DC polarography, CV, DPP, CPE and millicoulometry. They used DME as working electrode. Two peaks were observed in the reduction direction. Linear dynamic range was determined to be $3.01x10^{-9}$-$1.2x10^{-5}$ M**.** The developed DPP method for determination of dinobuton was also applied to agricultural formulations and spiked water. Percent recovery was found to be around 99% with % standart deviations of 0.012 - 0.021 in the agricultural formulations. In spiked distilled water percent recovery was found to be within 93.50-97.50 with % standart deviation of 0.012 -0.021%

Aruna et *al* (2018) studied determination of dinobuton by DPV and CV. Nanostructured Fe_2O_3-ZnO modified GCE was used as a working electrode. A single peak was observed at -560 mV. LOD, LOQ and linear working range were determined for validation of the proposed method. LOD and LOQ were within 0.01200 and 0.03636 μg/mL, respectively. Linear working range was within 0.05 - 30.00 μg/mL. The developed method was applied to environmental samples. The percent recoveries were found to be 97.8% and 99.8% in water and soil samples, respectively.

Espinosa-Mansilla *et al* (1999) recommended a semiautomatic method for the determination of dinobuton. A stopped-flow pneumtic system was used and detection limit was 0.40 μg/mL. The developed method was also applied to simultanoeus determination of dinobuton and dinoseb. Then the method was applied to commercial formulation of dinobuton.

Table 2.3. Comparison of studies for determination of dinobuton in literature in natural samples.

Sensing Material	Method	LOD(μg/mL)	LOQ(μg/mL)	Linear Operating Range (μg/mL)	Sample Applied	References
Kinetex C18 Column	HPLC-DAD	0.11	0.34	1-200	well water	Gebrehiwot, Erkmen and Uslu, 2020
		0.09	0.28	1-200	waste water	
		0.10	0.31	1-200	tap water	
		0.17	0.51	1-200	soil	
		0.09	0.28	1-200	tomato juice	
		0.09	0.29	1-200	serum	
		0.09	0.29	1-200	urine	
MWCNT	SWSV	0.878	2.92	3.99-11.54	apple juice	This study
	CV	0.398	1.33	4.27-10.38	tap water	

CV: Cyclic voltammetry, HPLC-DAD: High performance liquid chromatography-diode array detector, MWCNT: Multi-walled carbon nano tube, SWSV: Square wave stripping voltammetry

Gebrehiwot et al(2020) studied determination of buprofezin, dinobuton and chlorothalonil in food, environmental and biological samples. They used HPLC-DAD method. LOD and LOQ values were determined for dinobuton within 0.09 - 0.17 μg/mL and 0.28 - 0.51 μg/mL, respectively. Linear operating range was within 1 - 200 μg/mL. Percent recoveries were within 92.3 - 109.74% in different samples.

Table 2.4. Methods for the determination of dinitrophenyl pesticides in literature.

Analyte	Sensing Material	Method	LOD (M)	LOQ (M)	Linear Operating Range (M)	References
Dinoseb	CPE	DP-AdSV	$2x10^{-9}$	$6.6x10^{-9}$	$3x10^{-9}$-$4x10^{-7}$	Sreedhar, T.M. Reddy, Sirisha, S. Reddy and J. Reddy, 2003
	CMCPE		$1x10^{-10}$	$3x10^{-10}$	$2x10^{-10}$-$3x10^{-7}$	

Table 2.4. (continue) Methods for the determination of dinitrophenyl pesticides in literature.

Dinoterb	CPE CMCPE	DP-AdSV	$3.6x10^{-9}$ $5.4x10^{-10}$	$1.13x10^{-8}$ $1.8x10^{-9}$	$4x10^{-9}$-$8x10^{-7}$ $6x10^{-10}$-$6x10^{-7}$	Sreedhar and et al., 2003
Dinoseb	MFE	AdSV	$6.2x10^{-10}$ (t_{acc}=40 s) $1.1x10^{-10}$ (t_{acc}=300 s)	$2.1x10^{-9}$ (t_{acc}=40 s) $3.6x10^{-10}$ (t_{acc}=300 s)	$3.7x10^{-8}$ - $2.4x10^{-7}$ (t_{acc}=40 s) $6.5x10^{-10}$ - $5.5x10^{-9}$ (t_{acc}=300 s)	Pedrero, Casado, Villena and Pingarrón, 1994
Dinoseb Dinoterb DNOC	Electron Capture Electrode	GC	-	-	$3.06x10^{-8}$-$6.13x10^{-7}$ $3.06x10^{-8}$ – $6.13x10^{-7}$ $5.05x10^{-8}$-$1x10^{-6}$	Ohfuji, Chikamoto, Kamada and Komatsu, 1997
Dinoseb 2,6-dinitro-p-cresol	Quartz Cell	Spectro-Photometry	$4.16x10^{-6}$ $5.05x10^{-6}$	- -	0-$1.09x10^{-3}$ 0-$2.26x10^{-3}$	Arancibia, Delfa, Boschetti, Escandar and Olivieri, 2005
Dinocap	Electron capture detection system	GC	$6x10^{-4}$ ng	0.010 mg/kg	0.05-1 mg/kg	Bella, Saitta, Salvo Nicotina and Dugo, 2003
Dinoseb	High-speed spectro-photometric detector	HPLC	$1.04x10^{-7}$	-	-	Szeto and Price, 1991
Dinoseb 4,6-dinitro-2-methyl-phenol 2-nitro-phenol	LC pump coupled with UV-Vis Detector	LC	$2.5x10^{-7}$ $5.05x10^{-8}$ $1.44x10^{-7}$	- - -	$4.16x10^{-7}$-$1.25x10^{-4}$ $5.05x10^{-7}$-$1.51x10^{-4}$ $7.19x10^{-7}$-$2.16x10^{-4}$	Fernández-Salinero, Silva-Vargas, León-González, Párez-Arribas and Polo-Dáiez, 1999
Dinoterb	Cathodically-pretreated boron doped diamond electrode	SWAdSV	$9.16x10^{-9}$	$3.05x10^{-8}$	$3.12x10^{-8}$-$3.12x10^{-6}$	Pınar, Allahverdiya Yardım and Şentürk, 2020
Dinosulfon	GCE modified with ZnO/MWCNT	CV DPV	$1.24x10^{-8}$	$2.37x10^{-8}$	$5.4x10^{-8}$-$1.62x10^{-4}$	Reddy, Prasad and Sreedhar, 2016
Dinoseb Dinoterb	C-18 column, Negative ion electro-spray detection	LC-MS/MS	-	0.001 µg/g	$2.08x10^{-9}$-$1.66x10^{-7}$	Takahashi, Ishii, Nemoto and Matsuda, 2013

Table 2.4. (continue) Methods for the determination of dinitrophenyl pesticides in literature.

DNOC	UV-Vis Spectro-Photometer	Periodate spectro-photometry	$8.07x10^{-6}$	-	$3.78x10^{-5}$-$1.13x10^{-3}$	Uzer, Ercag, Parlar, Apak and Filik, 2006
		Cu(II)-neocuproine spectro-photometry	$1x10^{-6}$	-	$2.22x10^{-6}$-$2.24x10^{-5}$	
DNOC	Molecularly imprinted polymer based microsensor	SWV	$2.01x10^{-7}$	-	$8x10^{-7}$-10^{-4}	Gámez-Caballero, Unceta, Goicolea and Barrio, 2008
DNOC	Antimony film electrode	SWV	$1.12x10^{-6}$	$1.42x10^{-6}$	$1x10^{-6}$-$15x10^{-6}$	Betancourth, Cuellar, Ortiz and Pfaffen, 2018
DNOC	HMDE	SWSV	$2x10^{-8}$	-	$0.01x10^{-6}$-$0.55x10^{-6}$	Cuellar, Betancourth, Pfaffen and Ortiz, 2019
DNOC	Optical Biosensor	Fluorescence	$2.5x10^{-8}$	-	-	Védrine, Leclerc, Durrieu and Tran-Minh, 2003
2,4-DNP	UV detector	HPLC-UV	$3.73x10^{-5}$	-	$5.43x10^{-7}$-$5.43x10^{-4}$	Opeolu, Fatoki and Odendaal, 2010
DNOC			$9.99x10^{-6}$	-	$5.05x10^{-6}$-$1.51x10^{-4}$	
DNOC	Poly-fabricated capillary electro-phoresis microchip, Au working Electrode	CE PAD	$0.9x10^{-6}$	-	-	Ding and Garcia, 2006
2,4-DNP	Diode Array UV Detector	MMLLE	-	$2.86x10^{-10}$	$5.43x10^{-10}$-$6.79x10^{-8}$	Bartolomé, Lezamiz, Etxebarria, Zuloaga and Jönsson, 2007
DNOC				$9.79x10^{-11}$	$5.05x10^{-10}$-$6.31x10^{-8}$	
Dinoseb				$1.13x10^{-10}$	$4.16x10^{-10}$-$5.20x10^{-8}$	
Dinoterb				$9.82x10^{-11}$	$4.16x10^{-10}$-$5.20x10^{-8}$	

Table 2.4. (continue) Methods for the determination of dinitrophenyl pesticides in literature.

DNOC	SPE-HPLC UV Detector	SPE-HPLC	$3.03x10^{-10}$	-	$1x10^{-8}$-$5.05x10^{-6}$	Zhao, Wang, Yuan and Wang, 2009
DNOC	UV-detector, mass spectrometer	Pressure chemical ionisation MS-MS, LC	$2.02x10^{-10}$ (MeOH) $1.51x10^{-10}$ (ACN)	-	-	Geerdink, Kooistra-Sijpersma, Tiesnitsch, Kienhuis and Brinkman, 1999
Dinoseb			$8.33x10^{-11}$ (MeOH) $4.16x10^{-11}$ (ACN)	-	-	
Dinoterb			$8.33x10^{-11}$ (MeOH) $8.33x10^{-11}$ (ACN)	-	-	
2,4-DNP	Photoiodide array	LC	$5.43x10^{-9}$	-	-	Santana, Ferrera and Rodríguez, 2004
DNOC	detector		$6.56x10^{-9}$	-	-	
Dinoterbon	NiO-GO Nanosensor	AdSV	$8.97x10^{-8}$	-	$1.60x10^{-7}$-$1.60x10^{-4}$	Roja, Prasad, Sandhya and Sreedhar, 2016
Dinobuton	MWCNT	SWSV CV	$0.73x10^{-6}$	$2.43x10^{-6}$	$3.74x10^{-6}$-$25.8x10^{-6}$	This study

AdSV: Adsorptive stripping voltammetry, CE-Capillary electrophoresis, CMCPE: Clay modified carbon paste electrode, CPE: Carbon paste electrode, DPV: Differential pulse voltammetry, DPAdSV-Differential pulse adsorptive stripping voltammetry, GC-Gas chromatography, HMDE: Hanging mercury dropping electrode, HPLC: High performance liquid chromatography, LC:Liquid chromatography, MFE:Mercury film electrode, MMLLE:Microporous membrane liquid–liquid extraction, MS: Mass spectrometry, MWCNT: Multi-walled carbon nano tube, PAD: Pulse amperometric detection, SPE:Solid phase extraction, SWV:Square wave voltammetry, SWAdSV:Square-wave adsorptive stripping voltammetry, UV: Ultraviolet, Vis: Visible

Sreedhar et al (2003) studied the determination of dinoseb and dinoterb by DPAdSV at bare CPE and and clay modified CPE. For dinoseb, whereas LOD and LOQ were determined to be $2x10^{-9}$ M and $6.6x10^{-9}$ M, respectively and linear working range was $3x10^{-9}$ - $4x10^{-7}$ M at carbon paste electrode, LOD and LOQ were determined to be $1x10^{-10}$ M and $3x10^{-10}$ M, respectively and lienar working range was determined to be $2x10^{-10}$ - $3x10^{-7}$ M at clay modified carbon paste electrode. For dinoterb, LOD and LOQ were $3.6x10^{-9}$ M and $1.13x10^{-8}$ M, respectively. Linear working range was $4x10^{-9}$ - $8x10^{-7}$ M at carbon paste electrode. LOD and LOQ were $5.4x10^{-10}$ M and $1.8x10^{-9}$ M, respectively. Linear working range was $6x10^{-10}$ - $6x10^{-7}$ M at clay modified CPE. The recommended method was applied to environmental samples using CMPCPE. Percente recovery was found to be within

95.40 -96.40% for dinoseb and 95.20 – 98.0% for dinoterb in spiked tap water samples. Percent recovery was found to be within 96.60 - 98.50% for dinoseb and 95.40 -98.30% for dinoterb in soil samples. Percent recovery was found to be 98.04% for dinoseb and 98.29% for dinoterb on average in juice samples.

Pedrero et al. (1994) developed an adsorptive stripping voltammetric method for the determination of dinoseb using a MFE and LOD, LOQ and linear working ranges were obtained at different accumulation times. LOD and LOQ were $6.2x10^{-10}$ and $2.1x10^{-9}$ M, respectively and linear working range was determined to be $3.7x10^{-8}$ - $2.4x10^{-7}$ M at an accumulation time of 40 s. LOD and LOQ were $1.1x10^{-10}$ M and $3.6x10^{-10}$ M respectively, and linear working range was within $6.5x10^{-10}$ - $5.5x10^{-9}$ M at an accumulation time of 300 s. The recommended method was applied to spiked apple juie and % recovery was 91% at an accumulation time of 40 s and 90% at the accumulation time of 300 s in spiked apple juice samples.

Ohfuji et al (1997) developed a gas chromatographic method for determination of dinoseb, dinoterb and DNOC. An electron capture detector was connected to gas chromatograph and the linearity was within 0.01- 0.2 μg/mL ($3.06x10^{-8}$ – $6.13x10^{-7}$ M) in the calibration curve. The developed method was applied for the determination of dinoseb, dinoterb and DNOC in citrus fruit recovery within 7 3- 85%.

Arancibia et al (2005) studied the determination of dinoseb and 2,6-dinitro-p-cresol by spectrophotometry. The limit of detection was 1 μg/mL for both or $4.16x10^{-6}$ M for dinoseb and $5.05x10^{-6}$ M for 2,6-dinitro-p-cresol. The linear dynamic range was 0 - 261 μg/mL (0-$1.09x10^{-3}$ M) for dinoseb and 0 - 448 μg/mL (0 - $2.26x10^{-3}$ M) for 2,6-dinitro-p-cresol . The method was applied to natural samples. Simultaneous determination of dinoseb and 2,6-dinitro-p-cresol were performed by partial-least squares calibration. Percent recovery was within 96 - 102% for dinoseb and 95 - 104% for 2,6-dinitro-p-cresol, respectively in synthetic and natural samples.

A gas chromatographic method was used for the determination of azoxystrobin, dinocap, fenarimol, penconazole and quinoxyfen by Bella and et al (2003). High resolution gas chromatograph equipped with electron capture detection system exhibited a LOD and LOQ to be $6x10^{-4}$ ng and 0.010 mg/kg, respectively. Linear working range was within

0.05 - 1 mg/kg and residues of pesticides were determined in grapes, must, marc and wine. Percent recovery was within 89.4 - 94.1% in grapes, 81.8 - 93.8% in marc, 85.3 - 101.3% in must and 89.5 - 110.4% in wine, respectively.

Szeto and Price(1991) studied the determination of dinoseb by HPLC. High-speed spectrophotometric detector was used and LOD was determined 0.025 ppm ($1.04x10^{-7}$ M). The method was applied to raspberries and % recovery was within 78.6 -85.5%.

4,6-dinitro-2-methylphenol and 2-nitrophenol was determined by using liquid chromatography with UV-Vis detector by Fernández-Salinero et al. in 1999. LOD was 60 μg/L ($2.5x10^{-7}$ M), 10 μg/L ($5.05x10^{-8}$ M) and 20 μg/L ($1.44x10^{-7}$ M) for dinoseb, 4,6-dinitro-2-methylphenol and 2-nitrophenol, respectively. Linear dynamic range was 0.1-30 mg/L for all three species. These LOD values for dinoseb, 4,6-dinitro-2-methylphenol and 2-nitrophenol corresponds to $4.16x10^{-7}$- $1.25x10^{-4}$ M, $5.05x10^{-7}$- $1.51x10^{-4}$ M and $7.19x10^{-7}$ - $2.16x10^{-4}$ M, respectively. Chromatographic determination of dinoseb, 4,6-dinitro-2-methylphenol and 2-nitrophenol was applied to distilled water and lemon juice and % recovery was within 89- 100%.

Pınar et al (2020) investigated dinoterb by SWASV using cathodically pretreated boron-doped diamond electrode. LOD and LOQ was $9.16x10^{-9}$ and $3.05x10^{-8}$ M, respectively. Linear operating range was determined to be $3.12x10^{-8}$- $3.12x10^{-6}$ M. The recommended method was applied to river water and soil samples and % recovery was found to be in river water and soil sample 92% and 108%, respectively.

Reddy et al (2016) studied the voltammetric behavior of dinosulfon using DPV and CV. A GCE modified with ZnO/multiwalled carbon nanotubes nanocomposite was used as a working electrode. LOD and LOQ were 0.0046 μg/mL ($1.24x10^{-8}$ M) and 0.0088 μg/mL ($2.37x10^{-8}$ M), respectively. Linear dynamic range was within 0.02 - 60 μg/mL ($5.4x10^{-8}$-$1.62x10^{-4}$ M). The developed method was applied to water samples and % recovery was found to be in tap water and well water within 98 -99.70% and 99.45 -99.96%, respectively. % RSD was found to be within 0.16-0.22 and 0.11- 0.24, respectively.

A LC-MS/MS method was developed for the determination of dinoseb and dinoterb (Takahashi et al., 2013). A C18 column was used for LC seperation and negative ion electrospray detection was used for MS and LOQ was 0.001 μg/g for both compunds. The linear dynamic range was within 0.0005- 0.04 μg/mL ($2.08x10^{-9}$-$1.66x10^{-7}$ M) for both compunds and the method was applied to agricultural products, livestock products and seafood. The percent recovery and % RSD was within 77- 111% and 2-15% on average, respectively.

Uzer et al (2006) investigated spectrophotometric determination of DNOC. For two different spectrophometric methods used, LOD was determined 1.6 mg/L ($8.07x10^{-6}$ M) when periodate spectrophotometry applied, and 0.2 mg/L ($1x10^{-6}$ M) when Cu(II) neocuproine spectrophotometry applied. The linear working range was 7.5 - 225 mg/L ($3.78x10^{-5}$-$1.13x10^{-3}$ M) and 0.44- 4.44 mg/L ($2.22x10^{-6}$-$2.24x10^{-5}$ M) and the recommended method was applied to synthetically contaminated montmorillonite and lemon juice with a % recovery of 95% or slightly greater.

GÃmez-Caballero et al (2008) studied the determination of DNOC by SWV using molecularly imprinted polymer based microsensor and LOD was $2.01x10^{-7}$ M within a linear working range of $8x10^{-7}$ and 10^{-4} M.

Betancourth et al (2018) studied determination of DNOC by SWV using antimony film electrode prepared on GCE and LOD and LOQ were detected $1.12x10^{-6}$ M and $1.42x10^{-6}$ M, respectively. Linear working range was within $1x10^{-6}$ and $15x10^{-6}$ M and the developed method was applied to natural water samples with the recovery of 95- 106%.

Cuellar et al (2019) investigated DNOC by SWSV using a HMDE electrode. In the proposed method, LOD was $2x10^{-8}$ M within a linear working range of $0.01x10^{-6}$ and $0.55x10^{-6}$ M. The recommended method was applied to different water samples and % recovery was around 102%.

Védrine et al (2003) studied the determination of DNOC with optical biosensor using fluorescence spectroscopy and LOD was 5 μg/L ($2.5x10^{-8}$ M).

Opeolu et al (2010) studied the determination of phenols including 2,4-DNP and DNOC by HPLC-UV and LOD was 6.86 μg/mL ($3.73x10^{-5}$ M) for 2,4-DNP and 1.98 μg/mL ($9.99x10^{-6}$ M) for DNOC, respectively. Linear dynamic range for 2,4-DNP and DNOC was proposed to be 0.1 and 100 μg/mL ($5.43x10^{-7}$-$5.43x10^{-4}$ M) and 1-30 μg/mL ($5.05x10^{-6}$-$1.51x10^{-4}$ M), respectively. The recommended method was applied to Milli-Q water and % recovery for 2,4-DNP and DNOC was 83.74% and 93.28%, respectively. In the proposed HPLC-UV thecnique % RSD for 2,4-DNP and DNOC was 3% and 3.35%, respectively.

EPA's (Environmental Protection Agency) priority pollutants were studied by Ding and Garcia using capillary electrophores (CE) and PAD in 2006. Poly-fabricated capillary electrophoresis microchip was used for CE and Au working electrode and LOD for DNOC was 0.9 μM. The proposed method was applied to local city water sample and two over-the-counter sore throat medicines.

Bartolomé et al (2007) offered a microporous membrane liquid-liquid extraction for the determination of 2,4-DNP, DNOC, dinoseb and dinoterb using diode array UV detector. In the proposed method, LOQ values for 2,4-DNP, DNOC, dinoseb and dinoterb were 52.7 ng/L ($2.86x10^{-10}$ M), 19.4 ng/L ($9.79x10^{-11}$ M), 27.2 ng/L ($1.13x10^{-10}$ M) and 23.6 ng/L ($9.82x10^{-11}$ M), respectively with a linear working range of $5.43x10^{-10}$ and $6.79x10^{-8}$ M, $5.05x10^{-10}$ and $6.31x10^{-8}$ M, $4.16x10^{-10}$ and $5.20x10^{-8}$ M and $4.16x10^{-10}$ and $5.20x10^{-8}$ M.

Zhao et al (2009) studied phenols including DNOC by SPE-HPLC with SPE-HPLC UV detector and LOD was 0.06 ng/mL ($3.03x10^{-10}$ M). The linear working range was 2.0-100 ng/mL ($1x10^{-8}$- $5.05x10^{-6}$ M) and the recommended method applied to environmental water samples exhibited a % 81 recvery in tap water, 81.4% in groundwater, 120.1% in reservoir water, respectively. % RSD was 6% in tap water, 6.3% in groundwater and 6.2% reservoir water.

The DNOC, dinoseb and dinoterb was determined by Geerdink et al (1999) using pressure chemical ionisation MS-MS and LC method. When methanol was used as organic modifier, LOD for DNOC, dinoseb and dinoteb were 40 ng/L ($2.02x10^{-10}$ M), 20 ng/L ($8.33x10^{-11}$ M) and 20 ng/L ($8.33x10^{-11}$ M), respectively. When acetonitrile was used as an organic modifier, LOD for DNOC, dinoseb and dinoterb were 30 ng/L ($1.51x10^{-10}$ M), 10 ng/L ($4.16x10^{-11}$ M)

and 20 ng/L ($8.33x10^{-11}$ M), respectively. The recommended method was applied to surface water samples.

Liquid chromatography with photoiodide array detector was used for the determination of some phenolic derivatives (Santana et al. 2004) and LOD for 2,4-DNP and DNOC was 1 μg/L ($5.43x10^{-9}$ M) and 1.3 μg/L ($6.56x10^{-9}$ M), respectively. The proposed method was applied to water samples and % recovery for 2,4-DNP was 72.9% in water, 62% in seawater, 65.7% in waste water. The percent recoveries for DNOC in water, sea water and waste water samples were 92.4%, 85.7% and 72%, respectively.

Dinoterbon was determined by Roja et al (2016) using ASV and NiO electrochemical nanosensor modified with graphene oxide was prepared for detection. In the recommended method, LOD was 0.028 μg/mL ($8.97x10^{-8}$ M) and linear working range was within 0.05-50 μg/mL ($1.60x10^{-7}$-$1.60x10^{-4}$ M). The method applied to food samples exhibited a percent recovery within 97.40 - 99.88% with a RSD of 0.114%. AS voltammetry using NiO electrochemical nanosensor modified with graphene oxide showed 6.8% and 4.6% RSD for inter-assay and intra-assay studies, respectively.

Table 2.5. Comparison of studies for determination of dinitrophenylic pesticides in natural samples in literature.

Analyte	Sensing Material	Method	LOD (M)	LOQ (M)	Linear Operating Range (M)	Sample Applied	References
Dinoseb	MFE	AdSV	-	-	$2.0x10^{-8}$-$1.0x10^{-7}$ t_{acc}= 40 s $2.0x10^{-9}$-$1.0x10^{-8}$ t_{acc}= 300 s	Apple juice	Pedrero, Casado, Villena and Pingarrón, 1994
Dinoseb Dinoterb DNOC	Electron capture electrode	GC	0.005 μg/g	-	-	Citrus Fruits	Ohfuji, Chikamoto, Kamada and Komatsu, 1997
Dinoseb	Reversed-Phase Spherisorb 5 ODS Column	Chromatographic - Seperation	$7.08x10^{-8}$	-	-	Lemon Juice	Salinero, Vargas, González, Arribas and Diez, 1999

Table 2.5. (continue) Comparison of studies for determination of dinitrophenylic pesticides in natural samples in literature.

2,4-DNP	Photodiode Array Detector	UHPLC MS-USAEME	$1.68x10^{-8}$	-	$5.43x10^{-8}$-$5.43x10^{-6}$	Lake water	Chung, Leong and Huang, 2012
DNOC			$6.56x10^{-9}$		$2.52x10^{-8}$-$5.05x10^{-6}$		
			$1.74x10^{-8}$		$5.43x10^{-8}$-$5.43x10^{-6}$	Agriculture Water Sample	
			$7.07x10^{-9}$		$2.52x10^{-8}$-$5.05x10^{-6}$		
2-nitro-phenol	UV-Vis detector	LC	$2.37x10^{-8}$	-	-	Distilled water	Fernández-Salinero, Silva-Vargas, León-González, Párez-Arribas and Polo-Dáiez, 1999
4,6-dinitro-2-methyl-phenol			$1.16x10^{-8}$	-	-		
Dinoseb			$2.08x10^{-8}$	-	-		
				-			
Dinoseb			$7.08x10^{-8}$		-	Lemon juice	
Dinobuton	MWCNT	SWSV	$2.69x10^{-6}$	$8.96x10^{-6}$	$12.25x10^{-6}$-$35.38x10^{-6}$	Apple juice	This study
			$1.22x10^{-6}$	$4.08x10^{-6}$	$13.1x10^{-6}$-$31.81x10^{-6}$	Tap water	

AdSV: Adsorptive stripping voltammetry, GC:Gas chromatography, GC-ITMS:Gas chromatography-ion trap mass spectrometry, LC-Liquid chromatography, MFE-Mercury film electrode, MS-Mass spectrometry, MS-USAEME-Manuel shaking-enhanced, ultrasound-assisted emulsification microextraction, MWCNT-Multi-walled carbon nano tube, SWSV:Square wave stripping voltammtry, UHPLC:Ultrahigh pressure liquid chromatography, UPLC-MS/MS:Ultra performance liquid chromatography-tandem mass spectrometry, UV: Ultraviolet, Vis: Visible

Pedrero et al (1994) determined dinoseb by DPASV using MFE and the proposed method was applied to apple juice. Linear dynamic range was within $2.0x10^{-8}$ and $1.0x10^{-7}$ M at the accumulation time of 40 s and $2.0x10^{-9}$ and $1.0x10^{-8}$ M at the accumulation time of 300 s. In the recommended method, the percent recovery was 91% at the accumulation time of 40 s and 90% at the accumulation time of 300 s on average.

A gas chromatographic method for the determination of dinoseb, dinoterb and DNOC was developed by Ohfuji et al (1997) using electron capture detector (ECD). The method was applied to citrus fruits and LOD for dinoseb, dinoterb and DNOC was 0.005 μg/g and % recovery was within 73 and 85%.

Fernández-Salinero et al (1999) determined dinoseb in lemon juice by chromatographic technique and LOD was 17 μg/L ($7.08x10^{-8}$ M) with a % recovery of 89 – 100%.

UHPLC-MS-Ultrasound-assisted emulsification microextraction method was used by Chung et al (2012) for the determination of nitrophenols including 2,4-DNP and DNOC in water samples. LOD for 2,4-DNP and DNOC in lake water were determined 3 μg/L ($1.68x10^{-8}$ M) and 1.3 μg/L ($6.56x10^{-9}$ M), respectively. The linear working range for 2,4-DNP and DNOC in lake water were 10 - 1000 μg/L ($5.43x10^{-8}$ - $5.43x10^{-6}$ M) and 5 - 1000 μg/L ($2.52x10^{-8}$ - $5.05x10^{-6}$ M), respectively. LOD for 2,4-DNP and DNOC in agriculture water samples were 3.2 μg/L ($1.74x10^{-8}$ M) and 1.4 μg/L ($7.07x10^{-9}$ M), respectively. Linear working range for 2,4-DNP and DNOC in agricultural water samples was 10 - 1000 μg/L ($5.43x10^{-8}$ - $5.43x10^{-6}$ M) and 5 - 1000 μg/L ($2.52x10^{-8}$ - $5.05x10^{-6}$ M), respectively and % recovery was found to be 88% for 2,4-DNP and 110% for DNOC in lake water sample. In lake water and agricultural water samples % recovery for 2,4-DNP and DNOC were 80% and 106% with a 9%and 8% RSD, respectively.

Fernandez-Salinero et al (1999) determined 2-nitrophenol, 4,6-dinitro-2-methylphenol and dinoseb in distilled water by LC coupled with UV-Vis detector and LOD for 2-nitrophenol, 4,6-dinitro-2-methylphenol and dinoseb were 3.3 μg/L ($2.37x10^{-8}$ M), 2.3 μg/L ($1.16x10^{-8}$ M) and 5 μg/L ($2.08x10^{-8}$ M), respectively. The recommended method was also applied to lemon juice for dinoseb and LOD was 17.0 μg/L ($7.08x10^{-8}$ M) within the % recovery of 89 and 100%.

3. EXPERIMENTAL

3.1. Instrumentation

The BAS Epsilon model electrochemical analyzer (Bioanalytical Systems, Epsilon potentiostat/galvanostat, IN 47906, US) was used for recording voltammetric measurements. The electrochemical analyzer shown in Image 3.1 consists of potentiostat power supply, cell stand and computer. The BAS model cell stand of electrochemical analyzer shown in Image 3.2. The cell stand consist of three electrodes which are MWCNT paste electrode (BASi, MF-2012) as working electrode, Ag/AgCl (BASi, MF-2052) as reference electrode and platinum wire (BASi, MW-1032) as a counter electrode. The MWCNT paste electrode, Ag/AgCl reference electrode and the platinum wire electrode are shown in Image 3.3, 3.4 and 3.5, respectively. The pH values of the prepared solutions were measured by using portable HANNA 211 model, microprocessor pH meter with a combined glass electrode (Image 3.6). All samples were accurately weighted with portable, Sartorius analytical balance (precision to ± 0.0001) shown in Image 3.7.

Image 3.1. The BAS epsilon model potentiostat.

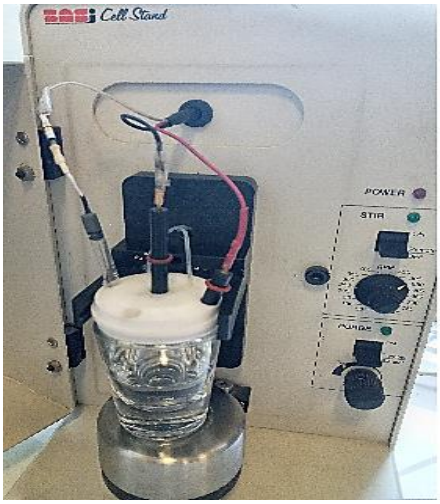

Image 3.2. The BAS model voltammetric cell stand.

Image 3.3. The MWCNT paste electrode.

Image 3.4. The Ag/AgCl reference electrode.

Image 3.5. The platinum wire electrode.

Image 3.6. The HANNA 211 model microprocessor pH meter.

Image 3.7. The Sartorius model analytical balance (± 0.0001 precision).

3.2. Reagents

Dinobuton and pesticides used in this work were of analytical grade. MWCNTs were obtained from Sigma Aldrich (O.D. 10-15 nm, I.D. 2-6 nm, lenght 0.1-10 μm, > 90% AS, MWCNT, Product of Arkema Inc.) and mineral oil was provided from Sigma Aldrich. The BR buffer solutions were prepared by mixing 2.5 grams of boric acid (Emsure® Merck KGaA 99.8%), 2.7 mL of acetic acid (Emprove®, Merck KGaA, 100%) and 2.3 mL of phosphoric acid (Merck KGaA, 85%) in 1 liter of distilled water.

2.0 M NaOH (prepared from pellets pure, Merck KGaA) and 2.0 M HCl (Sigma Aldrich, 37%) and 2.0 M H_2SO_4 (Merck, 95-98%) were used to make the pH of the supporting electrolyte to the desired pH value. All pesticides were dissolved in acetone (Sigma Aldrich, 99% and Emsure®, ACS, ISO, Reag. Ph Eur, Merck, 99%).

3.3. Preparation of Solutions

All solutions were prepared in either distilled water or acetone. The solubility of pesticides in water and in some organic solvents searched from literature and acetone was the best solvent for pesticides used in our voltammetric procedures. BR buffer stock solutions were kept in refrigerator at 4 ^{0}C. All pesticide stock solutions were prepared freshly before each experiment. NaOH and H_2SO_4 stock solutions were kept in the fridge at 2-8 °C.

3.3.1. Supporting electrolytes

0.1 M H_2SO_4 solution

0.1 M H_2SO_4 solution for pH ~1 was prepared from concentrated H_2SO_4 (Merck, 95-98%).

pH 2 supporting electrolytes

The Britton-Robinson universalbuffer (BR buffer) stock solution prepared originally by just mixing 2.5 gram H_3BO_3; 2.7 mL CH_3COOH; 2.3 mL H_3PO_4 in 1 L was used for the pH ~2 measurements.

pH 3 supporting electrolytes

2 M NaOH solution was dropped into pH ~ 2 BR buffer stock solution until pH 3 solution was obtained under the control of pH meter.

pH 4 supporting electrolytes

2 M NaOH solution was dropped into pH 2 BR buffer stock solution until pH 4 solution was obtained under the control of pH meter.

pH 5 supporting electrolytes

2 M NaOH solution was dropped into pH 2 BR buffer stock solution until pH 5 solution was obtained under the control of pH meter.

pH 6 supporting electrolyte

2 M NaOH solution was dropped into pH 2 BR buffer stock solution until pH 6 solution was obtained under the control of pH meter.

pH 7 supporting electrolyte

2 M NaOH solution was dropped into pH 2 BR buffer stock solution until pH 7 solution was obtained under the control of pH meter.

pH 8 supporting electrolyte

2 M NaOH solution was dropped into pH 2 BR buffer stock solution until pH 8 solution was obtained under the control of pH meter.

pH 9 supporting electrolyte

2 M NaOH solution was dropped into pH 2 BR buffer stock solution until pH 9 solution was obtained under the control of pH meter.

pH 10 supporting electrolyte

2 M NaOH solution was dropped into pH 2 BR buffer stock solution until pH 10 solution was obtained.

pH 11 supporting electrolyte

2M NaOH solution was dropped into BR buffer stock solution until pH 11 solution was obtained under the control of pH meter.

pH 12 supporting electrolyte

2 M NaOH solution was dropped into pH 2 BR buffer stock solution until pH 12 solution was obtained under the control of pH meter.

3.3.2. Stock solutions

Britton-Robinson buffer solution

The BR buffer solutions were prepared by mixing 2.5 grams of boric acid (99.8%), 2.7 mL of acetic acid (100%) and 2.3 mL of phosphoric acid (85%) in 1 liter of distilled water.

2 M NaOH solution

19.998 grams of NaOH (MW: 39.997 g/mol) in pure pellet form was weighted in analytical balance and completed to 0.25 L with distilled water in volumetric flask. In order to obtain BR buffer solutions at different pH values, 2 M NaOH was added in portions by pH control.

$1.50x10^{-3}$ M Dinobuton solution

0.0049 grams of dinobuton (MW: 326.304 g/mol)
was weighted in analytical balance and dissolved in 10 mL of aetone, so that $1.50x10^{-3}$ M dinobuton solution was obtained.

$1.54x10^{-3}$ M triasulfuron solution

0.0062 grams of triasulfuron (CGA 131036, analytical standart, %99,5; MW: 401.82 g/mol) was weighted in analytical balance and dissolved in 10 mL of acetone, so that $1.54x10^{-3}$ M triasulfuron solution was obtained. Molecular structure of triasulfuron is presented in Figure 3.1.

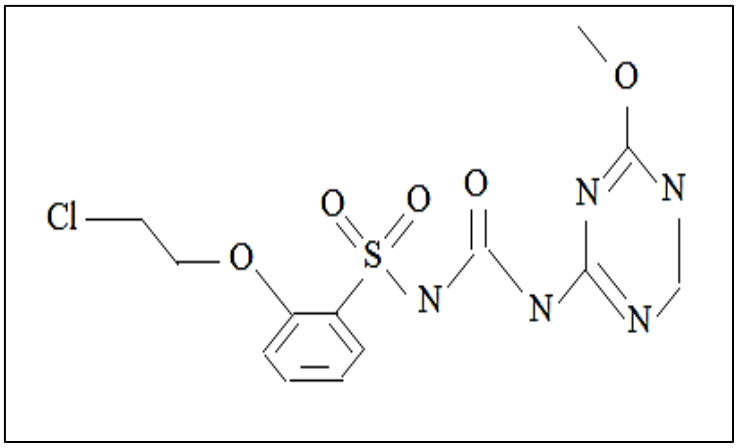

Figure 3.1. Molecular structure of triasulfuron

1.5x10^{-3} M azinphos-methyl solution

0.0049 grams of azinphos-methyl (Bayer, 99.5%; MW: 317.324 g/mol) was weighted in precision on analytical balance and dissolved in 10 mL of acetone. Molecular structure of azinphos-methyl is shown in Figure 3.2.

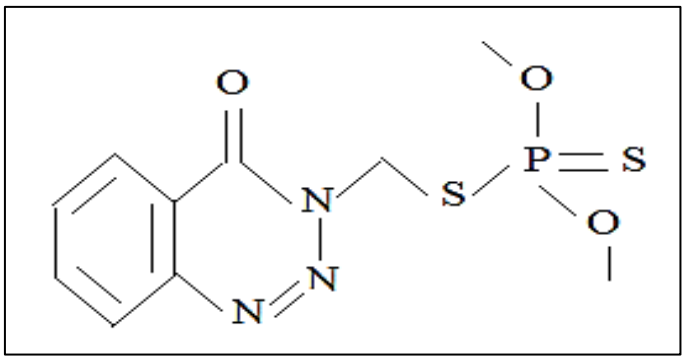

Figure 3.2. Molecular structure of azinphos-methyl.

1.46x10^{-3} M Bromoxynil-octanoate solution

0.0059 grams of bromoxynil-octanoate (MW of bromoxynil-octanoate: 403.10 g/mol) was weighted on analytical balance and dissolved in 10 mL of acetone so that 1.46x10^{-3} M bromoxynil-octanoate solution was prepared. Molecular structure of bromoxynil-octanoate is shown in Figure 3.3.

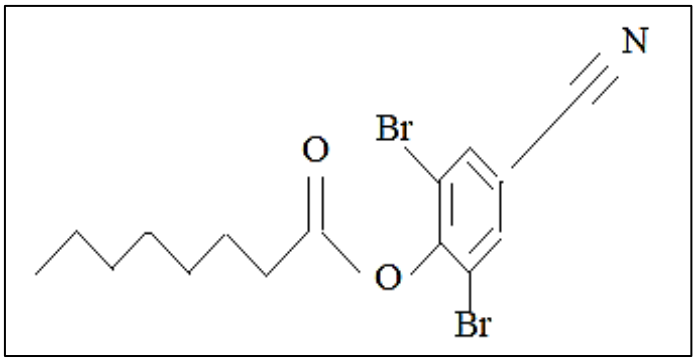

Figure 3.3. Molecular structure of bromoxynil-octanoate

1.60x10^{-3} M dialifos solution

0.0063 grams of dialifos (analytical standart, 99.7%) was dissolved in 10 mL of acetone (MW of dialifos: 393.85 g/mol) so that 1.6x10^{-3} M dialifos was prepared. Molecular structure of dialifos is shown in Figure 3.4.

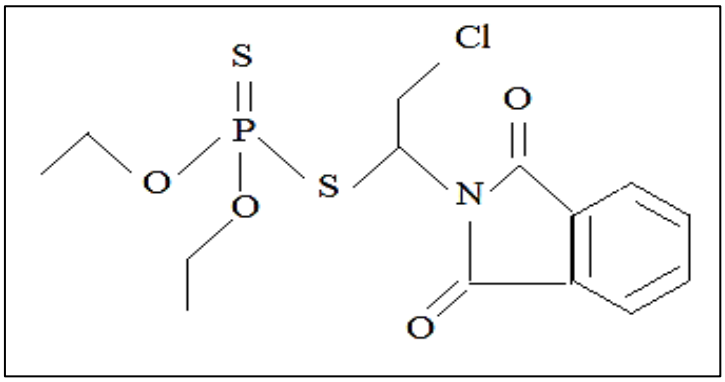

Figure 3.4. Molecular structure of dialifos

1.55x10^{-3} M fipronil solution

0.0068 grams of fipronil (Rhone-Poulenc, analytical standart) was weighted on anlytical balance and dissolved in 10 mL of acetone so that 1.55x10^{-3} M fipronil solution was prepared**.** (MW of fipronil: 437.15 g/mol). Molecular structure of fipronil is shown in Figure 3.5.

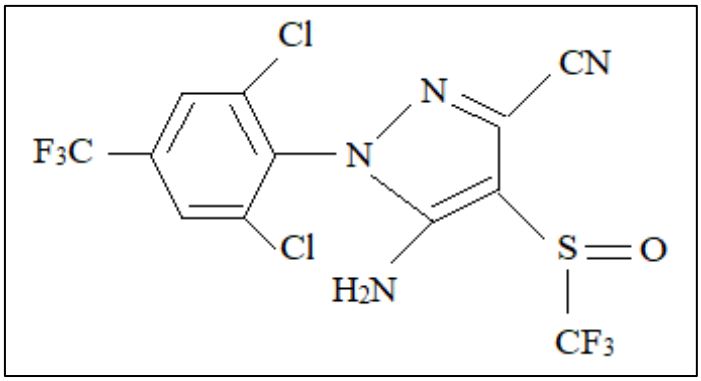

Figure 3.5. Molecular structure of fipronil.

1.64x10^{-3} M vinclozoline solution

0.0047 grams of vinclozolin (99,5%) pesticide was weighted on analytical balance and dissolved in 10 mL of acetone so that 1.64x10^{-3} M vinclozolin pesticide was prepared. (MW of vinclozolin: 286.11 g/mol). Molecular structure of vinclozoline is shown in Figure 3.6.

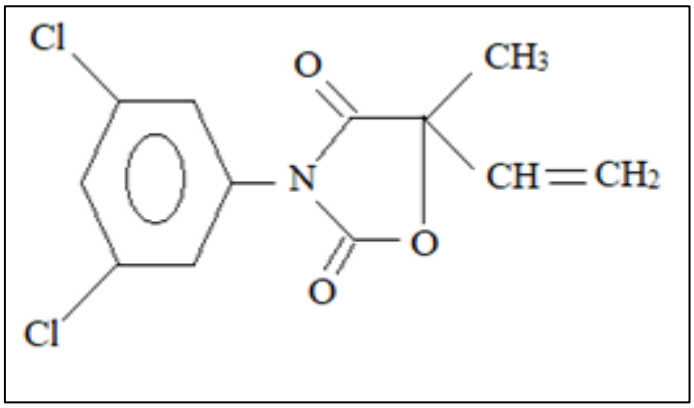

Figure 3.6. Molecular structure of vinclozoline.

1.64x10^{-3} M iprodione solution

0.0051 g of iprodione (Dr. Ehrenstorfer GmbH, 95%) was weighted on analytical balance and dissolved in 10 mL of acetone (MW of iprodione: 330.17 g/mol) so that 1.54x10^{-5} M stock solution of iprodine was prepared. Molecular structure of iprodione is shown in Figure 3.7.

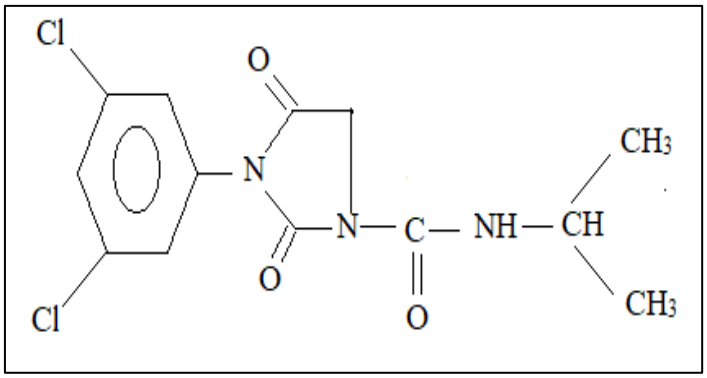

Figure 3.7. Molecular structure of iprodione.

1.64x10^{-3} M procymidone solution

0.0042 grams of procymidone (Sumitomo Chemical, Osaka, Japan, analytical standart, 100%) was weighted in analytical balance and dissolved in 10 mL of acetone(MW of procymidone: 284.14 g/mol) so that 1.48x10^{-3} M procymidone stock solution was prepared. Molecular structure of procymidone is shown in Figure 3.8.

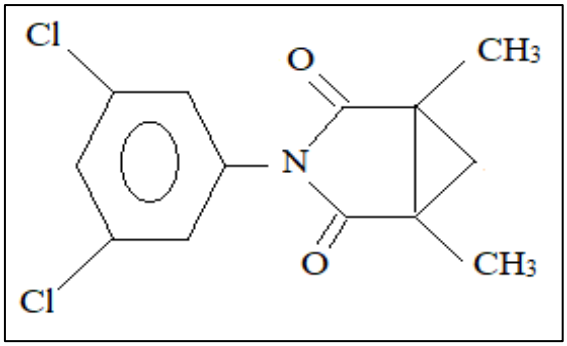

Figure 3.8. Molecular structure of procymidone

1.51x10^{-3} M Iron (III) solution

0.0061 grams of Fe (NO)3·9H_2O was weighted on precision balance and dissolved in 10 mL of distilled water. (MW of Fe $(NO)_3$·9H_2O: 404 g/mol) so that 1.51x10^{-3} M Fe $(NO)_3$·9H_2O was prepared.

1.56x10^{-3} M Magnesium solution

0.0040 grams of Mg $(NO_3)_2$·6H_2O was weighted on precision balance and dissolved in 10

mL of pure water (MW of Mg $(NO_3)_2{\cdot}6H_2O$: 256.41 g/mol) so that $1.56x10^{-3}$ M Mg $(NO_3)_2{\cdot}6H_2O$ solution was prepared.

<u>$1.57x10^{-3}$ M Lead solution</u>

0.0052 grams of Pb $(NO_3)_2$ was weighted on analytical balance and dissolved in 10 mL of distilled water (MW of Pb $(NO_3)_2$: 331.2 g/mol) so that $1.57x10^{-3}$ M Pb $(NO_3)_2$ solution was prepared.

3.3.3. Spiked samples

<u>Apple juice solution</u>

0.0204 grams of dinobuton (Mw:326.30 g/mol) was weighted on analytical balance and dissolved in 10 mL of acetone (6.25×10^{-3} M or 2040 ppm). 1 mL of this solution was taken and completed to 10 mL with apple juice so that 204 ppm or 10 mL of 6.25×10^{-4} M spiked dinobuton-apple juice solution was obtained.

<u>Tap water solution</u>

0.0218 grams of dinobuton was weighted and dissolved in 10 mL of acetone and 1 mL of this solution completed to 10 mL with tap water so that 218 ppm or 6.68×10^{-4} M spiked dinobuton-apple juice solution was obtained.

<u>Grape juice solution</u>

0.0202 grams of dinobuton was weighted on analytical balance and dissolved in 10 mL of acetone. 1 mL from this stock solution was taken and completed to 10 mL with 100% grape juice supplied from supermarket so that 202 ppm or $6.19x10^{-4}$ M spiked dinobutan-grape juice samples were obtained.

3.3.4. Multi-walled carbon nanotube paste electrodes

MWCNT paste was prepared by mixing of analytical grade multi-walled carbon nano tube

powder (O.D. 10-15 nm, I.D. 2-6 nm, lenght 0.1-10 μm, > 90 % AS, MWCNT, Product of Arkema Inc.) and mineral oil in a mortar and pestle. The MWCNT powder mixed with mineral oil is shown in Image 3.8. In general, MWCNTs and mineral oil were mixed with a 60:40 ratio (m/m). Mineral oil was added a little more proportion when necessary to obtain paste consistence. MWCNT paste was placed in the corpus of the bare carbon paste electrode (BASi, MF-2012) using a spatula. The surface of the MWCNT paste was polished and smoothed with spatula until it obtained a shinning appearance.

Image 3.8. MWCNT powder mixed with mineral oil.

4. RESULTS AND DISCUSSION

4.1. Cyclic voltammetric Behavior of Dinobuton

Cyclic voltammetry (CV) gives an idea whether the species analysed could be determined electrochemically or not so that it is usually the first step in voltammetric studies. To obtain knowledge about electrochemical behavior of analyte provides to decide the continuity of the experiment. Cyclic voltammetry was performed at optimum conditions in the determination of dinobuton. The electrode reaction of dinobuton was characterized through CV method.

Cyclic voltammetric study was performed in $1.36x10^{-4}$ M dinobuton solution at pH 7 (BR buffer) on MWCNT electrode. Scan rates were changed from 10 mV/s to 80 mV/s, when all other parameters were kept constant. The potential window was + 1000 mV to -1200 mV in two segment so that CV parameters were arranged as follows.

Initial potential (mV): 1000
Switching potential (mV): -1200
Final potential (mV): 1000
Scan rate (mV/s): 10-20-40-60-80

Firstly, electrode reaction of dinobuton in cathodic direction exhibited a peak at -765 mV. In the reverse scan, no peak was observed, indicating that electrode reaction is irreversible. Cyclic voltammogram of $1.36x10^{-4}$ M dinobuton at scan rate 20 mV/s was shown in Figure 4.1. Then cyclic voltammograms of dinobuton at different scan rates were also recorded.

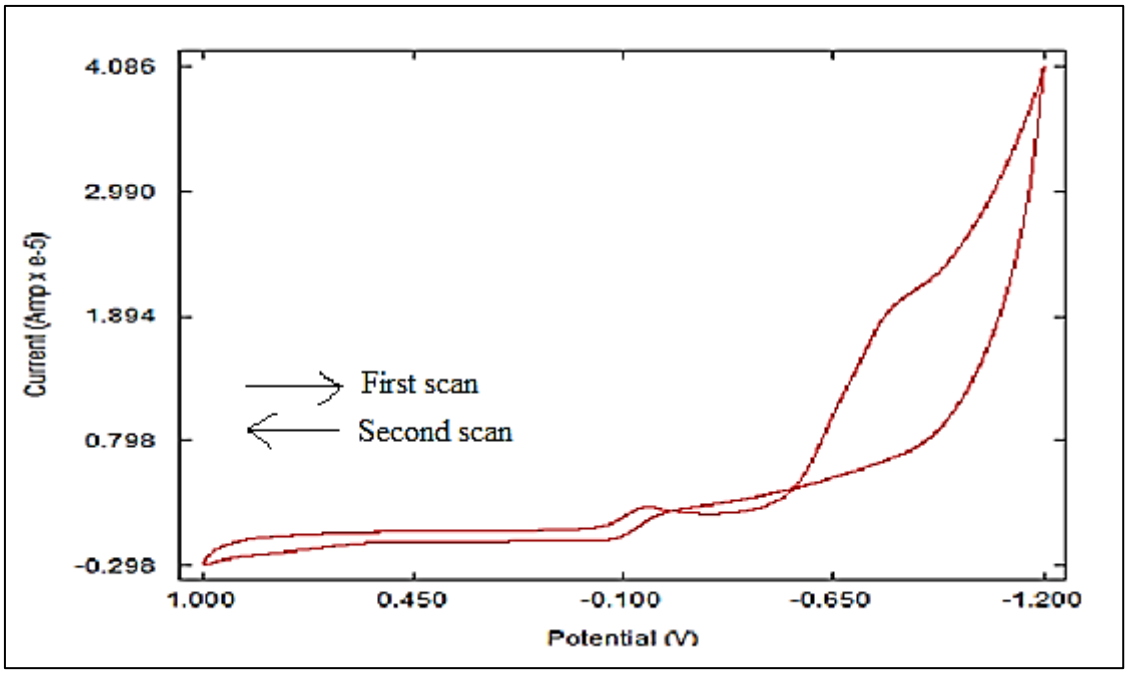

Figure 4.1. Cyclic voltammogram of dinobuton on MWCNTP electrode (at pH 7; $1.36x10^{-4}$ M dinobuton; scan rate:20 mVs^{-1})

The observation of a single peak in the negative scan and no peak in the positive scan indicates the irreversibility of the reaction. Cyclic voltammetry is important to determine the reversibility of the reaction.

Then different scan rates were tried to determine whether the reaction is diffusion controlled or adsorption controlled (Laviron, Roullier and Degrand, 1980). Voltammograms were recorded from scan rate of 10 mVs^{-1} to 80 mVs^{-1}. The CV voltammograms of dinobuton at scan rates (mVs^{-1}) from 10 to 80 are shown in Figure 4.2. and peak currents (µA) and potentials (mV) at different scan rates from 10 mVs^{-1} to 80 mVs^{-1} are shown in Table 4.1. The *log (Ip)* vs *log(v)* graph shown in Figure 4.3. was drawn to determine whether electrode reaction is diffusion or adsorption controlled.

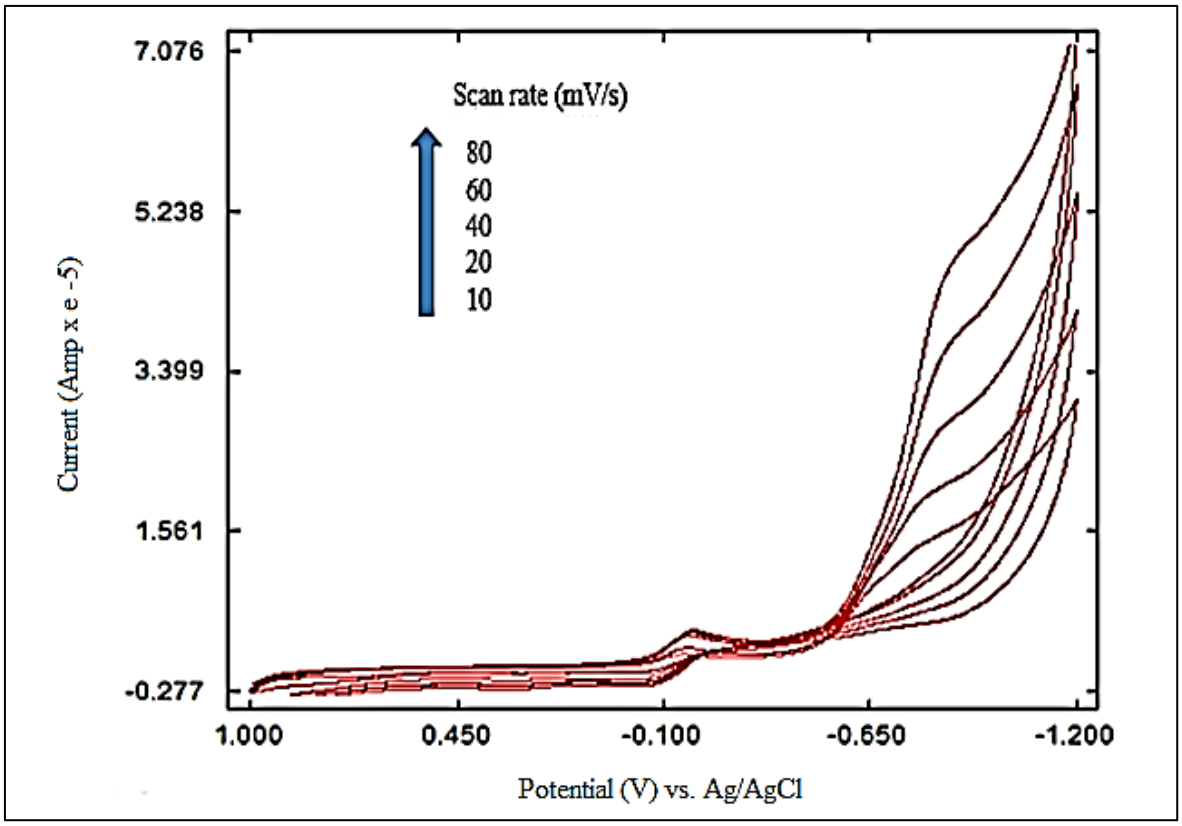

Figure 4.2. Cyclic voltammograms of dinobuton at different scan rates ($1.36x10^{-4}$ M dinobuton; pH 7 BR buffer solution; 10 mv/s to 80 mV/s)

Table 4.1. Effect of scan rate on peak currents and potentials in cyclic voltammetry.

Scan rate (mV/s)	Peak current (μA)	Peak potential (mV)
10	0.5005	-759
20	0.9400	-765
40	1.2726	-793
60	1.7212	-819
80	2.0262	-844

As shown in Table 4.1 when scan rate was increased, peak potential shifted to values that are more negative.

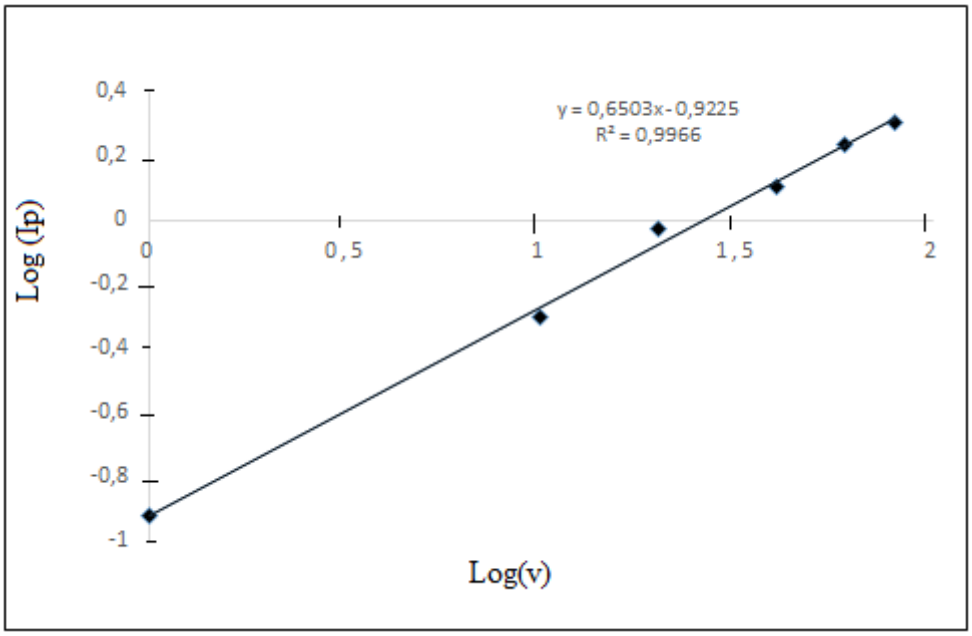

Figure 4.3. Log (*Ip*) versus Log(*ν*) graph for dinobuton in cyclic voltammetry ($1.36x10^{-4}$ M dinobuton).

The linear equation and slope obtained according to Figure 4.3 are given below.

$$\log Ip\ (\mu A) = 0.65 \log \nu\ (mV/s) - 0.92 \qquad (r=0.9966) \qquad (4.1)$$

Cyclic voltammetric experiments give an idea about the electrode reactions are diffusion or adsorption controlled. According the slope by the least squares line belonging to log (Ip) vs log (ν) graph, diffusion or adsorption controlled reactions could be determined. If the slope of log (Ip) vs log (ν) graph is nearly 0.5, the reaction is diffusion controlled, if the slope is nearly 1, the reaction is adsorption controlled (Laviron et al., 1980). The slope in the conducted study was found to be 0.65 and between 0.5 and 1.0. Therefore, electrode reaction is both diffusion and adsorption controlled or mixed controlled. Since it is close to 0.5, it can be said that the diffusion effect is more dominant than the adsorption effect for mass transfer.

According to peak currents (μA) at different scan rates (mV/s), peak current vs square root of scan rate and peak current *vs* scan rate graphs were drawn. I_p *vs* $\nu^{½}$ and I_p *vs* ν graphs are presented in Figure 4.4 and 4.5, respectively. A linear relationship was observed in both graphs.

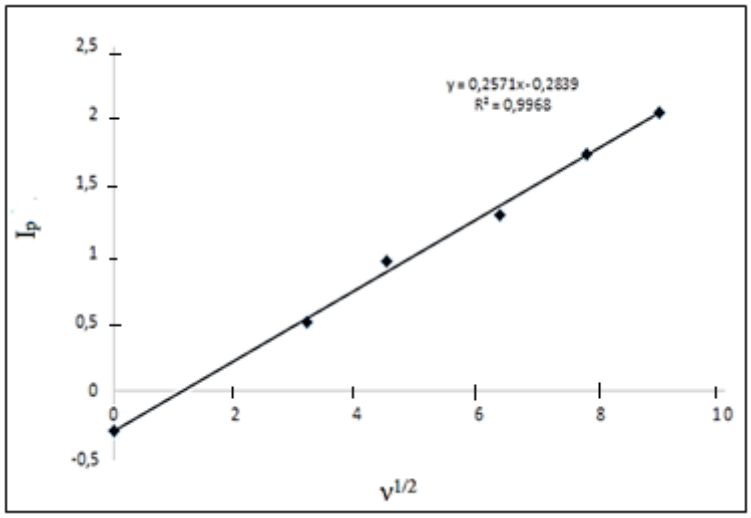

Figure 4.4. Peak current (μA) *vs* $\nu^{1/2}$ (mV/s) graph for dinobuton ($1.36x10^{-4}$ M dinobuton)

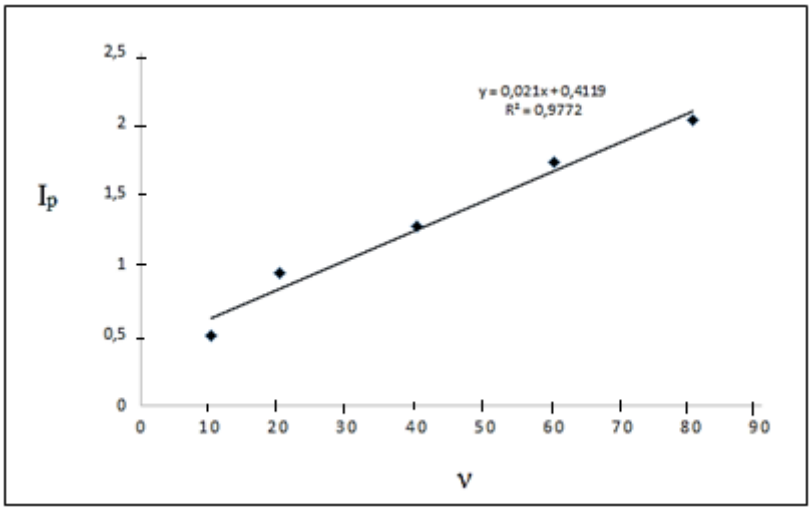

Figure 4.5. Ip (μA) *vs* ν (mV/s) graph for dinobuton ($1.36x10^{-4}$ M dinobuton)

4.2. Determination of Dinobuton Pesticide by SWV

Dinobuton pesticide was initially analyzed on the MWCNT electrode using SWS voltametry with random parameters in pH 2 BR buffer solution. Potential scan was applied between 1000 mV and -1000 mV in both oxidation and reduction directions. The potential range was kept in a broad range to increase the possibility of catching peak. Fortunately, the voltammetric peak was observed at -750 mV in the reduction direction and conluded that dinotuon can be studied by square stripping voltammetry.

4.3. Optimization of Experimental and Instrumental Parameters

Instrumental parameters were changed at a time while others were kept constant and voltammetric response of dinobuton was recorded by SWSV on MWCNT electrode. Instrumental parameters optimized in SWSV are listed below:

- Deposition potential (mV)
- Initial potential (mV)
- Final potential (mV)
- Full scale (µA)
- Deposition time (s)
- Step potential (mV)
- Frequency (Hertz)
- Amplitude (mV)

A single and suitable cathodic peak for dinobuton determination was observed at -750 mV (*vs* Ag/AgCl). Since the optimum parameters have not been determined yet, the SWSV parameters were taken randomly at the beginning and then the parameters were tried to be determined according to the obtained cathodic peak.

4.3.1. Optimization of pH

The pH of the electrochemical reactions has high effect on the electrode reactions of electroactive species so that optimum pH values should be determined to get the best efficiencies. Electrode reactions usually give different current and potential response with changing pH values. For the voltammetric determination of 1.48×10^{-5} M dinobuton on the MWCNT electrode, SWSV voltammograms were recorded using different pH values between pH 1 and 12, and optimum pH was tried to be found according to the currents obtained.

Voltammograms were recorded in BR buffer solutions within the pH 2 to 12 using 0.1 M H_2SO_4 solution for pH 1. BR buffer solutions prepared by mixing 2.5 grams of boric acid (99.8%), 2.7 mL of acetic acid (100%) and 2.3 mL of phosphoric acid (85%) in 1 liter of distilled water has a pH of nearly 2. For a higher desired pH values, 2 M NaOH solution

was added to the original BR buffer solution drop by drop with pH control.

To prepare the dinobuton solution, 0.0049 grams of dinobuton were weighed on an analytical balance and dissolved in 10 mL of acetone. 100 µL of $1.50x10^{-3}$ M dinobuton stock solution was added to 10 mL of blank solutions at different pH in the voltammetric cell. The optimum pH value was tried to be determined with $1.48x10^{-5}$ M dinobuton and SWSV parameters were arranged randomly at the beginning. The instrumental parameters were initially kept constant and only the pH value was changed. In this case, the intensity of the peak currents became directly pH dependent, and the optimum pH value was determined as 7.0 when the resulting peak currents were plotted against pH. Square wave stripping (SWS) voltammograms of dinobuton solution at different pHs are shown in Figure 4.6 and their data are shown in Table 4.2. As the peak current changed with pH, the peak potentials also changed and the graph of the peak potential plotted against pH is shown in Figure 4.7. The negative shift of the peak potentials with increasing pH indicates the participation of protons in the electrode mechanism, thus leading us to the mechanism of electrode reaction. As approved from the slope of the linear graph in figure 4.7, the peak potential shift in the negative direction of 27.7 mV per unit pH.

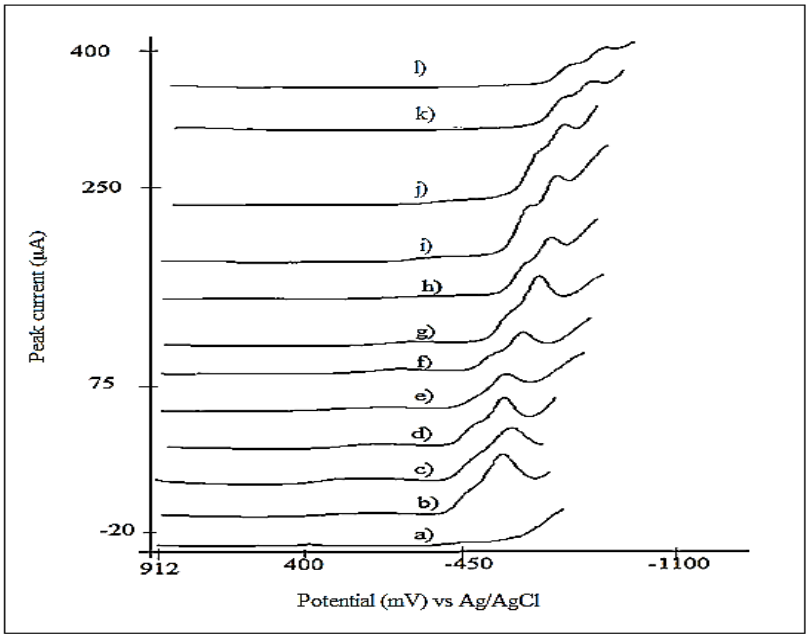

Figure 4.6. Effect of the pH's on the SWS voltammograms of dinobuton ($1.48x10^{-5}$ M dinobuton, pH 1 is H_2SO_4 and BR buffers from pH 2 to 12). a) pH 1, b) pH 2, c) pH 3, d) pH 4, e) pH 5, f) pH 6, g) pH 7, h) pH 8, i) pH 9, j) pH 10, k) pH 11, l) pH 12 (ΔE_s=5 mV, ΔE= 50 mV, *f*= 100 Hz., E_{acc}= 1000 mV, t_{acc}= 30 s

Table 4.2. Effect of pH on the peak potential of dinobuton in SWSV.

pH	Ep (mV)
1	-560
2	-585
3	-650
4	-650
5	-680
6	-700
7	-760
8	-785
9	-815
10	-825
11	-825
12	-865

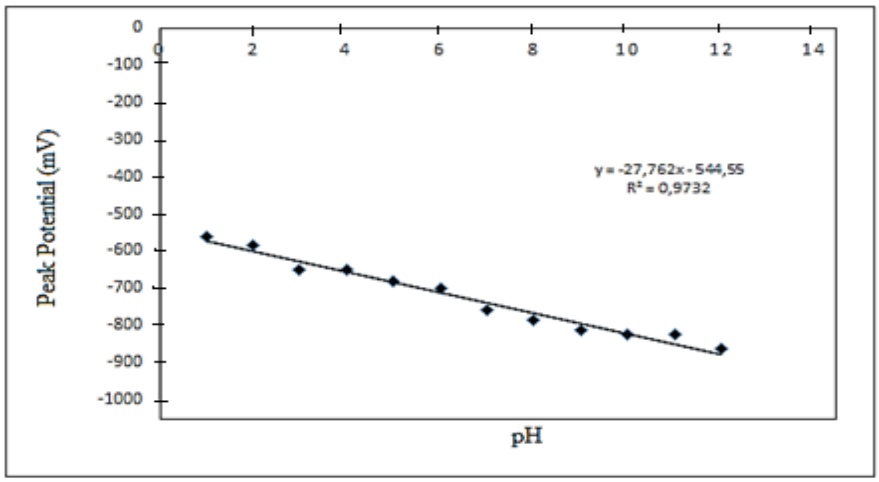

Figure 4.7. Peak potentials (mV) *versus* pH graph for dinobuton in SWSV ($1.48x10^{-5}$ M dinobuton).

The following equation with a slope of -27.8 mV/pH is derived from the linear graph of pH vs. peak potentials shown in Figure 4.7 above.

E_P (mV) = –27.8(pH) -544.5 $r^2 = 0.9732$ (4.2)

The resulting negative slope indicates that Ep shifts towards more negative potentials as pH increases. A linear relationship between pH and peak potential with a slope of -27.8 mV/pH indicates that H+ is involved in this electrode reaction. In other words, electron and H+ participation occur together in the reduction mechanism. In terms of the analytical use of these graphs, the maximum peak height for dinobuton in SWSV was observed at pH 7 with a peak potential of -760 mV, therefore, optimum pH 7 was chosen for further studies.

4.3.2. Optimization of step potential

0.0049 grams of dinobuton was weighted on analytical balance and dissolved in 10.0 mL of acetone so that $1.50x10^{-3}$ M of dinobuton stock solution was prepared. 100 µL of $1.50x10^{-3}$ M stock solution was added to the blank solution (10 ml of pH 7 BR buffer in voltammetric cell) and voltammograms were recorded at different step potentials (mV). Step potentials were optimized with $1.48x10^{-5}$ M dinobuton in 10 mL of pH 7 BR in the electrochemical cell. Different step potentials are applied from 1 mV to 10 mV in the following instrumental conditions.

Initial potential: 1000 mV
Final potential: -1100 mV
Deposition potential: 1000 mV
Full scale: 100 µA
Deposition time: 30 s
Quiet time: 5 s
Amplitude: 50 mV
Frequency: 100 Hertz

Effect of step potentials on the peak currents and potentials are summarized in Table 4.3. The graph of step potential versus peak currents are shown in Figure 4.8. The SWS voltammograms of $1.48x10^{-5}$ M dinobuton in pH 7 BR buffer at different step potentials (mV) are shown Figure 4.9.

Table 4.3. Effect of step potentials on peak currents and potentials.

Step potential (mV)	Peak current (mA)	Peak potential (mV)
1	Undefined peak	Undefined peak
2	0.0095	-728
3	0.0057	-728
4	0.0145	-756
5	0.0327	-755
6	0.0241	-824
8	0.0234	-760
9	0.0140	-773
10	0.0151	-780

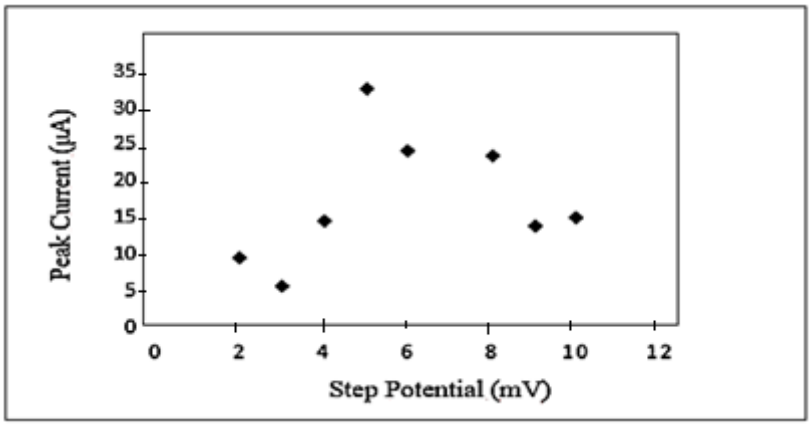

Figure 4.8. Peak currents (µA) versus step potentials (mV) (ΔE= 50 mV, *f*= 100 Hz., E_{acc}= 1000 mV, t_{acc}= 30 s).

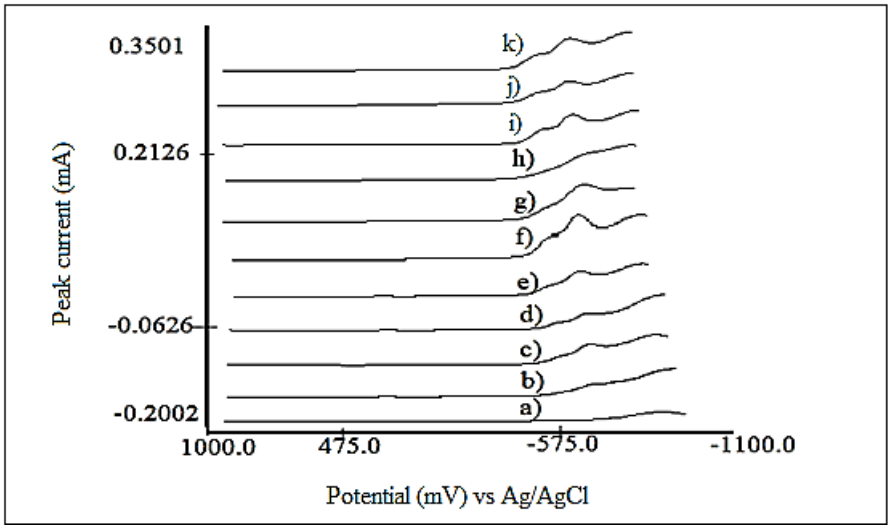

Figure 4.9. Effect of the step potentials on the square wave stripping voltammograms of dinobuton (mV) .a) blank, b) 1 mV, c) 2 mV, d) 3 mV, e) 4 mV, f) 5 mV, g) 6 mV, h) 7 mV, i) 8 mV, j) 9 mV, k) 10 mV. ($1.48x10^{-5}$ M dinobuton in pH 7 BRB solution; ΔE= 50 mV, *f*= 100 Hz., E_{acc}= 1000 mV, t_{acc}= 30 s)

4.3.3. Optimization of frequency

First, 0.0049 grams of dinobuton were weighed on an analytical balance and dissolved in 10 mL of acetone to prepare $1.50x10^{-3}$ M dinobuton stock solution. 100 µL of stock solution was added to the blank solution (pH 7 BR) and peak currents were measured at different frequencies (Hertz). Using the step potential (5 mV) parameter optimized in section 4.3.2, peak current measurements at different frequencies were recorded by fixing other instrumental parameters summarized below.

Initial potential: 1000 mV

Final potential: -1100 mV

Deposition potential: 1000 mV

Full scale: 1 mA

Deposition time: 30 s

Quiet time: 5 s

Step potential: 5 mV

Amplitude: 50 mV

Peak currents (μA) and peak potentials were obtained by recording SWS voltammograms with every 10 hertz increment between 10 and 100 Hertz in pH 7 BR buffer solution of $1.48x10^{-5}$ M dinobuton, and the data (mV) are presented in Table 4.4. The graph of the peak currents (μA) obtained against the applied frequency (Hertz) is presented in Figure 4.10.

Table 4.4. Effect of frequency on peak currents and potentials.

Frequency (Hertz)	Peak current (μA)	Peak potential (mV)
10	5.6	-695
20	19.6	-710
30	26	-690
40	17.5	-745
50	22.9	-710
60	19.2	-720
70	21.7	-710
80	18	-710
90	Undefined peak	Undefined peak
100	12.9	-755

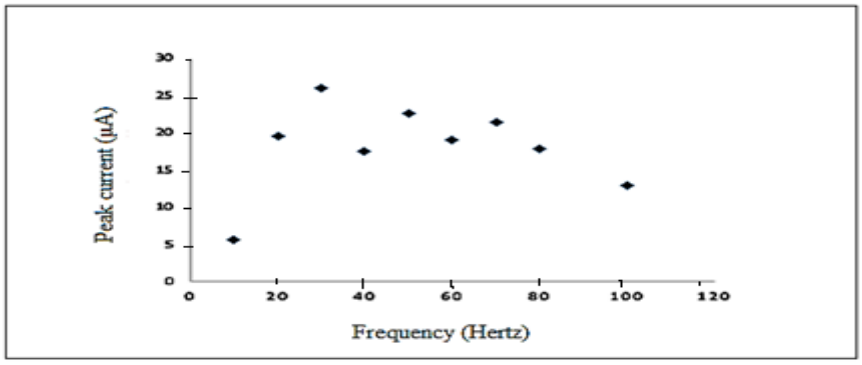

Figure 4.10. Peak current (μA) versus frequency (Hertz) of dinobuton in SWSV. ($1.50x10^{-3}$ M dinobuton; pH 7; ΔE_s=5 mV, ΔE= 50 mV, E_{acc}= 1000 mV, t_{acc}= 30 s)

In the frequency (*f*) versus peak current (μA) study, the maximum peak current was observed as 30 Hertz. At a frequency of 30 Hertz, at which the maximum peak current was obtained, the peak shape was quite smooth and was therefore used as the optimum frequency in further studies. Square wave stripping voltammograms of $1.48x10^{-5}$ M dinobuton in pH 7 BR buffer solution at different frequency are shown in Figure 4.11.

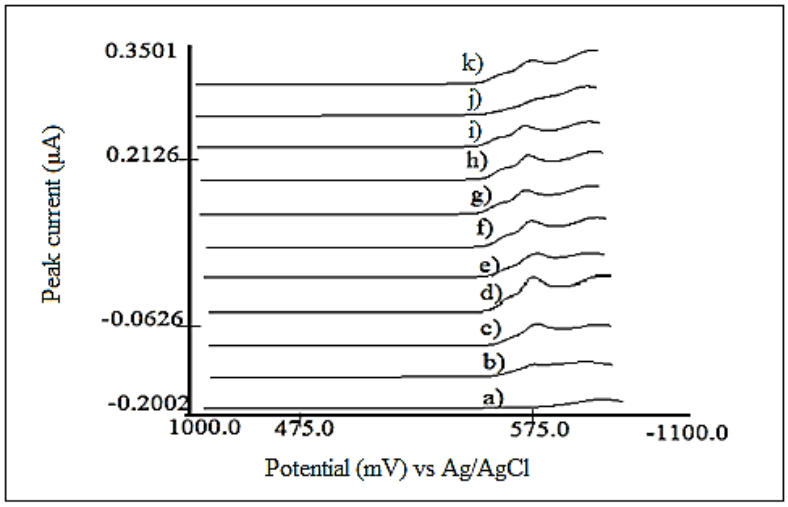

Figure 4.11. Square wave stripping voltammograms of dinobuton at different frequencies (Hertz). a) blank (10 mL pH 7 BR solution), b) 10 Hz, c) 20 Hz, d) 30 Hz, e) 40 Hz, f) 50 Hz, g) 60 Hz, h) 70 Hz, i) 80 Hz, j) 90 Hz, k) 100 Hz. ($1.48x10^{-5}$ M dinobuton; ΔE_s= 5 mV, ΔE: 50 mV, E_{acc}= 1000 mV, t_{acc}= 30 s) in pH 7 BRB solution.

4.3.4. Optimization of amplitude

Firstly, 0.0049 grams of dinobuton was weighted in analytical balance and dissolved in 10 mL of acetone so that $1.50x10^{-3}$ M of dinobuton stock solution was prepared. 100 μL stock solution was added to the blank solution (10 mL of pH 7.0 BR) for each measurement at different amplitudes (mV). The step potential (5 mV) and frequency (30 Hz) parameters optimized previously were used and other instrumental parameters fixed were:

Initial potential: 1000 mV

Final potential: -1100 mV

Deposition potential: 1000 mV

Full scale: 1 mA

Deposition time: 30 s

Quiet time: 5 s

Step potential: 5 mV

Frequency: 30 Hertz

In this study, voltammograms with different amplitudes between 10 mV and 100 mV were recorded and SWS voltammograms of dinobuton with different amplitudes were presented in Figure 4.12. Experimental data on the effect of amplitude on peak current and potentials are summarized in Table 4.5.

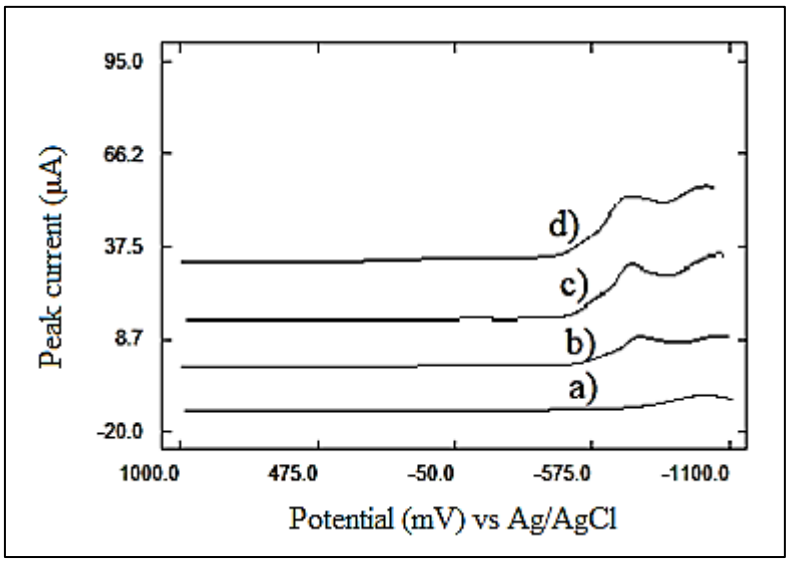

Figure 4.12. Square wave stripping voltammograms voltammograms of dinobuton at different amplitudes a) blank (10 mL pH 7 BR solution), b) 10 mV, c) 20 mV, d) 30 mV. ($1.48x10^{-5}$ M dinobuton ; ΔE_s= 5 mV, *f*= 30 Hz., E_{acc}= 1000 mV, t_{acc}= 30 s)

Table 4.5. Effect of amplitude on peak current and potentials of dinobuton in SWSV.

Amplitude (mV)	Peak current (µA)	Peak potential (mV)
10	3.1189	-760
20	5.2644	-745
30	5.1575	-770

4.3.5. Optimization of deposition time

Before examining the effect of accumulation time, 0.0049 grams of dinobuton was weighed on an analytical balance and dissolved in 10 mL of acetone to prepare a $1.50x10^{-3}$ M dinobuton stock solution. After that, 100 µL of stock solution was added to the blank solution of 10 mL of pH 7 BR and voltammograms were recorded at different accumulation times(s). Since step potential, frequency and amplitude parameters were previously optimized as (5 mV), (30 Hertz) and (20 mV), respectively, these values were used for optimization of the deposition time. All other instrumental parameters used are summarized below:

Initial potential: 1000 mV
Final potential: -1100 mV
Deposition potential: 1000 mV
Full scale: 1 ųA
Quiet time: 5 s
Step potential: 5 mV
Amplitude:20 mV
Frequency: 30 Hertz

Peak currents (µA) and potentials (mV) recorded at different deposition times (s) are summarized in Table 4.6. The peak current (µA) versus deposition time (s) is shown in Figure 4.13. Square wave stripping voltammograms of $1.48x10^{-5}$ M dinobuton at different deposition times are presented in Figure 4.14 and accordingly the deposition time was chosen as 50 s because of the highest and sensitive analytical response.

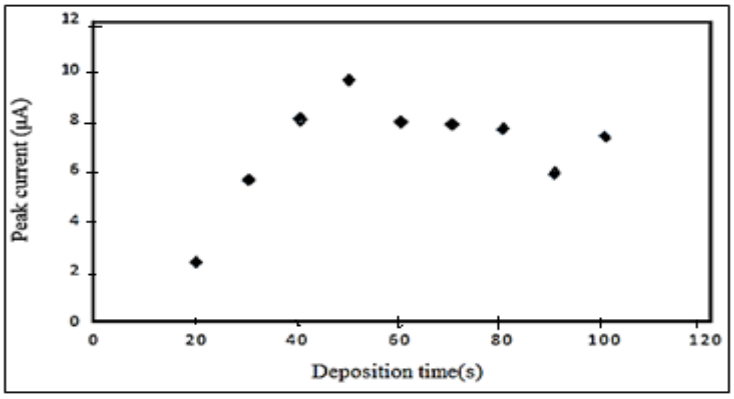

Figure 4.13. Peak current (µA) versus deposition time (s). (pH 7 and $1.50x10^{-3}$ M dinobuton ; ΔE_s= 5 mV, *f*= 30 Hz., ΔE= 20 mV, E_{acc}= 1000 mV)

Table 4.6. Effect of deposition time on peak current and potentials.

Deposition time (s)	Peak current (µA)	Peak potential (mV)
10	Undefined peak	Undefined peak
20	2.3407	-750
30	5.5787	-755
40	8.0812	-760
50	9.6071	-765
60	7.9530	-790
70	7.8676	-790
80	7.6143	-800
90	5.8473	-810
100	7.3945	-805

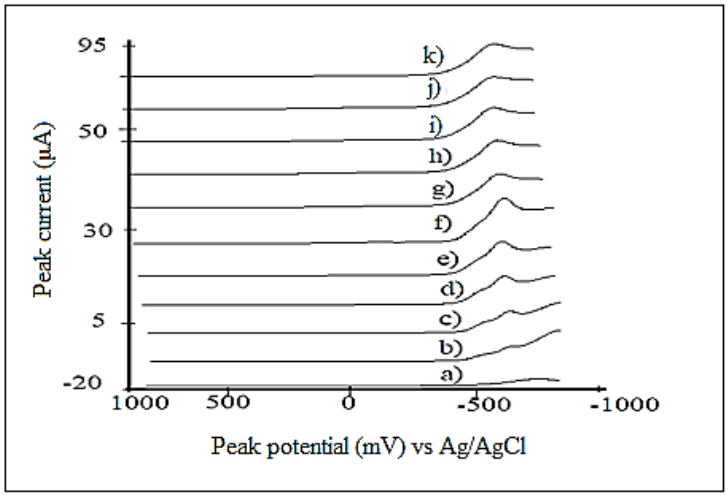

Figure 4.14. SWS voltammograms of dinobuton at different deposition times(s). a) blank (10 mL of pH 7 BR), b) 10 s, c) 20 s, d) 30 s, e) 40 s, f) 50 s, g) 60 s, h) 70 s, i) 80 s, j) 90 s, k) 100 s. ($1.48x10^{-5}$ M dinobuton ; ΔE_s= 5 mV, *f*= 30 Hz., ΔE= 20 mV, E_{acc}= 1000 mV)

4.3.6. Optimization of deposition potential

First, 0.0049 grams of dinobuton were weighed on an analytical balance, and $1.50x10^{-3}$ M dinobuton stock solution was prepared by dissolving in 10 mL of acetone. 100 µL of stock solution was added to blank solution (10 mL of pH 7 BR) for each measurement at different deposition potentials (mV). Because step potential, frequency, amplitude and deposition time were optimized as 5 mV, 30 Hertz, 20 mV and 50 s, respectively, only deposition potential was changed by just keeping other parameters constant. Effect of deposition potential (mV) on peak currents (µA) and peak potentials (mV) are presented in Table 4.7. The peak currents versus deposition potentials are shown in Figure 4.15. SWS voltammograms of $1.48x10^{-5}$ M dinobuton at different deposition potentials are presented in Figure 4.16. For the analytical determination of dinobuton, the deposition potential was chosen as -500 mV due to the most sensitive and smooth peak shape.

Table 4.7. Effect of deposition potentials on peak currents and potentials.

Deposition potential (mV)	Peak current (µA)	Peak potential (mV)
-500	6.7231	-750
-300	6.0029	-755
-100	4.6265	-760
0	4.3305	-760
100	3.9521	-765
300	3.3814	-765
500	2.7161	-765

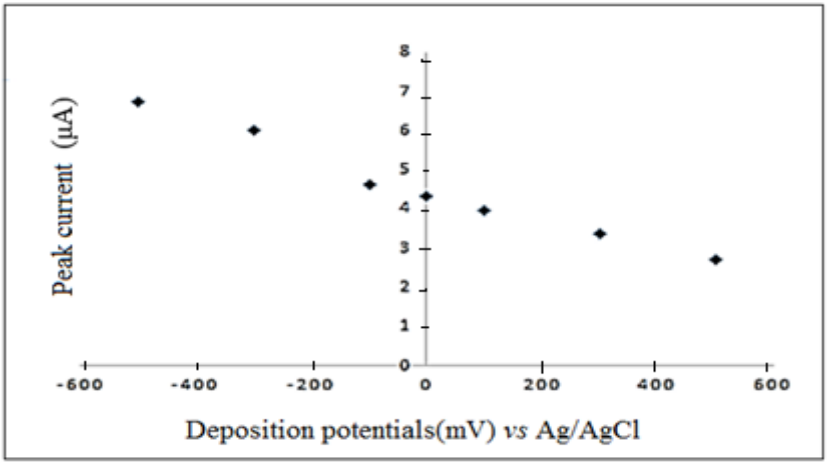

Figure 4.15. A graph of peak current (µA) versus deposition potentials (mV) in SWSV. ($1.50x10^{-5}$ M dinobuton, pH 7 BR ; ΔE_s= 5 mV, *f*= 30 Hz., ΔE= 20 mV, t_{acc}= 50 s)

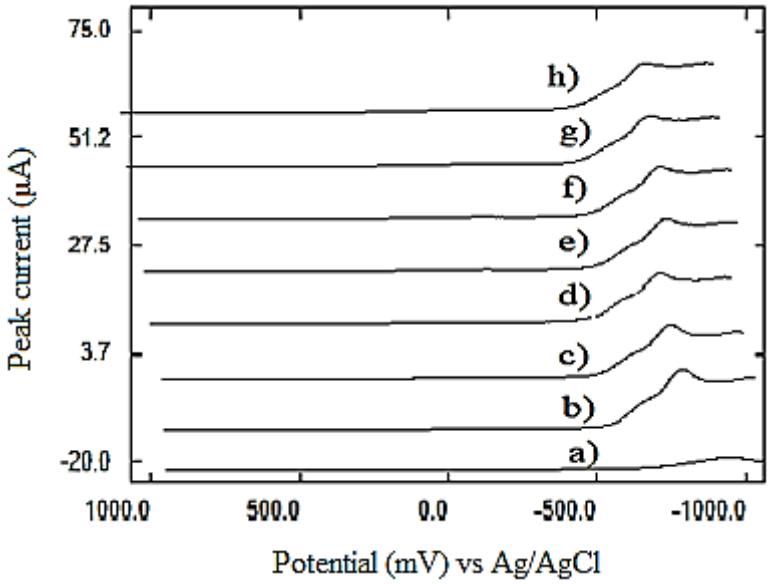

Figure 4.16. SWS voltammograms of dinobuton at different deposition potentials (mV). a) blank (10 mL of pH 7 BR), b) -500 mV, c) -300 mV, d) -100 mV, e) 0 mV, f) 100 mV, g) 300 mV, h) 500 mV. ($1.48x10^{-5}$ M dinobuton ; pH 7; ΔE_s= 5 mV, *f*= 30 Hz, ΔE= 20 mV, t_{acc}= 50 s)

At the end of all these experiments for the optimization of instrumental parameters for dinobuton determination in SWS voltammetry, step potential, frequency, amplitude, deposition time and deposition potential parameters were optimized. All optimum parameters are summarized in Table 4.8.

Table 4.8. Optimum parameters for determinaton of dinobuton by SWSV.

Optimum Parameters	
Supporting electrolyte pH	7.0
Step potential (mV)	5
Frequency (Hertz)	30
Amplitude (mV)	20
Deposition time (s)	50
Deposition potential (mV)	–500

4.4. Construction of Calibration Graph

Drawing the calibration graph is a fundamental step in establishing an analytical method, and for this purpose, standard additions were made from the dinobuton stock solution to 10 mL of pH 7 buffer in the voltammetric cell and the corresponding analytical signals were recorded. The least squares regression method was used to obtain the calibration parameters.

Calibration

The linear calibration plot is used to determine the relationship between the analytical concentration and the corresponding signal response. Before determining the concentration of unknown samples, analytical signals of known samples were recorded and compared with unknown samples using the calibration graph obtained accordingly. (Skoog et al., 2004; 192). A linear calibration curve is often difficult to obtain because analytical signals do not increase in exact proportion with increasing concentrations. Therefore, the least squares method is used to obtain the best line closest to linearity.

Calibration method

There are several steps in calibration process:

1. Preparation of sample
2. Preparation of standart solutions
3. Measurement of signals of sample and standart solutions
4. Plotting of calibration graph
5. Comparing signals of sample which has unknown concentration and samples which have known concentrations. (Kościelniak, Wieczorek, Kozak and Herman, 2011)

Kościelniak et al. (2003) suggested that calibration methods could be divided into three main sections:

1. The conventional method (calibration curve method or external method)
2. Indirect method
3. Internal standart method

In the indirect method, the signal of the analyte is not measured directly, but the signal of the reagent reacting with the analyte. This method is used when the analysis signal cannot be measured directly.This reagent is added to the sample and standard solutions, the signals are recorded, and the calibration graph is drawn. The variation in the sample is determined according to the calibration graph equation. After determining the reagent concentration in the sample, the analyte concentration is determined indirectly. In the internal standard

method, an internal standard with the same physicochemical properties as the analyte is added to the sample and standard solutions, a calibration graph is drawn depending on its concentration, and the signals are recorded. The analyte concentration in the sample could be determined using calibration graph constructred with the signals measured from the ratio of standard and internal standard solutions (Kościelniak et al., 2011).

4.4.1. Linear calibration plot for dinobuton

In this study, the traditional method from the calibration methods was used and the calibration graph of the dinobuton with SWSV was drawn, ignoring the dilution factor, and the increasing amounts of dinobuton concentrations were plotted against the peak currents. For this purpose, $1.50x10^{-3}$ M dinobuton stock solution was prepared by first weighing 0.0049 grams of dinobuton on an analytical balance and dissolving it in 10.0 mL of acetone. Standard additions of 25 µL of this stock solution were made to the voltammetric cell (10 mL of pH 7 BR buffer). Recorded peak currents (µA) for different concentrations of dinobuton solutions are shown in Table 4.9. Peak current heights (µA) from 3.74 µM to 25.8 µM were plotted in Excel Software 2016 and calibration graph of the dinobutton is presented in Figure 4.17. SWS voltammograms for the linear calibration curve of dinobuton in pH 7 BR buffer solution are shown in Figure 4.18.

Table 4.9. Peak currents obtained from dinobuton calibration.

Dinobuton concentration (µM)	Peak currents (µA)
3.74	2.13±0.25
7.46	4.4±0.46
11.16	7.37±0.15
14.85	9.73±0.57
18.52	12.93±0.49
22.17	15.7±0.3
25.80	17.7±0.61

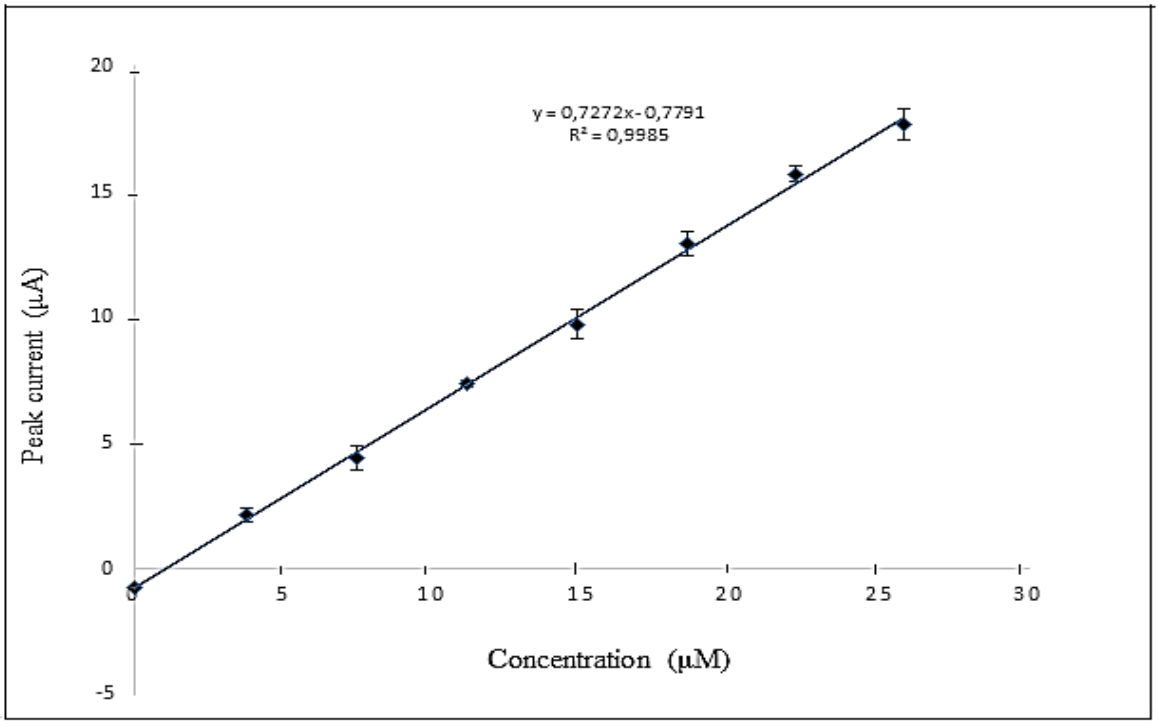

Figure 4.17. Calibration graph of dinobuton by SWSV on MWCNT electrode. Vertical bars show standart deviations (n=3) of peak currents (µA). (pH 7 BR buffer; ΔE_s: 5 mV, f: 30 hertz, ΔE: 20 mV, t_{acc}: 50 s, E_{acc}: -500 mV).

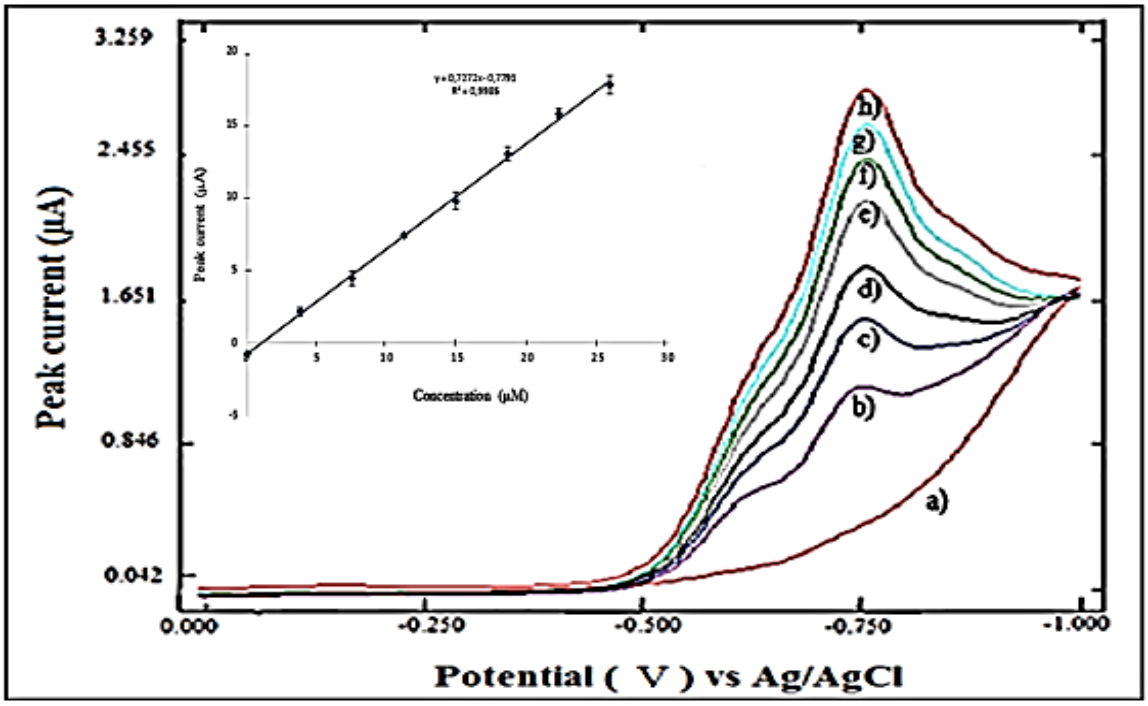

Figure 4.18. SWS voltammograms for linear calibration curve of dinobuton (a)blank-10 mL pH 7 BR buffer, b) 3.74 µM, c) 7.46 µM, d) 11.16 µM, e) 14.85µM, f) 18.52 µM, g)22.17 µM, h)25.8 µM). (pH 7 BR buffer solution, ΔEs: 5 mV, f: 30 hertz, ΔE: 20 mV, tacc: 50 s, Eacc: -500 mV).

4.4.2. Least squares method for dinobutton calibration.

The linear increase in Figure 4.17 is plotted using the least squares method in Excel. All points are expected to lie on this line, but not always possible due to undetected errors. The regression analysis to obtain this line is based on the least squares method for two-dimensional data.

As shown in Figure 4.17, each point has vertical deviation from its linear line and these vertical errors are called deviation. The line found by the least squares method gives the minimum value when all the squares of the deviations are added up. Slope and standard deviation values are calculated from here (Skoog et al., 2004; 196).

The use of the Least Squares Method in Excel is described in the book "The Fundamentals of Analytical Chemistry" (Skoog et al. (2004)). The Least Squares Method was applied in Excel after the calibration graph was drawn and the parameters of the calibration curve were calculated using Excel 2016 software. Least squares analysis could be done simply in Excel, using basic functions and regression data analysis (Skoog et al., 2004; 204).

In least squares analysis, several steps could be applied simultaneously with the point function. For this, an area of two cells wide and five cells high was selected, then "Add function" (fx) was used. The point is then selected and known x and y values are entered. Enter "True" in the box with the fixed label, click F2+ctrl+shift+enter at the same time, the numbers are displayed in the selected cells. The amounts found by the point function (dot function) are shown in Table 4.10 (Skoog et al., 2004; 204, 205).

Table 4.10. Quantities found by dot function(Skoog et al., 2004; 204, 205)

Slope	starting ordinate (cut-off point)
standart deviation of slope	standart deviation of starting ordinate
R^2 (coefficient of determination)	s_r (standart deviation of regression)
F	degree of freedom relation to error
sum of squares of regression	sum of squares of deviations

As shown in Table 4.9, peak current height increases as concentration of dinobuton increases and a linear increase is observed in peak current from 3.74 µM to 25.8 µM. Therefore, the concentrations providing linearity were taken into consideration and calibration study shows

us dinobuton can certainly be determined by SWSV on MWCNT electrode within 3.74 µM or 25.8 µM.

According to calibration graph of dinobuton shown in Figure 4.17, the equation of the linear line was:

I_p (μA) = (0.73 ± 0.01) C (μA/µM) – (0.78 ± 0.18) r = 0.9985 (4.3)

A regression coefficient close to 1 means that this graph has good linearity. According to the linear curve, some parameters were found, for example, LOD and LOQ values were determined. The positive and negative standard deviations of the peak currents were added to the resulting graph.

The point function was used in least squares analysis to determine the slope and standard deviation of the cutoff point. The standard deviation of the slope and cutoff point (The slope and standart deviation of cut off point) is used to determine the LOD and LOQ, and the LOD and LOQ values are calculated as follows:

$$\text{LOD}= \frac{3s}{m} \quad \text{and} \quad \text{LOQ}= \frac{10s}{m}$$

The *s* and *m* in the equation are standart deviation of cut-off point and slope of the calibration line, respectively.

LOD and LOQ values were calculated using the cutoff point and the standard deviation of the slope (slope and the standart deviation of the cut-off point) and accordingly, the values found with the point function in the Least Squares Method analysis with Excel 2016 software are as follows:

Slope, *s* = 0.727 µA/µM
Standard deviation of the cutoff point, *s*= 0.177 µA

The LOD and LOQ found with the point function using the least squares method are calculated as follows:

LOD= $\frac{3x0.1768\mu A}{0.7272\mu A/\ \mu M}$ =0.73 µM

and

LOQ= $\frac{10x0.1768\mu A}{0.7272\mu A/\ \mu M}$ =2.43 µM

The linear working range determined from 3.74 µM to 25.8 µM means that dinobuton could be determined within the concentration of 3.74 µM to 25.8 µM by SWS voltammetric technique under the stated conditions. Parameters obtained by dinobuton calibration graph with SWSV in pH 7 BR buffer solution are summarized in Table 4.11.

Table 4.11. Parameters obtained by dinobuton calibration graph

Parameters (Units)	Values
Peak potential (mV)	− 760
Slope (µA/µM)	0.73 ± 0.01
Cut-off point (µA)	− 0.78 ± 0.18
Correlation coefficient	0.9985
Limit of detection (µM)	0.73
Limit of quantification (µM)	2.43
Linear operating range (µM)	3.74 − 25.8
Repeability of peak current (RSD%)	4.31
Repeability of peak potential (RSD%)	1.15

N = 3; RSD % = $\frac{s}{\bar{x}}$ x100

Least Squares Method was described as "The best trendline as statistically can be provided from the minimum value of sum of squares of the deviations from the line (Christian, Dasgupta and Schug, 2021; 100). "There is a changing *x* value and accordingly a changing *y*. The *y* values are obtained according to the concentrations. Accordingly, how to find the slope of the least squares line is shown as follows:

$$m= \frac{\sum x_i\, y_i - [(\sum x_i \sum y_i)/n]}{\sum {x_i}^2 - [(\sum x_i)^2/n]} \quad (4.4)$$

It is shown how to prepare a linear graph with the least squares method, and accordingly, a cut-off point is obtained from the equation determined by the least squares method. Therefore, the cut-off point of the calibration graph of dinobuton determination with SWSV was taken as 0 and -0.78. The values obtained from the calibration graph that will be used to calculate LOD and LOQ values are shown in Table 4.12.

The following formulas are given to calculate the standard deviation of the cut-off point, accordingly standard deviation of the y-axis Sy

$$S_y = \sqrt{\frac{[\sum y_i{}^2 - (\sum y_i)^2/\mathrm{N}] - m^2[\sum x_i{}^2 - (\sum x_i)^2/\mathrm{N}]}{N-2}} \quad (4.5)$$

Standart deviation of cut-off point, S_b is

$$S_b = S_y \sqrt{\frac{1}{\mathrm{N} - (\sum x_i)^2/\sum x_i{}^2}} \quad (4.6)$$

Table 4.12. Data obtained from the calibration graph of dinobuton.

x (μM)	x^2	*y (μA)*	y^2	*x·y*
0	0	-0.78	0.6084	0
3.74	13.9876	2.13	4.5369	7.9662
7.46	55.6516	4.4	19.36	32.824
11.16	124.5456	7.37	54.3169	82.2492
14.85	220.5225	9.73	94.6729	144.4905
18.52	342.9904	12.93	167.1849	239.4636
22.17	491.5089	15.7	246.49	348.069
25.8	665.64	17.7	313.29	456.66

$\overline{x}$=12.9625

$\overline{y}$ =8.6475

The parts in the above formulas (Equal 4.5 and 4.6) are calculated according to the x, y values as follows:

$\sum x_i = 103.7$

$\sum x_i^2 = 1914.8466$

$(\sum x_i)^2 = 10753.69$

$\sum y_i = 69.18$

$\sum y_i^2 = 900.46$

$(\sum y_i)^2 = 4785.8724$

$\sum x_i.y_i = 1311.7225$

According to the least squares method, the slope was 0.7272, S_y was 0.28, and S_b was 0.18 accordingly. Since LOD and LOQ were $3S_b/m$ and $10S_b/m$, respectively, LOD and LOQ were determined as 0.74 and 2.47 µM, respectively, using these formulas. Previously, LOD and LOQ had calculated as 0.73 and 2.43 µM, respectively, by Excel 2016 software with point function in Least Squares Method analysis.

4.5. Interference Study in the Presence of co-existing Species

Voltammetric determination of dinobuton pesticide was carried out in the presence of different pesticides, that is, in the presence of species that may interfere. Some interfering pesticides at different concentrations were added to the dinobuton solution and voltammograms were recorded using the optimized parameters, and the currents of the peaks were measured in each application. Percent recoveries were calculated by dividing the dinobuton peak current obtained when dinobuton and interfering species were together in the same solution to that peak current recorded in the presence of only dinobuton. In calculations, 10% variation was accepted as the tolerance limit. The interference studies were carried out by taking the "dinobuton/interference pesticide" ratios at 1:1, 1:5 and 1:10 mole ratios. Pesticides used to investigate whether dinobuton can be detected in matrix medium, ie pesticides tested for dinobuton determination will be discussed in the following sections as given below.

4.5.1. Triasulfuron

Triasulfuron, a sulfonylurea herbicide, is mainly used to control broadleaf weeds in wheat and rye production. 0.0052 grams of dinobuton was weighted precisely and dissolved in 10 mL of acetone to prepare $1.59x10^{-3}$ M dinobuton stock solution. 0.0062 grams of

triasulfuron (M_{wt}: 401.82 g/mol) was weighted precisely using analytical balance and dissolved in 10 mL of acetone to prepare $1.54x10^{-3}$ M stock solution. Triasulfuron is more likely to dissolve in acetone compared to water and other organic solvents such as *n*-hexane, toluene and ethyl acetate. The molecular structure of triasulfuron has been shown below.

For the interference study, 200µL of dinobuton stock solution was transferred to 10.0 mL pH 7 BR buffer solution in the voltammetric cell and SWS voltammograms were recorded in the presence of dinobuton only. Then, interference study was performed by adding triasulfuron (1:1, in mol-molar) and (1:5, in mol-molar) to the cell under the same experimental conditions. Dinobuton and dinobuton-triasulfuron peaks were superimposed on the same graph to facilitate comparison. These voltammograms are shown in Figures 4.19. and 4.20. and recovery data on dinobuton determination in the presence of triasulfuron are given in Table 4.13.

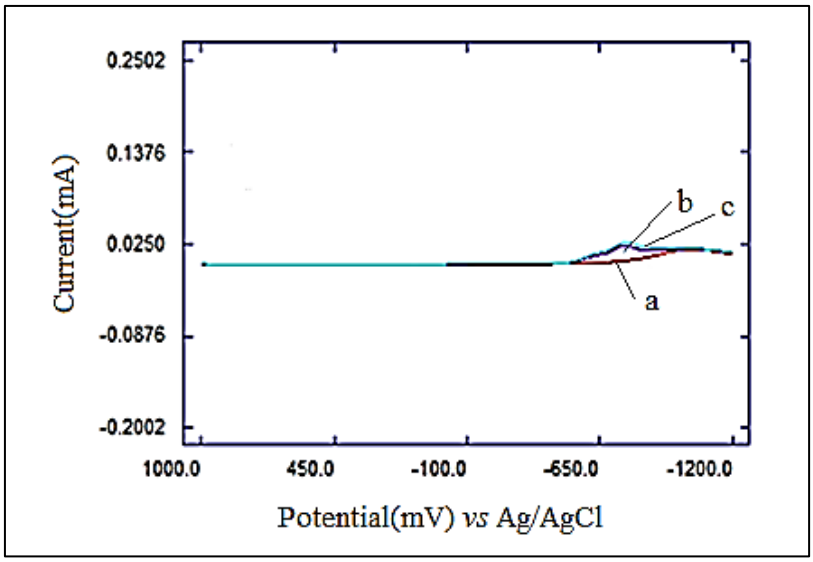

Figure 4.19. SWS voltammogram of dinobuton with triasulfuron at 1:1 mole ratio a) blank (10 mL pH 7 BR buffer), b) $3.12x10^{-5}$ M dinobuton, c) $3.06x10^{-5}$ M dinobuton-$2.96x10^{-5}$ M triasulfuron solutions (pH 7, ΔE_s: 5 mV, *f*: 30 hertz, ΔE: 20 mV, t_{acc}: 50 s, E_{acc}: -500 mV).

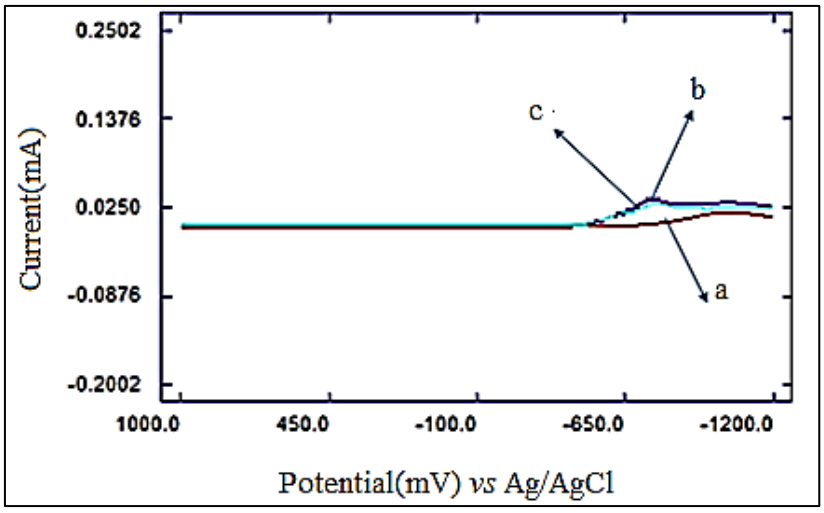

Figure 4.20. SWS voltammogram of dinobuton with triasulfuron at 1:5 mole ratio a) blank (10 mL pH 7 BR buffer), b) $3.12x10^{-5}$ M dinobuton, c) $2.84x10^{-5}$ M dinobuton-$1.37x10^{-4}$ M triasulfuron solutions (pH 7, ΔE_s: 5 mV, f: 30 hertz, ΔE: 20 mV, t_{acc}: 50 s, E_{acc} : -500 mV).

Table 4.13. Interferring effect of triasulfuron and % recoveries*

Mole to mole	Dinobuton (M)	Triasulfuron(M)	Recovery % $\bar{x}$ ±s	Relative error %
1:1	$3.06x10^{-5}$	$2.96x10^{-5}$	102.69±1.99	+2.69
1:5	$2.84x10^{-5}$	$1.37x10^{-4}$	93.39±2.51	-6.61

**n=3*

The percent recovery was calculated by simply taking the ratio of the dinobuton's peak current (μA) to that in the presence of triasulfuron. (The percent recovery was calculated by simply taking the ratio of the dinobuton's peak current in the presence of triasulfuron and to that without triasulfuron).

4.5.2. Azinphos-methyl

Azinphos-methyl, an organophosphate insecticide, was first registered in 1959 and is widely used in agriculture. It provides significant pest control specially to fruit, nut and other crop growers. 0.0050 g dinobuton was weighed on an analytical balance and dissolved in 10.0 mL acetone to prepare $1.53x10^{-3}$ M dinobuton stock solution. 0.0049 grams of azinphos-methyl was accurately weighed using an analytical balance and dissolved in 10 mL of acetone to prepare a stock solution of $1.54x10^{-3}$ M azinphos-methyl (Mwt: 317.324 g/mol). Azinphos-methyl is readily soluble in ethyl acetate and acetone, but

since acetone was used for dinobuton, it was also used for azinphos-methyl to ensure compatibility.

For interference study, 100 µL dinobuton stock solution was transferred to the voltammetric cell including 10.0 mL of BR buffer solution at pH 7 then SWS voltammogram was recorded. Interference study with azinphos-methyl (1:1, mole to mole; 1:5, mole to mole and 1:10, mole to mole) was repeated under the same experimental conditions. Dinobuton and dinobuton-azinphos methyl peaks were overlapped on the same graph to facilitate comparison. These voltammograms of dinobuton in the presence of azinphos-methyl are shown in Figures 4.21, 4.22 and 4.23. The recovery data on dinobuton determination in the presence of triasulfuron are given in Table 4.14.

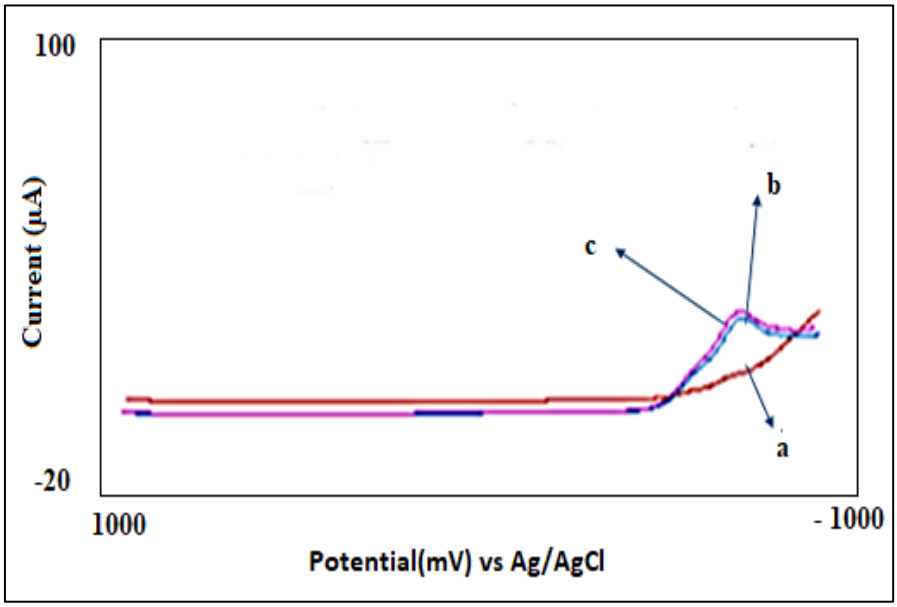

Figure 4.21. SWS voltammogram of dinobuton with azinphos-methyl at 1:1 mole ratio a) blank (10 mL pH 7 BR buffer), b) $1.51x10^{-5}$ M dinobuton, c) $1.5x10^{-5}$ M dinobuton-$1.51x10^{-5}$ M azinphos-methyl solutions (pH 7, ΔE_s: 5 mV, f: 30 hertz, ΔE: 20 mV, t_{acc}: 50 s, E_{acc}: -500 mV

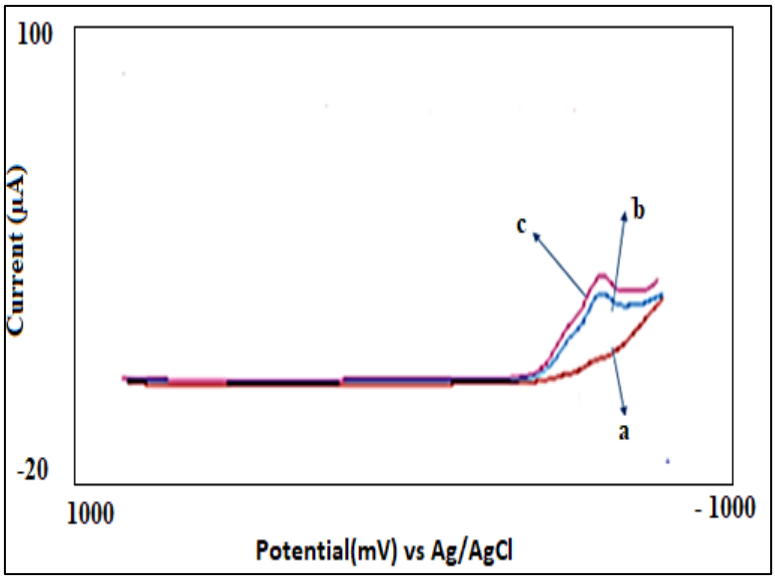

Figure 4.22. SWS voltammogram of dinobuton with azinphos-methyl at 1:5 mole ratio a) blank (10 mL pH 7 BR buffer), b) $1.51x10^{-5}$ M dinobuton, b) $1.44x10^{-5}$ M dinobuton-$7.26x10^{-5}$ M azinphos-methyl solutions (pH 7, ΔE_s: 5 mV, f: 30 hertz, ΔE: 20 mV, t_{acc}: 50 s, E_{acc} : -500 mV).

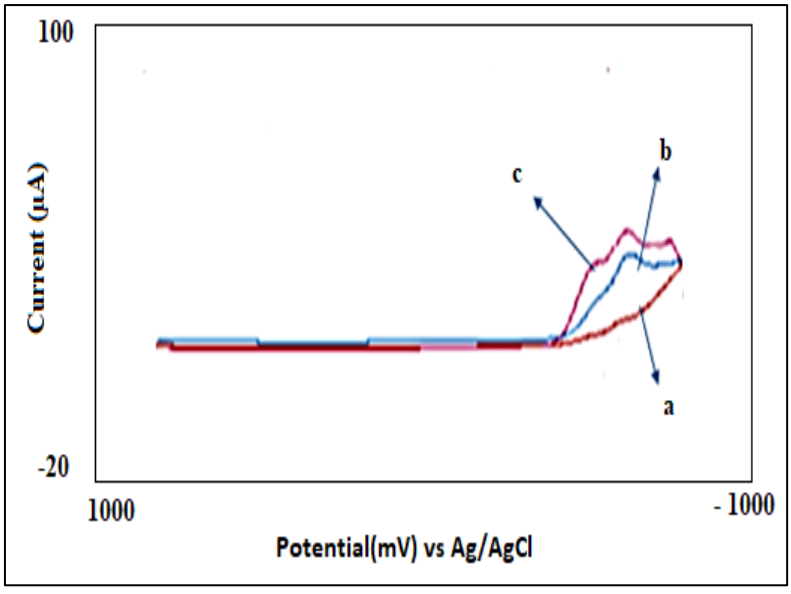

Figure 4.23. SWS voltammogram of dinobuton with azinphos-methyl at 1:10 mole ratio a) blank (10 mL pH 7 BR buffer), b) $1.51x10^{-5}$ M dinobuton, c**)** $1.38x10^{-5}$ M dinobuton-$1.39x10^{-4}$ M azinphos-methyl solutions (pH 7, ΔE_s: 5 mV, f: 30 hertz, ΔE: 20 mV, t_{dep}: 50 s, E_{dep}: -500 mV).

Table 4.14. Interfering effect of azinphos-methyl and % recoveries*

Mole to mole	Dinobuton (M)	Azinphos-methyl(M)	Recovery %	Relative error %
1:1	1.50×10^{-5}	1.51×10^{-5}	99.97 ± 1.56	-0.03
1:5	1.44×10^{-5}	7.26×10^{-5}	109.21 ± 2.61	9.21
1:10	1.38×10^{-5}	1.39×10^{-4}	131.59 ± 7.14	31.59

**n=3*

The percent recovery was calculated by simply taking the ratio of the dinobuton's peak current (μA) to that in the presence of azinphos-methyl. (The percent recovery was calculated by simply taking the ratio of the dinobuton's peak current in the presence of triasulfuron and to that without azinphos-methyl).

4.5.3. Bromoxynil-octanoate

Bromoxynil-octanoate is a widely used herbicide for post emergence weed control of crops. 0.0050 grams of dinobuton was weighted precisely and dissolved in 10 mL of acetone to prepare 1.53×10^{-3} M dinobuton stock solution. 0.0059 grams of bromoxynil-octanoate (Mwt: 403.11 g/mol) was weighted precisely on analytical balance and dissolved in 10 mL of acetone to prepare 1.46×10^{-3} M bromoxynil-octanoate stock solution. Bromoxynil-octanoate is more soluble in acetone than in other solvents.

For interference study, 100 μL dinobuton stock solution was transferred to the voltammetric cell including 10 mL of BR buffer solution at pH 7 and SWS voltammogram was recorded with only dinobuton. Then, interference study with bromoxynil-octanoate with 1:1 and 1:5 mole ratio was repeated under the same experimental conditions. Dinobuton and dinobuton-bromoxynil octanoate peaks were overlapped on the same graph to facilitate the comparison. These voltammograms of dinobuton in the presence of bromoxynil-octanoate are shown in Figures 4.24. and 4.25. The recovery data on dinobuton determination in the presence of bromoxynil-octanoate are given in Table 4.15.

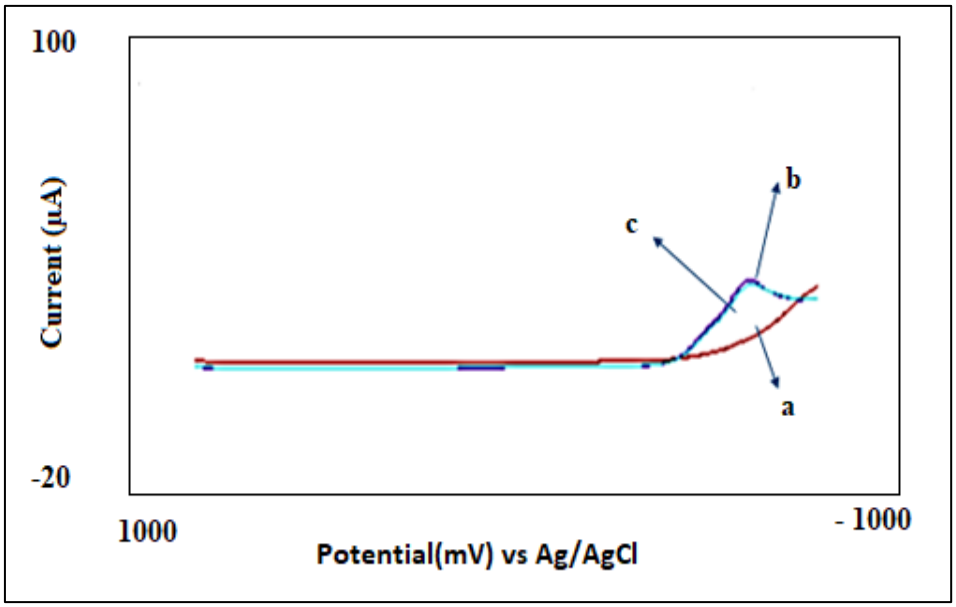

Figure 4.24. SWS voltammogram of dinobuton with bromoxynil-octanoate at 1:1 mole ratio a) blank (10 mL pH 7 BR buffer), b) $1.51x10^{-5}$ M dinobuton, b) $1.5x10^{-5}$ M dinobuton-$1.43x10^{-5}$ M bromoxynil-octanoate solutions (pH 7, ΔE_s: 5 mV, f: 30 hertz, ΔE: 20 mV, t_{acc}: 50 s, E_{acc}: -500 mV).

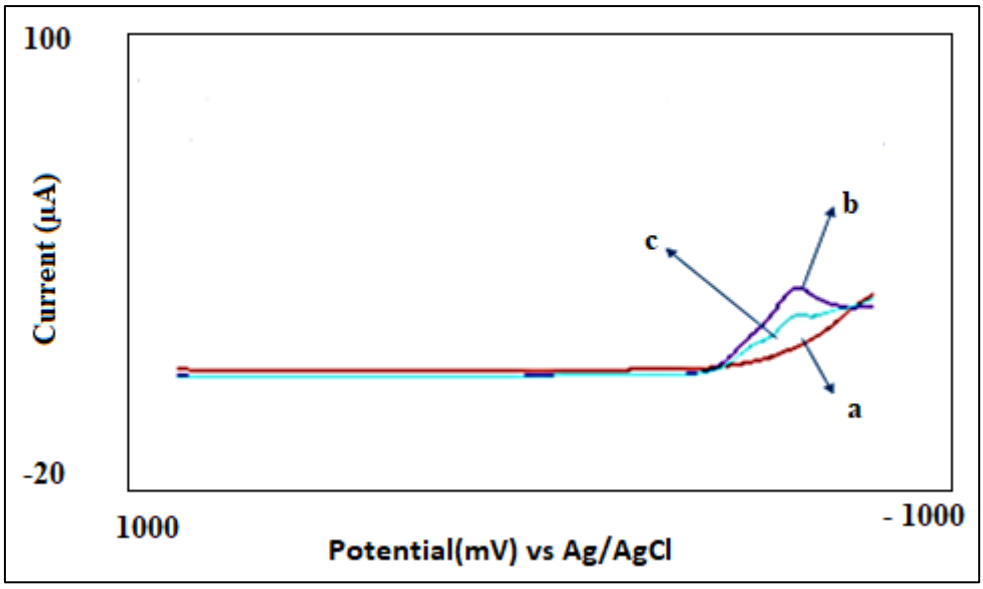

Figure 4.25. SWS voltammogram of dinobuton with bromoxynil-octanoate at 1:5 mole ratio a) blank (10 mL pH 7 BR buffer), b) $1.51x10^{-5}$ M dinobuton, c) $1.44x10^{-5}$ M dinobuton-$6.88x10^{-5}$ M bromoxynil-octanoate solutions (pH 7, ΔE_s: 5 mV, f: 30 hertz, ΔE: 20 mV, t_{acc}: 50 s, E_{acc}: -500 mV).

Table 4.15. Interfering effect of bromoxynil-octanoate and % recoveries*

Mole to mole	Dinobuton (M)	Bromoxynil-octanoate (M)	Recovery %	Relative error %
1:1	1.5×10^{-5}	1.43×10^{-5}	96.55 ± 4.26	-3.45
1:5	1.44×10^{-5}	6.88×10^{-5}	27.29 ± 3.6	-72.70

*n=3

The percent recovery was calculated by simply taking the ratio of the dinobuton's peak current (μA) to that in the presence of bromoxynil-octanoate.

4.5.4. Dialifos

Dialifos is an ancient organophosphate insecticide and is highly toxic to honey bees and moderately toxic to birds and fish. 0.0051 grams of dinobuton (Mwt:326.304 g/mol) was weighted precisely and dissolved in 10 mL of acetone to prepare 1.56×10^{-3} M dinobuton stock solution. The solubility of dialifos was investigated from references and since acetone is a good solvent for dialifos, it was used in the preparation of stock solutions. 0.0063 grams of dialifos (Mwt: 393.85 g/mol) was weighted precisely on analytical balance and dissolved in 10 mL of acetone to prepare 1.6×10^{-3} M dialifos stock soluton.

For interference study, 100 μL of dinobuton stock solution was transferred to the voltammetric cell including 10 mL of BR buffer solution at pH 7 and SWS voltammogram was recorded with only dinobuton. Then, interference study with dialifos with 1:1 and 1:5 mole ratio was repeated under the same experimental conditions. Dinobuton and dinobuton-dialifos peaks were overlapped on the same graph to facilitate comparison. The solubility of dialifos was searched and acetone which is a good solvent for dialifos was used to prepare dialifos stock solution. These voltammograms of dinobuton in the presence of dialifos are shown in Figures 4.26. and 4.27. The recovery data on dinobuton determination in the presence of dialifos are given in Table 4.16.

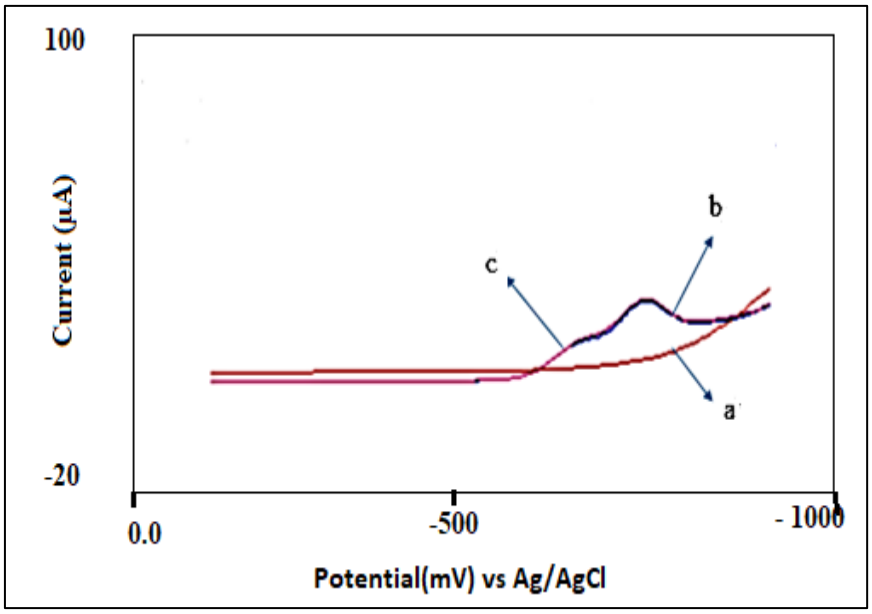

Figure 4.26. SWS voltammogram of dinobuton with dialifos at 1:1 mole ratio a) blank (10 mL pH 7 BR buffer), b) $1.54x10^{-5}$ M dinobuton, c) $1.53x10^{-5}$ M dinobuton-$1.57x10^{-5}$ M dialifos solutions. (pH 7, ΔE_s: 5 mV, *f*: 30 hertz, ΔE: 20 mV, t_{acc}: 50 s, $E_{acc:}$ −500 mV)

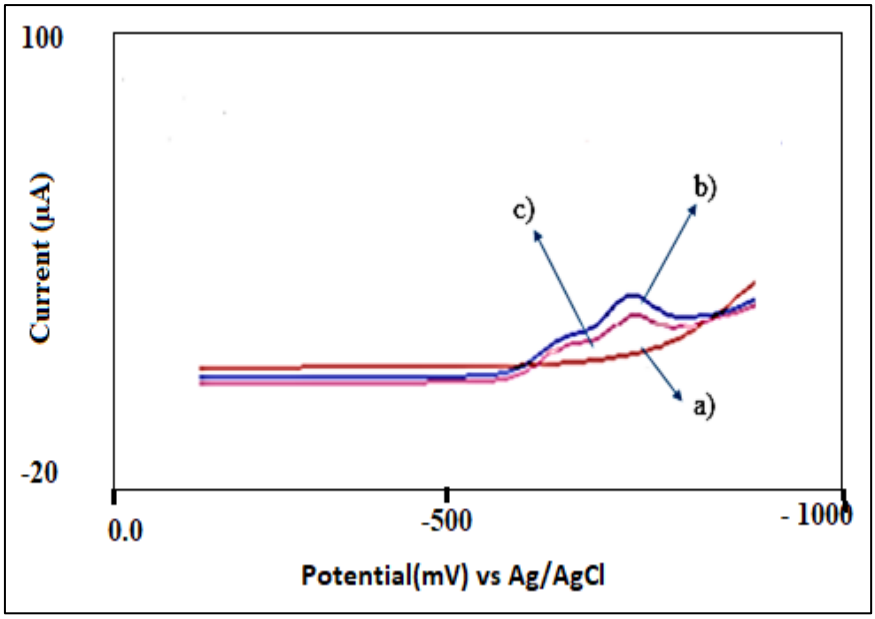

Figure 4.27. SWS voltammogram of dinobuton with dialifos at 1:5 mole ratio a) blank (10 mL pH 7 BR buffer), b) $1.54x10^{-5}$ M dinobuton, c) $1.47x10^{-5}$ M dinobuton -$7.55x10^{-5}$ M dialifos solutions. (pH 7, ΔE_s: 5 mV, f: 30 hertz, ΔE: 20 mV, t_{acc}: 50 s, E_{acc}: -500 mV).

Table 4.16. Interfering effect of dialifos and % recoveries*

Mole to mole	Dinobuton (M)	Dialifos (M)	Recovery %	Relative error %
1:1	$1.53 \times 1\ 0^{-5}$	1.57×10^{-5}	98.91 ± 1.08	-1.09
1:5	1.47×10^{-5}	7.55×10^{-5}	69.93 ± 4.53	-30.07

**n=3*

The percent recovery was calculated by simply taking the ratio of the dinobuton's peak current (μA) to that in the presence of dialifos.

4.5.5. Fipronil

Fipronil pesticide is a broad-spectrum insecticide belonging to the phenylpyrazole group. 0.0052 grams of dinobuton (Mwt:326.304 g/mol) was weighted precisely and dissolved in 10 mL of acetone to prepare 1.59×10^{-3} M dinobuton stock solution. 0.0068 grams of fipronil (Mwt: 437.15 g/mol) was weighted precisely using analytical balance and dissolved in 10 mL of acetone to prepare 1.55×10^{-3} M fipronil stock solution.

For interference study, 100 μL from dinobuton stock solution was transferred to the voltammetric cell including 10 mL of BR buffer solution at pH 7 and SWS voltammogram was recorded with only dinobuton. Then, interference study in the presence of fipronil with 1:1, 1:5 and 1:10 mole ratio was repeated under the same experimental conditions. Dinobuton and dinobuton plus fipronil peaks were overlapped on the same graph to facilitate comparison. These voltammograms of dinobuton in the presence of fipronil are shown in Figures 4.28., 4.29. and 4.30. The recovery data on dinobuton determination in the presence of fipronil are given in Table 4.17.

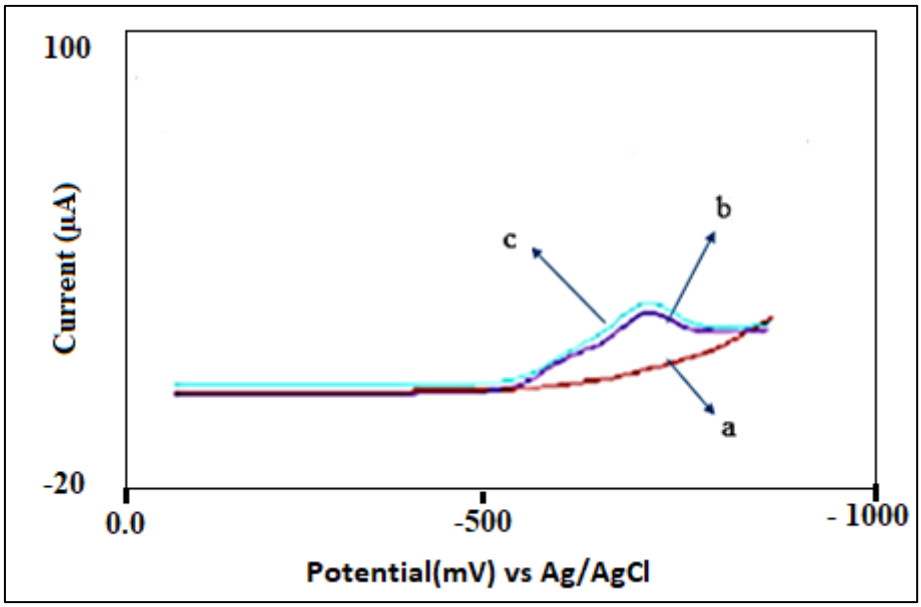

Figure 4.28. SWS voltammogram of dinobuton with fipronil at 1:1 mole ratio a) blank (10 mL pH 7 BR buffer), b) $1.57x10^{-5}$ M dinobuton, b) $1.56x10^{-5}$ M dinobuton-$1.52x10^{-5}$ M fipronil solutions

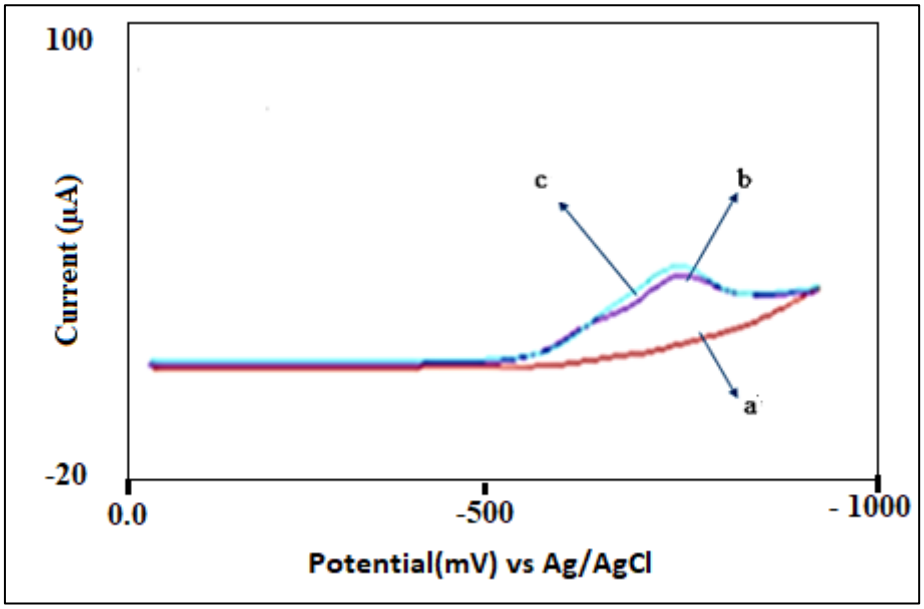

Figure 4.29. SWS voltammogram of dinobuton with fipronil at 1:5 mole ratio a) blank (10 mL pH 7 BR buffer), b) $1.57x10^{-5}$ M dinobuton, c) $1.5x10^{-5}$ M dinobuton-$7.31x10^{-5}$ M fipronil solutions

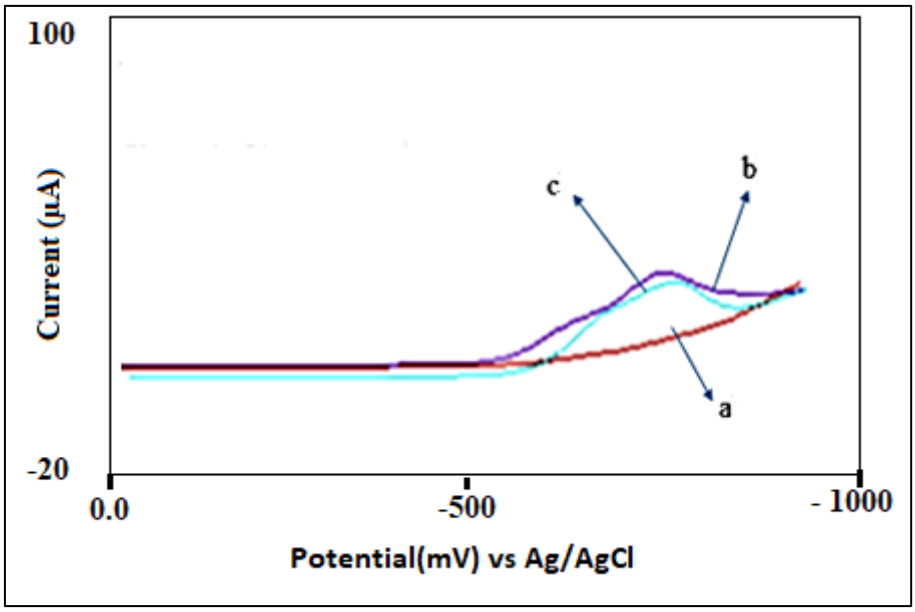

Figure 4.30. SWS voltammogram of dinobuton with fipronil at 1:10 mole ratio a) blank (10 mL pH 7 BR buffer), b) $1.57x10^{-5}$ M dinobuton, c) $1.43x10^{-5}$ M dinobuton-$1.4x10^{-4}$ M fipronil solutions

Table 4.17. Interfering effect of fipronil and % recoveries*

Mole to mole	Dinobuton (M)	Fipronil (M)	Recovery %	Relative error %
1:1	1.56×10^{-5}	1.52×10^{-5}	102.54 ± 0.55	2.54
1:5	1.5×10^{-5}	7.31×10^{-5}	101.27 ± .91	1.27
1:10	1.43×10^{-5}	1.40×10^{-4}	86.98 ± 1.10	-13.01

**n=3*

The percent recovery was calculated by simply taking the ratio of the dinobuton's peak current (µA) to that in the presence of fibronil.

4.5.6. Vinclozolin

Vinclozolin pesticide is used in grape production to control burns, rot and mold; It is also a dicarboximide fungicide used to control diseases in fruits and vegetables such as lettuce, kiwi, beans and onions. 0.0053 grams of dinobuton (Mwt: 326.304 g/mol) was weighted precisely and dissolved in 10 mL of acetone to prepare $1.62x10^{-3}$ M dinobuton stock solution. 0.0047 grams of vinclozolin (Mwt: 286.11 g/mol) was weighted precisely using analytical balance and dissolved in 10 mL of acetone to prepare $1.64x10^{-3}$ M vinclozoline stock solution.

For interference study, 100 µL of dinobuton stock solution was transferred to 10.0 mL of voltammetric cell including BR buffer solution at pH 7 and SWS voltammogram was recorded with only dinobuton. Then interference study in the presence of vinclozolin with 1:1, 1:5 and 1:10 mole ratio was repeated under the same experimental conditions. Dinobuton and dinobuton plus vinclozolin peaks were overlapped on the same graph to facilitate comparison. These voltammograms of dinobuton in the presence of vinclozolin are shown in Figures 4.31., 4.32. and 4.33. The recovery data on dinobuton determination in the presence of vinclozolin are given in Table 4.18.

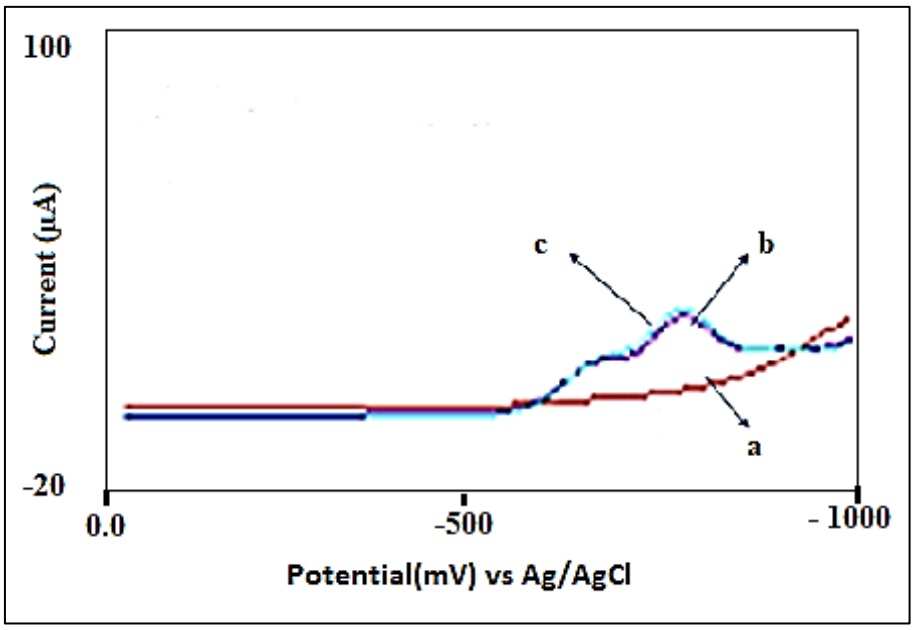

Figure 4.31. SWS voltammogram of dinobuton with vinclozolin at 1:1 mole ratio a) blank (10 mL pH 7 BR buffer) b) 1.60×10^{-5} M dinobuton, c) 1.59×10^{-5} M dinobuton– 1.61×10^{-5} M vinclozolin solutions. (pH 7, ΔE_s: 5 mV, *f*: 30 hertz, ΔE: 20 mV, t_{acc}: 50 s, E_{acc}: -500 mV).

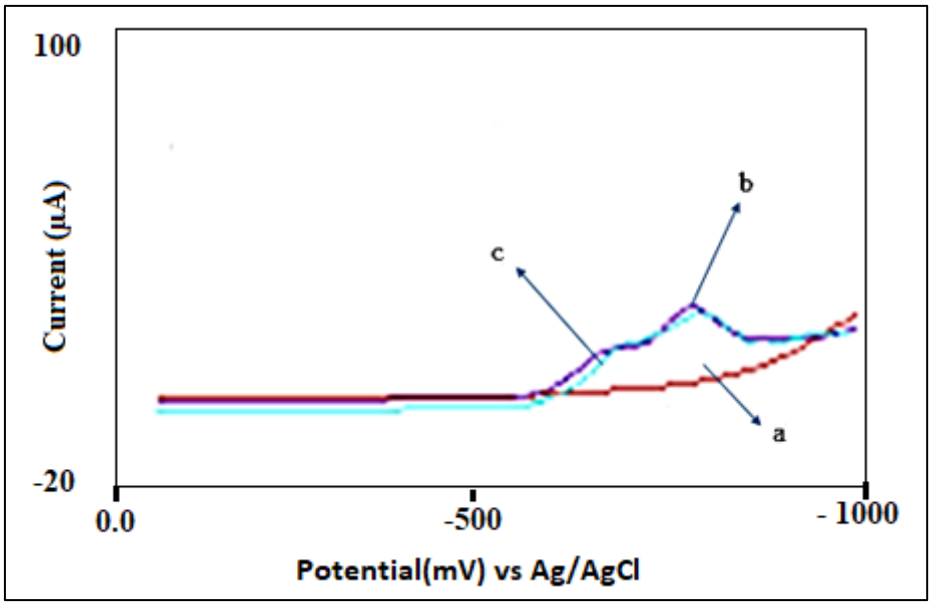

Figure 4.32. SWS voltammogram of dinobuton with vinclozolin at 1:5 mole ratio a) blank (10 mL pH 7 BR buffer) b) 1.60×10^{-5} M dinobuton, c) 1.53×10^{-5} M dinobuton -7.73×10^{-5} M vinclozolin solutions. (pH 7, ΔE_s: 5 mV, f: 30 hertz, ΔE: 20 mV, t_{acc}: 50 s, E_{acc} : -500 mV).

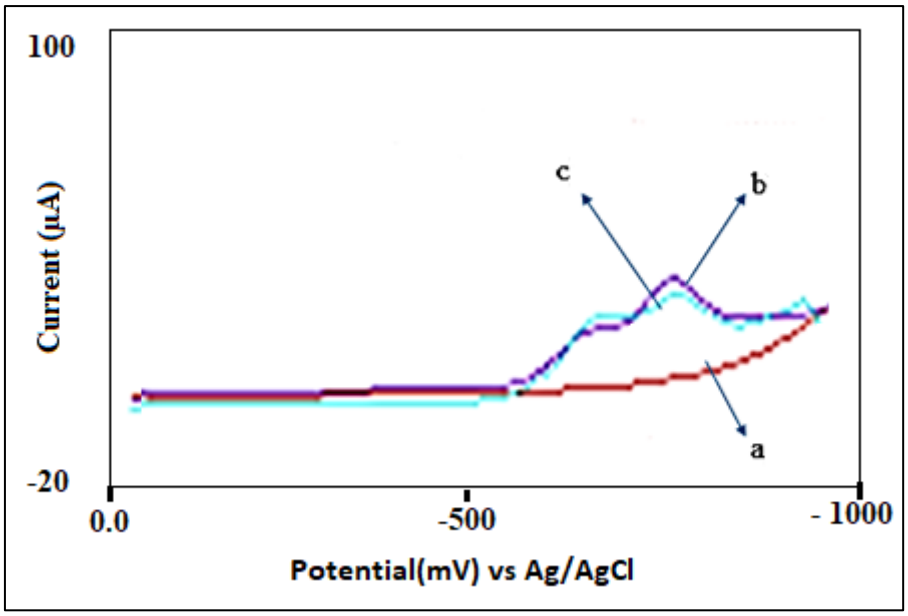

Figure 4.33. SWS voltammogram of dinobuton with vinclozolin at 1:10 mole ratio a) blank (10 mL pH 7 BR buffer), b) 1.60×10^{-5} M dinobuton, c) 1.46×10^{-5} M dinobuton - 1.48×10^{-4} M vinclozolin solutions. (pH 7, ΔE_s: 5 mV, f: 30 hertz, ΔE: 20 mV, t_{acc}: 50 s, E_{acc}: -500 mV).

Table 4.18. Interfering effect of vinclozolin and % recoveries*

Mole to mole ratio	Dinobuton (M)	Vinclozolin (M)	Recovery %	Relative error %
1:1	1.59×10^{-5}	1.61×10^{-5}	100.17 ± 0.86	0.17
1:5	1.53×10^{-5}	7.73×10^{-5}	98.73 ± 3.27	-1.26
1:10	1.46×10^{-5}	1.48×10^{-4}	76.86 ± 6.04	-23.14

**n=3*

The percent recovery was calculated by simply taking the ratio of the dinobuton's peak current (μA) to that in the presence of vinclozolin.

4.5.7. Iprodione

It is used as the active ingredient of fungicide to fight against gray mold on vegetables, early leaf blight on vegetables, and white rot on cucumbers, with formulas developed with this active ingredient. 0.0051 grams of dinobuton (Mwt: 326.306 g/mol) was weighted precisely and dissolved in 10 mL of acetone to prepare 1.56×10^{-3} M dinobuton stock solution. 0.0051 grams of iprodione (Mwt: 330.17 g/mol) was weighted precisely using analytical balance and dissolved in 10 mL of acetone to prepare 1.54×10^{-3} M iprodione stock solution.

For interference study, 100 μLof dinobuton stock solution was transferred to the voltammetric cell including 10.0 mL of BR buffer solution at pH 7 and SWS voltammograms were recorded with only dinobuton. Then, interference study in the presence of iprodione with 1:1, 1:5 and 1:10 mole ratio was repeated under the same experimental conditions. Dinobuton and dinobuton-iprodione peaks were overlapped on the same graph to facilitate comparison. These voltammograms of dinobuton in the presence of iprodione are shown in Figures 4.34, 4.35. and 4.36. The recovery data on dinobuton determination in the presence of iprodione are given in Table 4.19.

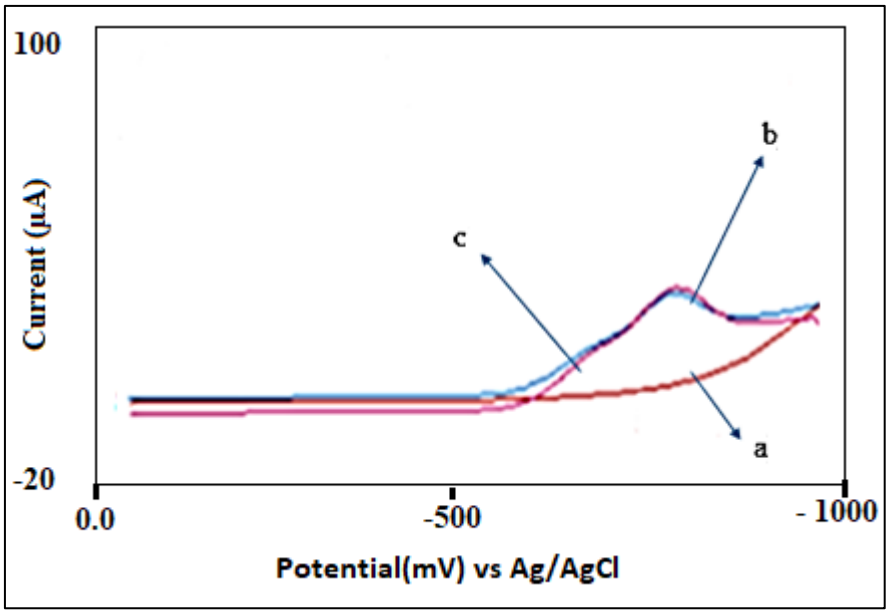

Figure 4.34. SWS voltammogram of dinobuton with iprodione at 1:1 mole ratio a) blank (10 mL pH 7 BR buffer), b) $1.54x10^{-5}$ M dinobuton, c) $1.53x10^{-5}$ M dinobuton-$1.51x10^{-5}$ M iprodione solutions. (pH 7, ΔE_s: 5 mV, f: 30 hertz, ΔE: 20 mV, t_{acc}: 50 s, E_{acc}: -500 mV).

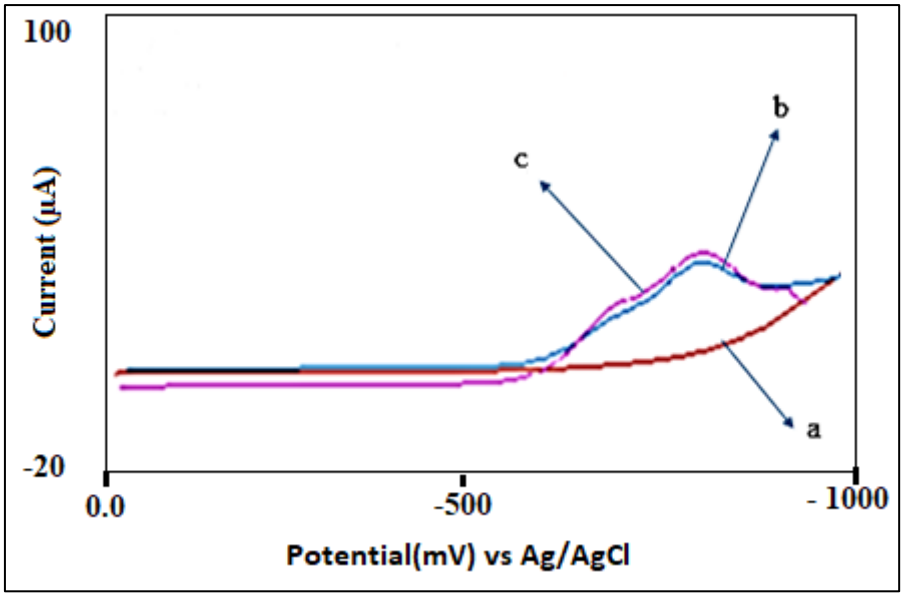

Figure 4.35. SWS voltammogram of dinobuton with iprodione at 1:5 mole ratio a) blank (10 mL pH 7 BR buffer), b) $1.54x10^{-5}$ M dinobuton, c) $1.47x10^{-5}$ M dinobuton-$7.26x10^{-5}$ M iprodione solutions. (pH 7, ΔE_s: 5 mV, f: 30 hertz, ΔE: 20 mV, t_{acc}: 50 s, E_{acc}: -500 mV).

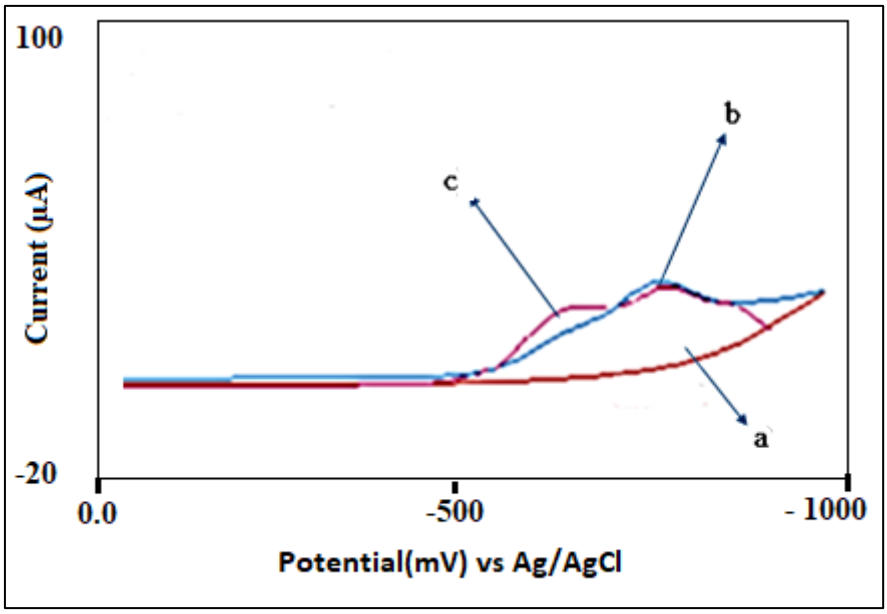

Figure 4.36. SWS voltammogram of dinobuton with iprodione at 1:10 mole ratio a) blank (10 mL pH 7 BR buffer), b) $1.54x10^{-5}$ M dinobuton, c) $1.40x10^{-5}$ M dinobuton-$1.39x10^{-4}$ M iprodione solutions. (pH 7, ΔE_s: 5 mV, *f*: 30 hertz, ΔE: 20 mV, t_{acc}: 50 s, E_{acc}: -500 mV).

Table 4.19. Interfering effect of iprodione and % recoveries*

Mole to mole ratio	Dinobuton (M)	Iprodione (M)	Recovery %	Relative error %
1:1	1.53×10^{-5}	1.51×10^{-5}	101.65 ± 1.51	1.65
1:5	1.47×10^{-5}	7.26×10^{-5}	102.97 ± 0.99	2.97
1:10	1.40×10^{-5}	1.39×10^{-4}	91.82 ± 2.94	-8.18

**n=3*

The percent recovery was calculated by simply taking the ratio of the dinobuton's peak current (µA) to that in the presence of iprodione.

4.5.8. Procymidone

Procymidone is used as the main active ingredient of some pesticides produced against fungicides. It is used against gray mold disease on tomatoes, monilia disease on quince, white rot disease on cucumber and some diseases on apricots. 0.0050 grams of dinobuton (Mwt:326.304 g/mol) was weighted precisely and dissolved in 10.0 mL of acetone to prepare $1.53x10^{-3}$ M dinobuton stock solution. 0.0042 grams of procymidone (Mwt:284.14 g/mol) was weighted precisely using analytical balance and dissolved in 10.0 mL acetone to prepare $1.48x10^{-3}$ M procymidone stock solution.

For interference study, 100 µL from dinobuton stock solution was transferred to the voltammetric cell including 10.0 mL of BR buffer solution at pH 7 and SWS voltammogram was recorded with only dinobuton. Then, interference study in the presence of procymidone with 1:1, 1:5 and 1:10 mole ratio was repeated under the same experimental conditions. Dinobuton and dinobuton-procymidone peaks were overlapped on the same graph to facilitate comparison. These voltammograms of dinobuton in the presence of procymidone are shown in Figures 4.37, 4.38 and 4.39. The recovery data on dinobuton determination in the presence of procymidone are given in Table 4.20.

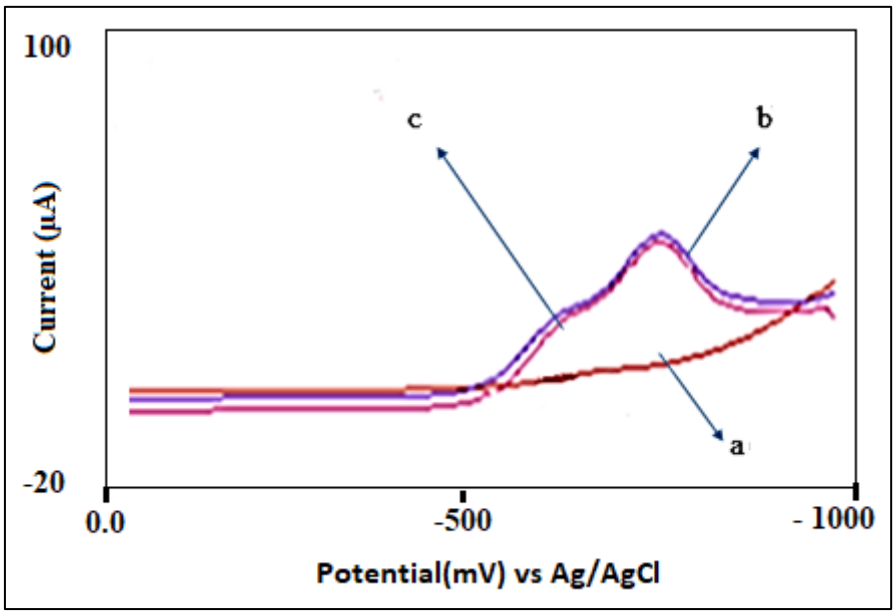

Figure 4.37. SWS voltammogram of dinobuton with procymidone at 1:1 mole ratio a) blank (10 mL pH 7 BR buffer), b) 1.51×10^{-5} M dinobuton, c) 1.50×10^{-5} M dinobuton-1.45×10^{-5} M procymidone solutions. (pH 7, ΔE_s: 5 mV, *f*: 30 hertz, ΔE: 20 mV, t_{acc}: 50 s, E_{acc}: -500 mV).

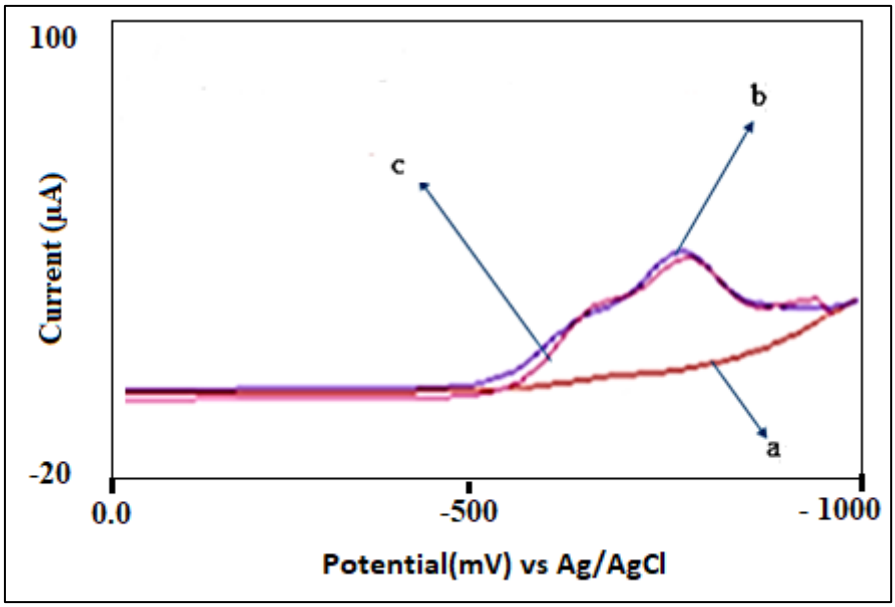

Figure 4.38. SWS voltammogram of dinobuton with procymidone at 1:5 mole ratio a) blank (10 mL pH 7 BR buffer), b) $1.51x10^{-5}$ M dinobuton, c) $1.44x10^{-5}$ M dinobuton - $6.98x10^{-5}$ M procymidone. (pH 7, ΔE_s: 5 mV, *f*: 30 hertz, ΔE: 20 mV, t_{acc}: 50 s, E_{acc}: -500 mV).

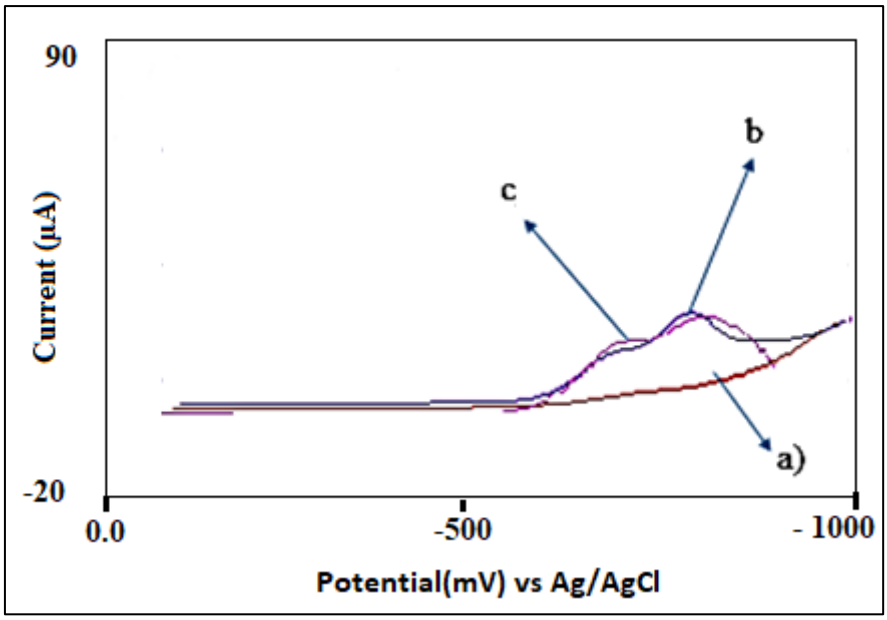

Figure 4.39. SWS voltammogram of dinobuton with procymidone at 1:10 mole ratio a) blank (10 mL pH 7 BR buffer), b) $1.51x10^{-5}$ M dinobuton, b) $1.38x10^{-5}$ M dinobuton-$1.33x10^{-4}$ M procymidone solutions. (pH 7, ΔE_s: 5 mV, *f*: 30 hertz, ΔE: 20 mV, t_{acc}: 50 s, E_{acc}: -500 mV).

Table 4.20. Interfering effect of procymidone and % recoveries*

Mole to mole ratio	Dinobuton (M)	Procymidone (M)	Recovery %	Relative error %
1:1	1.5×10^{-5}	1.45×10^{-5}	98.69 ± 0.99	-1.31
1:5	1.44×10^{-5}	6.98×10^{-5}	97.82± 0.99	-2.18
1:10	1.38×10^{-5}	1.33×10^{-4}	98.9 ± 1.71	-1.1

**n=3*

The percent recovery was calculated by simply taking the ratio of the dinobuton's peak current (μA) to that in the presence of procymidone.

4.5.9. Influence of some metal ions

Metals ions could actually co-exist with pesticides in agricultural areas. Therefore, the electrochemical determination of pesticides in the presence of metal ions is a useful study. The concentration range in which quantitative and qualitative determinations of pesticides can be made in such environments should be determined. For this purpose, the effects of Fe^{3+}, Mg^{2+}, Pb^{2+} ions were investigated.

Iron (III)

The iron element is the fourth most common mineral on the earth's surface and the most abundant metal in the earth's crust. Iron is obtained as a metal from iron ores and is rarely found in nature in elemental form. In general, the iron ores found in the earth's crust are: hematite (Fe_2O_3), limonite, goethite, magnetite (Fe_3O_4), siderite and pyrite (FeS_2). Foremost, 0.005 grams of dinobuton (Mwt: 326.304 g/mol) was weighted precisely and dissolved in 10.0 mL of acetone to prepare 1.53×10^{-3} M dinobuton stock solution, later on 0.0061 grams of $Fe(NO)_3 \cdot 9H_2O$ (Mwt: 404 g/mol) was weighted precisely using analytical balance and dissolved in 10.0 mL of distilled water to prepare 1.51×10^{-3} M Fe^{3+} stock solution.

For interference study, 100 μL of dinobuton stock solution was transferred to the voltammetric cell including 10.0 mL of BR buffer solution at pH 7 and SWS voltammogram was recorded with only dinobuton. Then, interference study in the presence of Fe^{3+} with 1:1, 1:5 and 1:10 mole ratio was repeated under the same experimental conditions. Dinobuton and dinobuton plus Fe^{3+} peaks were overlapped on the same graph to facilitate comparison. These voltammograms of dinobuton in the presence of Fe^{3+} are shown in Figures 4.40., 4.41.

and 4.42. The recovery data on dinobuton determination in the presence of Fe^{3+} are given in Table 4.21.

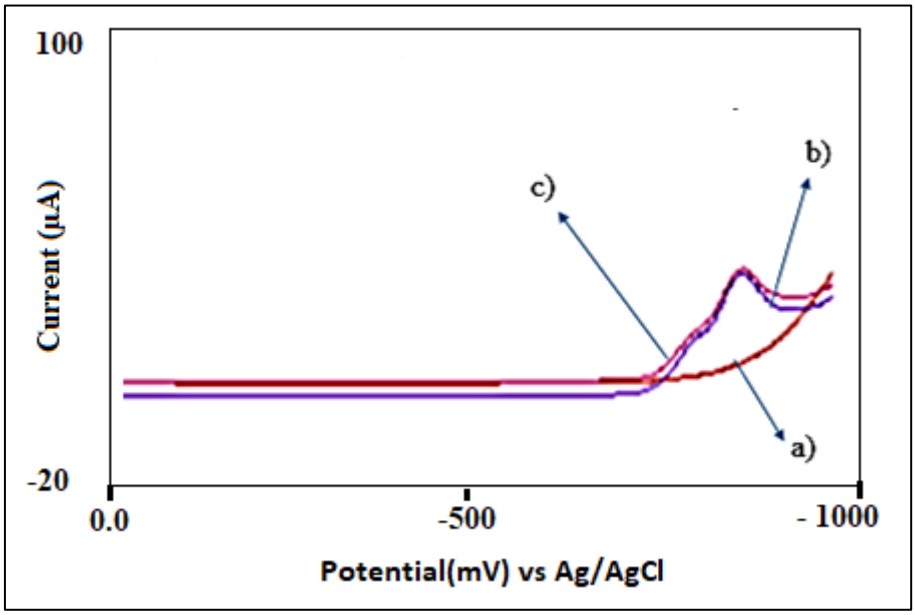

Figure 4.40. SWS voltammogram of dinobuton with Fe^{3+} at 1:1 mole ratio a) blank (10 mL pH 7 BR buffer), b) $1.51x10^{-5}$ M dinobuton, c) $1.5x10^{-5}$ M dinobuton-$1.48x10^{-5}$ M Fe^{3+}. (pH 7, ΔE_s: 5 mV, *f*: 30 hertz, ΔE: 20 mV, t_{acc}: 50 s, E_{acc}: -500 mV).

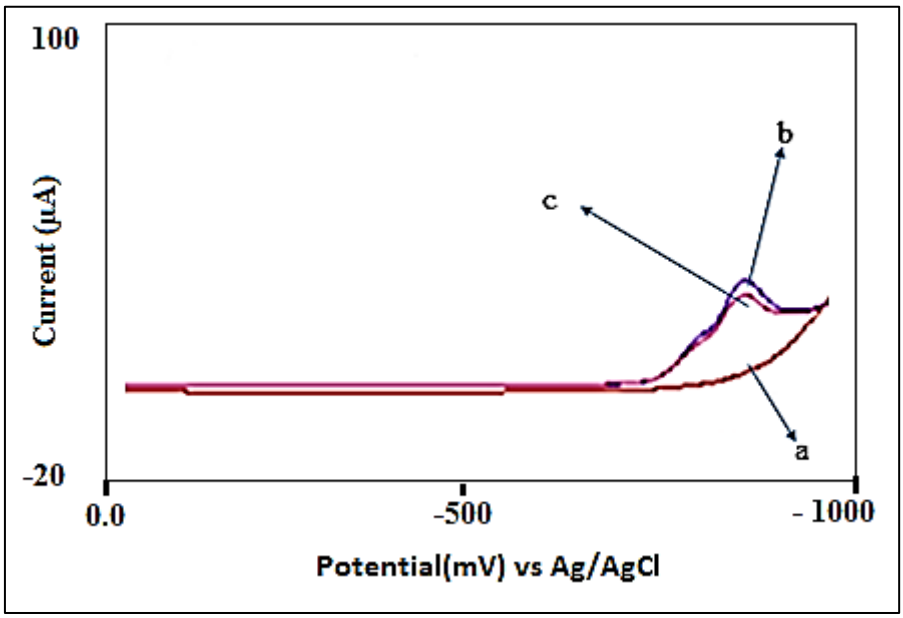

Figure 4.41. SWS voltammogram of dinobuton with Fe^{3+} at 1:5 mole ratio a) blank (10 mL pH 7 BR buffer), b) $1.51x10^{-5}$ M dinobuton, c) $1.44x10^{-5}$ M dinobuton-$7.12x10^{-5}$ M Fe^{3+}. (pH 7, ΔE_s: 5 mV, *f*: 30 hertz, ΔE: 20 mV, t_{acc}: 50 s, E_{acc}: -500 mV).

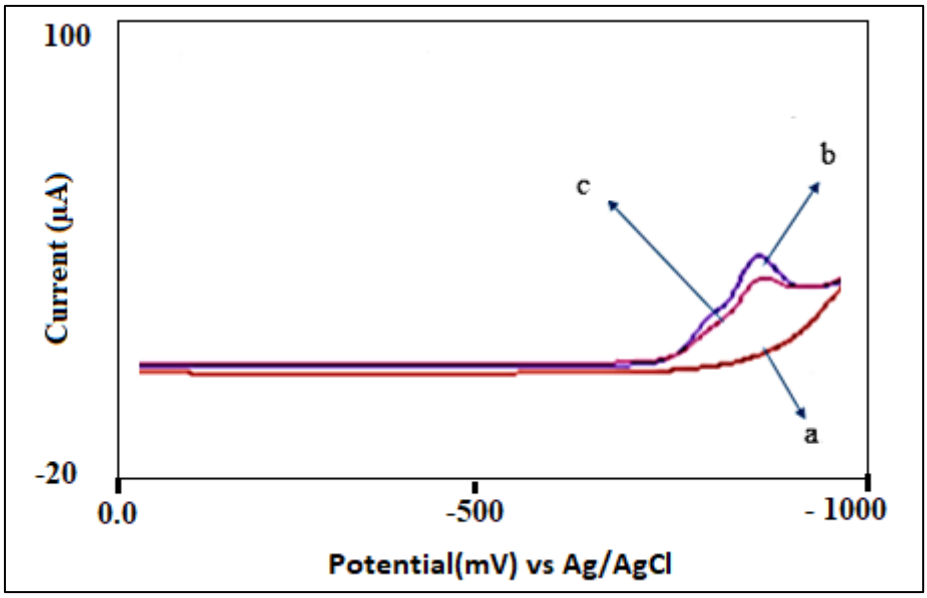

Figure 4.42. SWS voltammogram of dinobuton with Fe^{3+} at 1:10 mole ratio a) blank (10 mL pH 7 BR buffer), b)$1.51x10^{-5}$ M dinobuton, c) $1.38x10^{-5}$ M dinobuton-$1.40x10^{-4}$ M Fe^{3+}. (pH 7, ΔE_s: 5 mV, *f*= 30 hertz, ΔE: 20 mV, t_{acc}: 50 s, E_{acc}: -500 mV).

Table 4.21. Interfering effect of Fe^{3+} and % recoveries*

Mole to mole ratio	Dinobuton (M)	Fe^{3+} (M)	Recovery %	Relative error %
1:1	1.50×10^{-5}	1.48×10^{-5}	101.98 ± 4.32	1.98
1:5	1.44×10^{-5}	7.12×10^{-5}	90.2 ± 0.85	-9.8
1:10	1.38×10^{-5}	1.36×10^{-4}	74.26 ± 4.54	-25.74

**n=3*

The percent recovery was calculated by simply taking the ratio of the dinobuton's peak current (µA) to that in the presence of Fe^{3+}.

Magnesium

It is the sixth most abundant element, constituting 2% of the total mass of the earth's crust, and the important mineral forms of magnesium are magnesite $MgCO_3$ (27% Mg), dolomite $MgCO_3 \cdot CaCO_3$ (13% Mg), carnallite $KClMgCl_2 \cdot 6H_2O$ (8% Mg) and 0.13 % Mg^{2+} in seawater. At the outset, 0.0050 grams of dinobuton (Mwt: 326.304 g/mol) was weighted precisely and dissolved in 10.0 mL of acetone to prepare $1.53x10^{-3}$ M dinobuton stock solution. Later on, 0.0040 grams of $Mg(NO_3)_2 \cdot 6H_2O$ (Mwt: 256.41 g/mol) was weighted

precisely on analytcial balance and dissolved in 10.0 mL of distilled water to prepare 1.56 x 10^{-3} M Mg^{2+} stock solution.

For voltammetric measurement, 100 µL of dinobuton stock solution was transferred to the voltammetric cell including 10.0 mL of BR buffer solution at pH 7 and SWS voltammogram was recorded with only dinobuton. Then, interference study in the presence of Mg^{2+} with 1:1, 1:5 and 1:10 mole ration was repeated under the same experimental conditions. Dinobuton and dinobuton plus Mg^{2+} peaks were overlapped on the same graph to facilitate comparison. These voltammograms of dinobuton in the presence of Mg^{2+} are shown in Figures 4.43., 4.44. and 4.45. The recovery data on dinobuton determination in the presence of Mg^{2+} are given in Table 4.22.

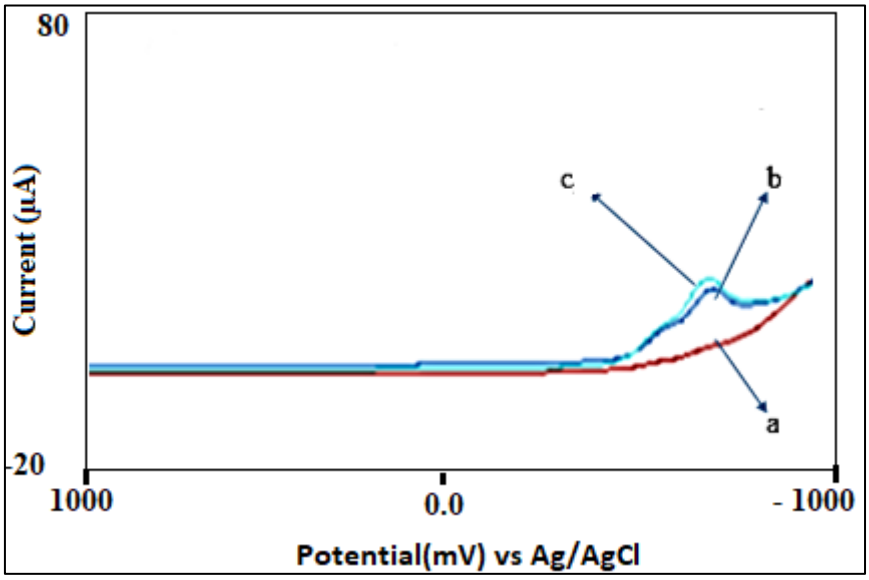

Figure 4.43. SWS voltammogram of dinobuton with Mg^{2+} at 1:1 mole ratio a) blank (10 mL pH 7 BR buffer) b) 1.51x10^{-5} M dinobuton, c) 1.50x10^{-5} M dinobuton plus 1.53x10^{-5} M Mg^{2+}. (pH 7, ΔE_s: 5 mV, *f*: 30 hertz, ΔE: 20 mV, t_{acc}: 50 s, E_{acc}: -500 mV).

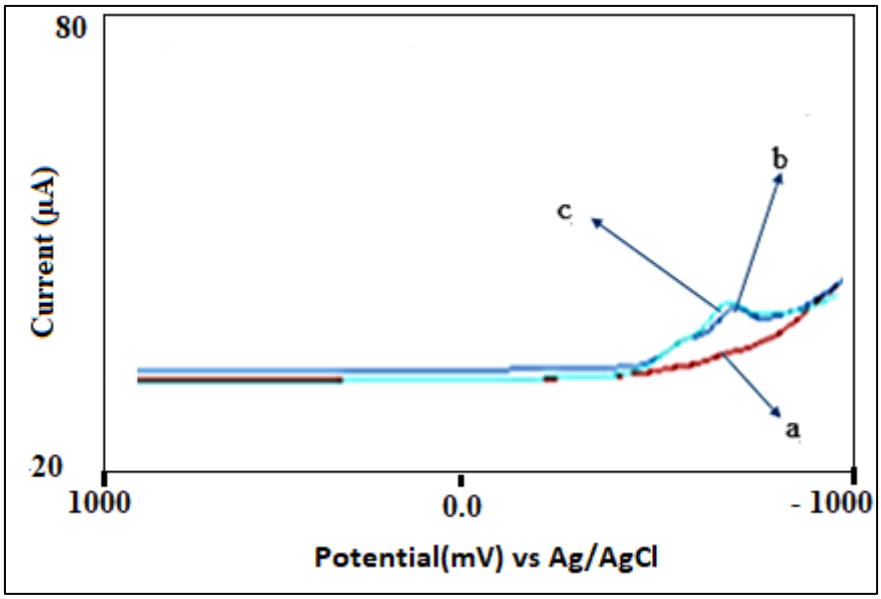

Figure 4.44. SWS voltammogram of dinobuton with Mg^{2+} at 1:5 mole ratio a) blank (10 mL pH 7 BR buffer), b) $1.51x10^{-5}$ M dinobuton, c) $1.44x10^{-5}$ M dinobuton plus $7.36x10^{-5}$ M Mg^{2+}. (pH 7, ΔE_s: 5 mV, *f*: 30 hertz, ΔE: 20 mV, t_{acc}: 50 s, E_{acc}: -500 mV).

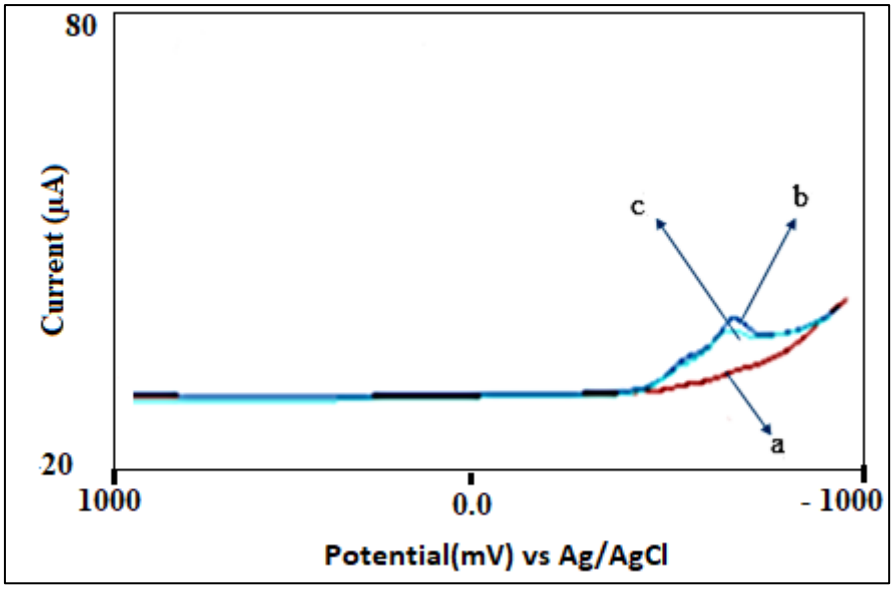

Figure 4.45. SWS voltammogram of dinobuton with Mg^{2+} at 1:10 mole ratio a) blank (10 mL pH 7 BR buffer), b) $1.51x10^{-5}$ M dinobuton, c) $1.38x10^{-5}$ M dinobuton plus $1.40x10^{-4}$ M Mg^{2+} solutions. (pH 7, ΔE_s: 5 mV, *f*: 30 hertz, ΔE: 20 mV, t_{acc}: 50 s, E_{acc}: -500 mV).

Table 4.22. Interfering effect of Mg^{2+} and % recoveries*

Mole to mole ratio	Dinobuton (M)	Mg^{2+} (M)	Recovery %	Relative error %
1:1	1.5×10^{-5}	1.53×10^{-5}	105.43 ± 4.84	5.43
1:5	1.44×10^{-5}	7.36×10^{-5}	100.77 ± 3.55	0.78
1:10	1.38×10^{-5}	1.40×10^{-4}	86.82 ± 3.55	-13.18

**n=3*

The percent recovery was calculated by simply taking the ratio of the dinobuton's peak current (μA) to that in the presence of Mg^{2+}.

Lead

The most important ores of lead are the sulfur mineral galena (PbS) and its oxidized products, cerucite ($PbCO_3$) and anglesite ($PbSO_4$). At the start of the experiment 0.0050 grams of dinobuton (Mwt: 326.304 g/mol) was weighted precisely and dissolved in 10.0 mL of acetone to prepare 1.53×10^{-3} M dinobuton stock solution. Later on, 0.0052 grams of $Pb(NO_3)_2$ (Mwt:331.2 g/mol) was weighted in precisely using analytical balance and dissolved in 10.0 mL of distilled water to prepare 1.57×10^{-3} M Pb^{2+} stock solution.

For the interference study, 100 μL of dinobuton stock solution was transferred to the voltammetric cell including 10.0 mL of BR buffer solution at pH 7 and SWS voltammogram was recorded with only dinobuton. Then, interference study in the presence of Pb^{2+} with 1:1, 1:5 and 1:10 mole ratio was repeated under the same experimental conditions. Dinobuton and dinobuton plus Pb^{2+} were overlapped on the same graph to facilitate comparison. These voltammograms of dinobuton in the presence of Pb^{2+} are shown in Figures 4.46., 4.47. and 4.48. The recovery data on dinobuton determination in the presence of Pb^{2+} are given in Table 4.23.

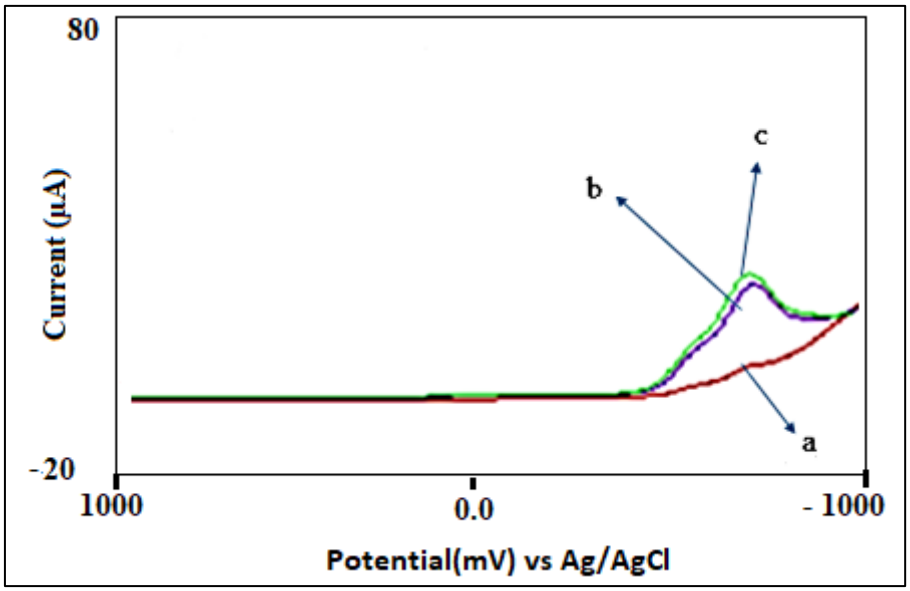

Figure 4.46. SWS voltammogram of dinobuton with Pb^{2+} at 1:1 mole ratio a) blank (10 mL pH 7 BR buffer), b) $1.51x10^{-5}$ M dinobuton, c) $1.50x10^{-5}$ M dinobuton plus $1.54x10^{-5}$ M Pb^{2+} solutions. (pH 7, ΔE_s: 5 mV, *f*: 30 hertz, ΔE: 20 mV, t_{acc}: 50 s, E_{acc}: -500 mV).

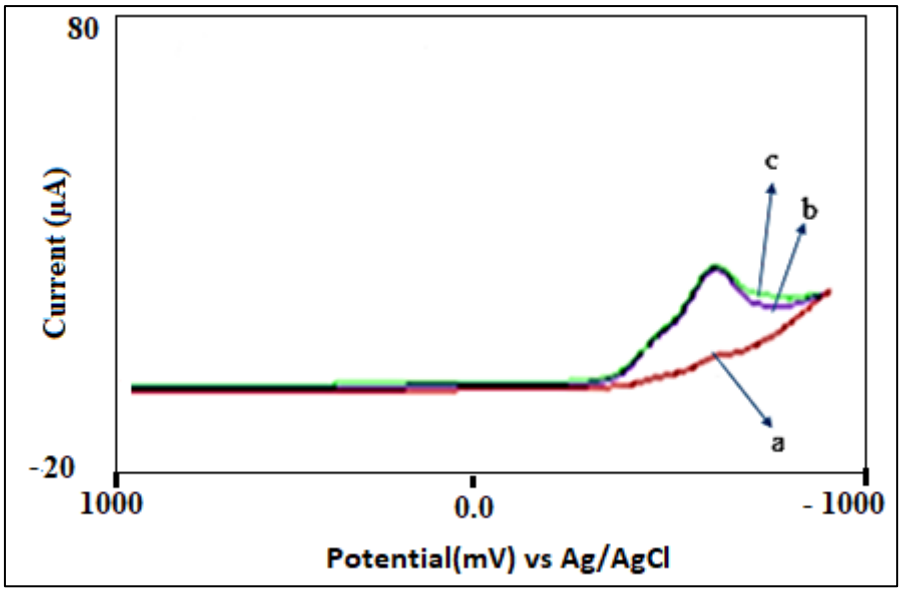

Figure 4.47. SWS voltammogram of dinobuton with Pb^{2+} at 1:5 mole ratio a) blank (10 mL pH 7 BR buffer), b) $1.51x10^{-5}$ M dinobuton, c) $1.44x10^{-5}$ M dinobuton plus $7.40x10^{-5}$ M Pb^{2+} solutions. (pH 7, ΔE_s: 5 mV, *f*: 30 hertz, ΔE: 20 mV, t_{acc}=50 s, E_{acc}: -500 mV).

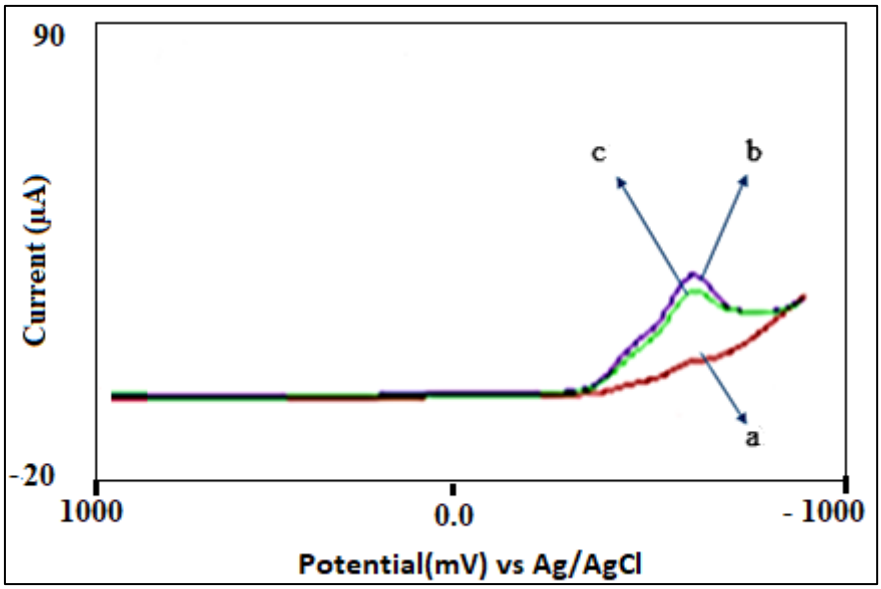

Figure 4.48. SWS voltammogram of dinobuton with Pb^{2+} at 1:10 mole ratio a) blank (10 mL pH 7 BR buffer), b) $1.51x10^{-5}$ M dinobuton, c) $1.38x10^{-5}$ M dinobuton plus $1.41x10^{-4}$ M Pb^{2+}. (pH 7, ΔE_s: 5 mV, *f*: 30 hertz, ΔE: 20 mV, t_{acc}: 50 s, E_{acc}: -500 mV).

Table 4.23. Interfering effect of Pb^{2+} and % recoveries*

	Dinobuton (M)	Pb^{2+} (M)	Recovery %	Relative error %
1:1	1.5×10^{-5}	1.54×10^{-5}	105.02 ± 2.83	5.02
1:5	1.44×10^{-5}	7.40×10^{-5}	100.17 ± 0.22	0.17
1:10	1.38×10^{-5}	1.41×10^{-4}	78.27 ± 1.66	-21.73

**n=3*

The percent recovery was calculated by simply taking the ratio of the dinobuton's peak current (µA) to that in the presence of Pb^{2+}.

Recovery calculations of dinobuton herbicide in the presence of some other pesticides and metal cations are a valuable tool for performing dinobuton determination in matrix media. Dinobuton determination in various matrices was made using the SWS voltammetric method. Recovery calculations were made with reference to the analytical signal of the dinobuton and proportioning it to the analytical signal recorded in the presence of the matrix. The results of the dinobuton determination performed in the presence of all pesticides and metal ions given above are displayed in Table 4.24 and 4.25, respectively.

Table 4.24. Interference of some pesticides in summary and percent recoveries*.

Mole Ratio ($M_{dinobuton}/M_{interfering\ type}$)			
	1:1	1:5	1:10
Interfering pesticide	Recovery (%)	Recovery (%)	Recovery (%)
Triasulfuron	102.69 ± 1.99	93.39 ± 2.51	Undefined peak
Azinphos-methyl	99.97 ± 1.56	109.21 ± 2.61	131.59
Bromoxynil octanoate	96.55 ± 4.26	27.29 ±3 .6	-
Dialifos	98.91 ± 1.08	69.93 ± 4.53	-
Fipronil	102.54 ± 0.55	101.27 ± 2.91	86.98 ± 1.10
Vinclozolin	100.17 ± 0.86	98.73 ± 3.27	76.86 ± 6.04
Iprodione	101.65 ± 1.51	102.97 ± 0.99	91.82 ± 2.94
Procymidone	98.69 ± 0.99	97.82 ± 0.99	98.9 ± 1.71

**n=3*

Table 4.25. Interference of some metal ions in summary and percent recoveries*.

Mole Ratio ($M_{dinobuton}/M_{interfering}$)			
	1:1	1:5	1:10
Interfering Ion	Recovery (%)	Recovery (%)	Recovery (%)
Fe^{3+}	101.98±4.32	90.2±0.85	74.26±4.54
Mg^{2+}	105.43±4.84	100.77±3.55	86.82±3.55
Pb^{2+}	105.02±2.83	100.17±0.22	78.27±1.66

**n=3*

4.6. Determination of Dinobuton in Spiked Samples

4.6.1. Apple juice

The proposed method was validated from the recovery of spiked apple juice using the conventional calibration method in apple juice. Utilizing the slope of the calibration graph obtained from the plot of concentration (µM) versus peak current (µA), LOD and LOQ values (3s/m and 10s/m) from the standard deviation of the cutoff point were determined as 2.69 µM and 8.96 µM, respectively. Dinobuton was added to the apple juice sample for recovery studies, and a dinobuton standard between 12.2 and 60.8 µM was added to the voltammetric cell for recovery.

Plotting of calibration graph

At first, 0.0204 grams of dinobuton was weighted in an analytical balance and dissolved in 10.0 mL of acetone to prepare $6.25x10^{-3}$ M dinobuton stock solution and then 1.0 mL was delivered to the 10.0 mL volumetric flask and completed to volume with apple juice, so that $6.25x10^{-4}$ M dinobuton spiked apple juice was obtained. 100 µL of standard additions were

made successively from the spiked apple juice sample to 10.0 mL of pH 7 BR buffer solution in the voltammetric cell, and voltammograms were immediately recorded. These additions were continued as long as the peak current increased linearly. The calibration graph of dinobuton in apple juice with SWSV is shown in the Figure 4.49. The voltammograms and related analytical parameters determined from the calibration chart of dinobuton in apple juice are presented in Figure 4.50 and Table 4.26, respectively.

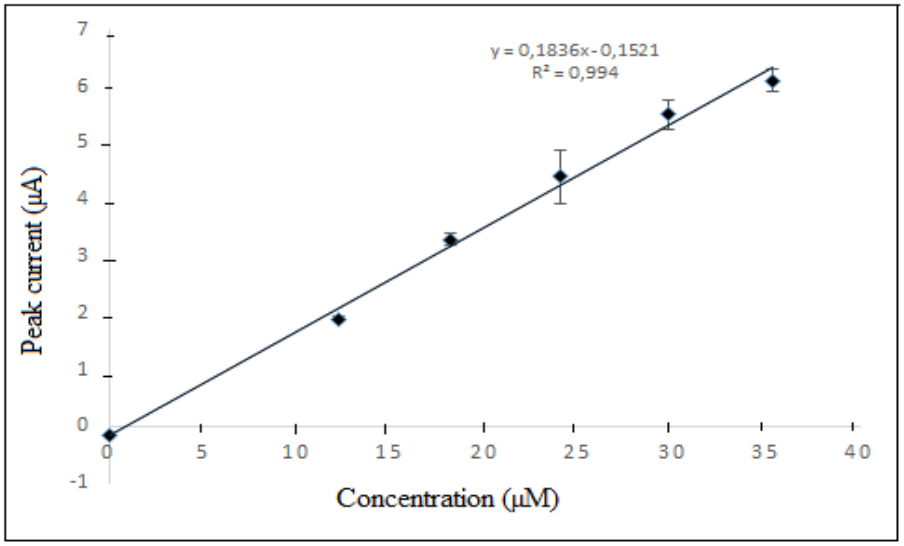

Figure 4.49. Calibration graph of dinobuton in an apple juice sample.

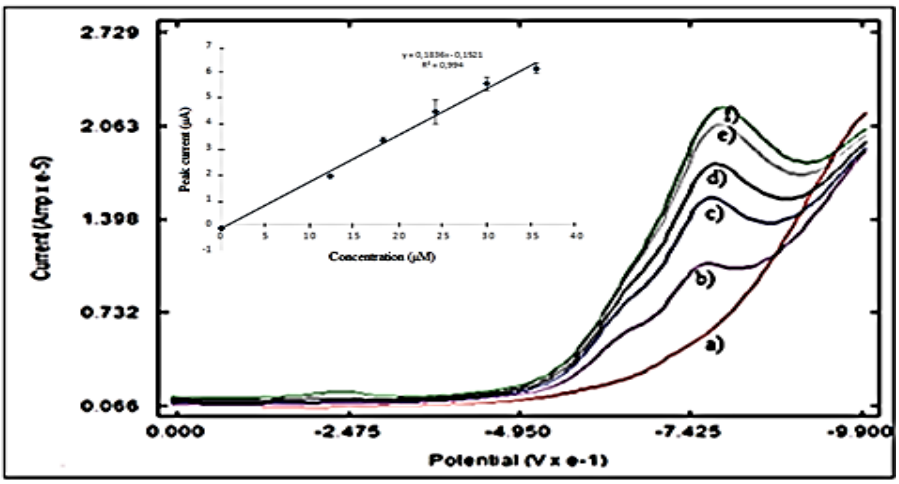

Figure 4.50. SWS voltammograms for the linear calibration curve of dinobuton in apple juice (a)blank-10 mL BR buffer, b) 12.25 µM, c)18.20 µM, d)24.04 µM, e)29.76 µM, f) 35.38 µM.

Table 4.26. Parameters obtained from calibration of dinobuton in apple juice.

Paremeters	
Slope (µA/µM)	0.18357 ± 0,007129
Cut-off point (µA)	-0.15209 ± 0,164553
LOD (µM)	2.69
LOQ (µM)	8.96
Linear operating range (µM)	12.25 – 35.38

Recovery studies were performed from apple juice solution containing 12.25 µM dinobuton in 10 mL voltammetric cells. It was made with standard additions of 20, 40, 60 and 80 µL from $6.25x10^{-3}$ M dinobuton stock solution. From the obtained voltammograms, four different dinobuton concentrations were recorded by SWSV. SWS voltammograms of dinobuton peaks increaments with their standard additions are presented in the Figure 4.51.

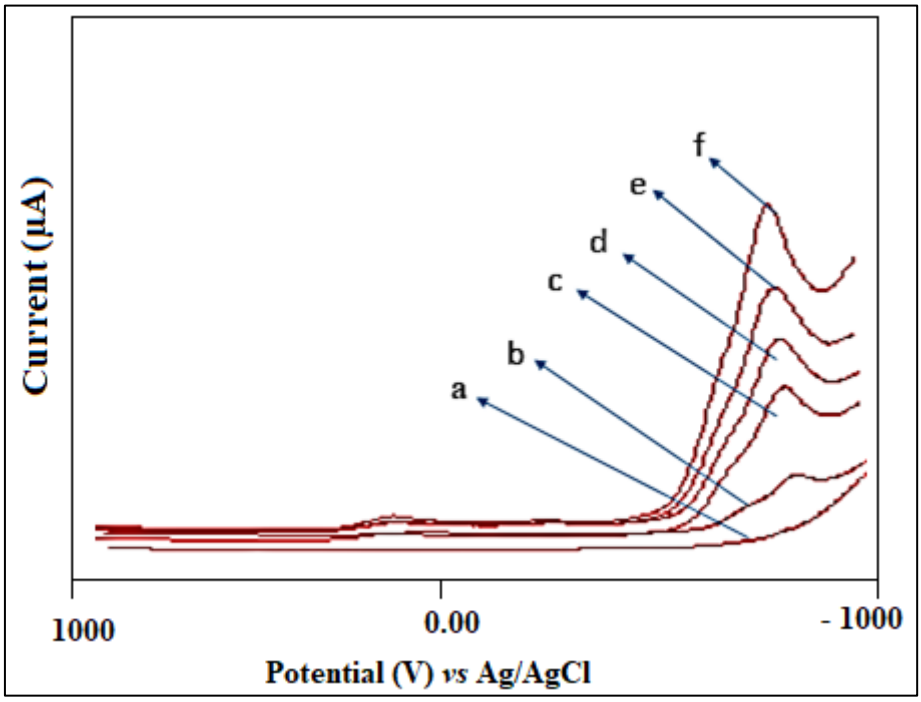

Figure 4.51. SWS voltammograms of dinobuton in spiked apple juice (a)10 mL blank- BR 7 buffer , b) $1.225x10^{-5}$ c) $2.45x10^{-5}$ M, d) $3.66x10^{-5}$ M, e) $4.87x10^{-5}$ M, f) $6.07x10^{-5}$ M) (pH 7, ΔEs: 5 mV, *f*: 30 hertz, ΔE: 20 mV, t_{acc}: 50 s, E_{acc}: -500 mV).

For recovery study, 0.2 mL of the spiked apple juice sample was transferred to 10.0 mL of BR 7 buffer in the voltammetry cell, and the resulting 12.25 µM dinobuton in the cell was accepted unknown true value. In other words, the 12.25 µM dinobuton concentration in the voltammetry cell was considered as unknown, and the % recovery values in the apple juice

sample were calculated from that content. The first measurement was made by SWS voltammetry when there was no dinobuton in apple juice, that is, only in the blank solution and no peak was observed as expected. The peak current height (μA) due to the 12.25 μM dinobuton resulting from the addition of spiked apple juice was then measured as unknown.

Since the blank solution did not give a peak current, it was accepted as zero, and then four identical standards were added from the stock dinobuton solution into the voltammetric cell, and the corresponding peak currents were measured and quantified after successive recording. That is, the spiked amounts in apple juice were calculated from the difference between the peak current height that obtained after each standard addition and the first peak arising from 12.25 μM dinobutton in the cell (Figure 4.51). The standard deviation from the four assays was calculated and the relative standard deviations (RSD%) was determined by dividing it to that of the avarages. The dilution factor is not neglected and the % recovery, %RSD and %RE values are given in the Table 4.27.

Table 4.27. Percent recovery values of dinobuton in spiked apple juice*.

Spiked apple juice (M)	Found (M)	Recovery %	RSD %	RE %
$1.225x10^{-5}$	$(1.297\pm0.052)x10^{-5}$	105.9±4.3	4.0	5.9

*N=4

4.6.2. Tap water

Validation studies on real samples such as tap water were performed by drawing a calibration graph and recovery studies were carried out accordingly. In the calibration method, LOD and LOQ values were determined as 1.22 and 4.08 μM, respectively.

Plotting of calibration graph

In order to construct a calibration graph, 0.0218 grams of dinobuton was weighed on an analytical balance and dissolved in 10.0 mL of acetone to obtain $6.68x10^{-3}$ M dinobuton stock solution. 1.0 mL of this solution was transferred to a 10.0 mL volumetric flask and the volume was completed with tap water, thus $6.68x10^{-4}$ M spiked dinobuton sample was prepared. 100 μL of spiked tap water was transfered to the voltammetric cell containing 10.0 mL of pH 7.0 BR buffer and a calibration graph was constructed by adding equal

amounts of standard dinobuton solutions. The calibration graph obtained for the determination of dinobuton in tap water by SWS voltammetry is presented in Figure 4.52. The voltammograms from which the linear calibration curve of the dinobuton in tap water is shown in Figure 4.53.

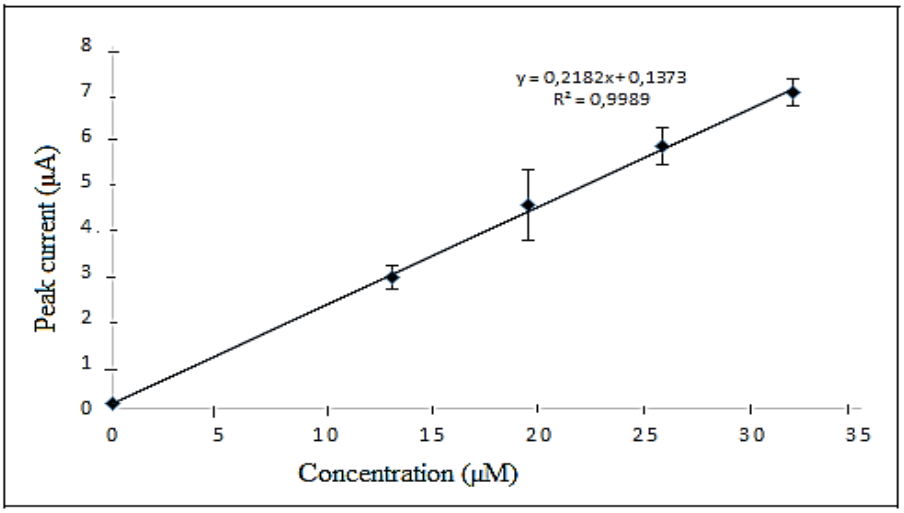

Figure 4.52. Calibration graph of dinobuton by SWS voltammetry in tap water.

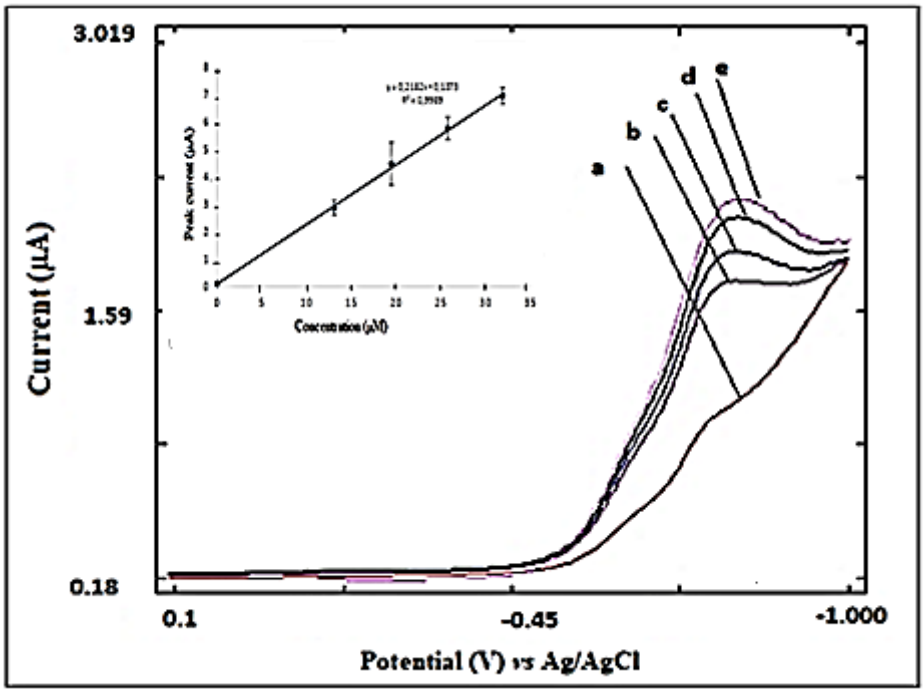

Figure 4.53. SWS voltammograms for the calibration of dinobuton in spiked tap water (a)10 mL blank- BR 7 buffer, b) 1.31×10^{-5} c) 1.946×10^{-5} M, d) 2.569×10^{-5} M, e) 3.181×10^{-5} M (pH 7, ΔEs: 5 mV, f: 30 hertz, ΔE: 20 mV, tacc: 50 s, Eacc: -500 mV).

Parameters obtained from calibration graph of dinobuton by SWS voltammetry in tap water is presented in Table 4.28.

Table 4.28. Parameters obtained from calibration of dinobuton in tap water.

Parameters (Units)	Values
Peak potential (mV)	-760
Slope (µA/µM)	0.218 ± 0.004
Cut-off point (µA)	0.137± 0.089
Correlation coefficient	0.9989
Limit of detection (µM)	1.22
Limit of quantification (µM)	4.08
Linear operating range (µM)	13.1 - 31.81

After constructing of calibration graph in tap water by SWS voltammetry, the validity of the proposed method was evaluated by the recoveries of the spiked tap water. In this procedure, 0.0209 grams of dinobuton was dissolved in 10.0 mL of acetone and 6.40 $x10^{-3}$ M dinobuton stock solution was obtained. 1.0 mL of dinobuton stock solution was transferred to the 10.0 mL of volumetric flask and the volume was completed with tap water. Thus, 6.40$x10^{-4}$ M spiked dinobuton sample was obtained. After 200 µL of dinobuton spiked tap water was delivered into the cell containing 10.0 mL of pH 7 BR buffer solution, standard additions of 60 µL of 6.40 $x10^{-3}$ M dinobuton stock solution were made four times. SWS voltammograms in spiked tap water has been shown in the Figure 4.54.

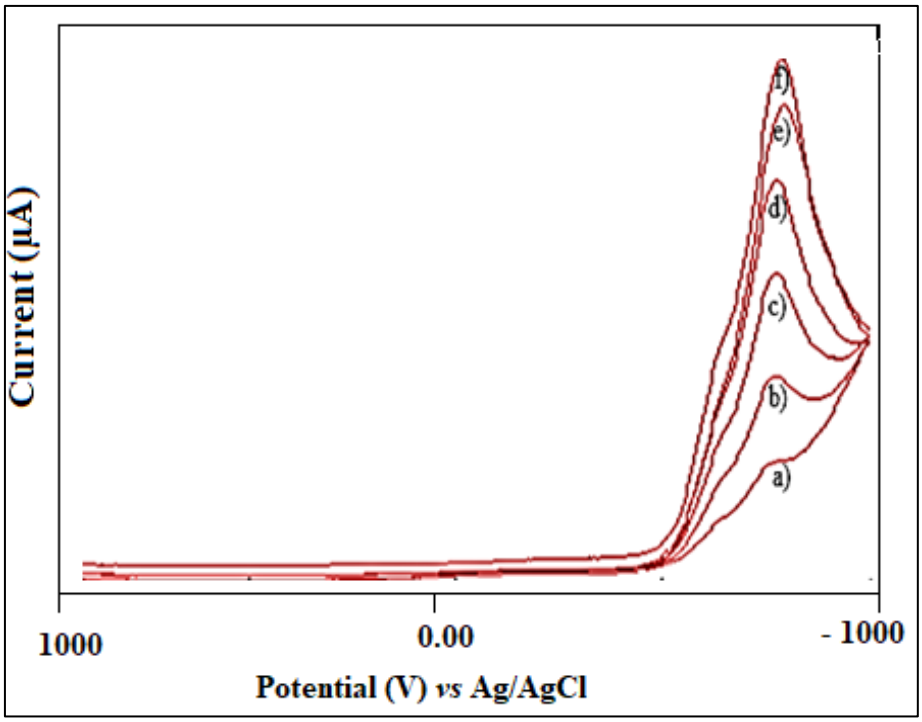

Figure 4.54. SWS voltammograms of dinobuton in spiked tap water (a)10 mL blank- BR 7 buffer, b)1.25x10^{-5} M, c) 5x10^{-5} M, d)8.68x10^{-5} M, e)1.23x10^{-4} M, f)1.59x10^{-4} M (pH 7, ΔEs: 5 mV, *f*: 30 hertz, ΔE: 20 mV, tacc: 50 s, Eacc: -500 mV).

Recovery in tap water was carried out from the spiked samples containing 12.55-µM dinobuton with standard additions. The 12.55 µM dinobuton concentration was accepted as the unknown real sample. The percent recovery was determined by the standard addition method. The difference between the peak current height obtained after each standard addition and the peak current observed for unknown sample in the cell was compared. The mean and standard deviations were calculated and the percent recoveries were determined as the ratio of mean value to that of actual spiked value (12.55 µM). The percent recovery, percent RSD and percent RE are given in the Table 4.29.

Table 4.29. Percent recovery values of dinobuton in spiked tap water sample*.

Spiked tap water (M)	Found (M)	Recovery %	RSD %	RE %
1.255x10^{-5} M	(1.234 ± 0.012)x10^{-5}	98.3±0.9	0.97	-1.65

n=4.

4.6.3. Grape juice

At last, validation studies in real samples were performed in grape juice. The validity of the recommended method was investigated with recoveries of spiked grape juice. 0.0202 grams of dinobuton dissolved in 10 mL of acetone, thus, $6.19x10^{-3}$ M dinobuton stock solution was prepared. 1.0 mL of dinobuton stock solution was transferred to a 10.0 mL volumetric flask and made up to volume with grape juice supplied from the market. Thus, $6.19x10^{-4}$ M dinobuton in grape juice stok solution was obtained. After adding 400-µL $6.19x10^{-4}$ M dinobuton-grape juice stock solution to 10.0 mL of pH 7 BR buffer in a voltammetric cell, sequential standard additions from 40 µL dinobuton stock solution were performed four times. SWS voltammograms overlayed of dinobuton in grape juice sample is presented in Figure 4.55.

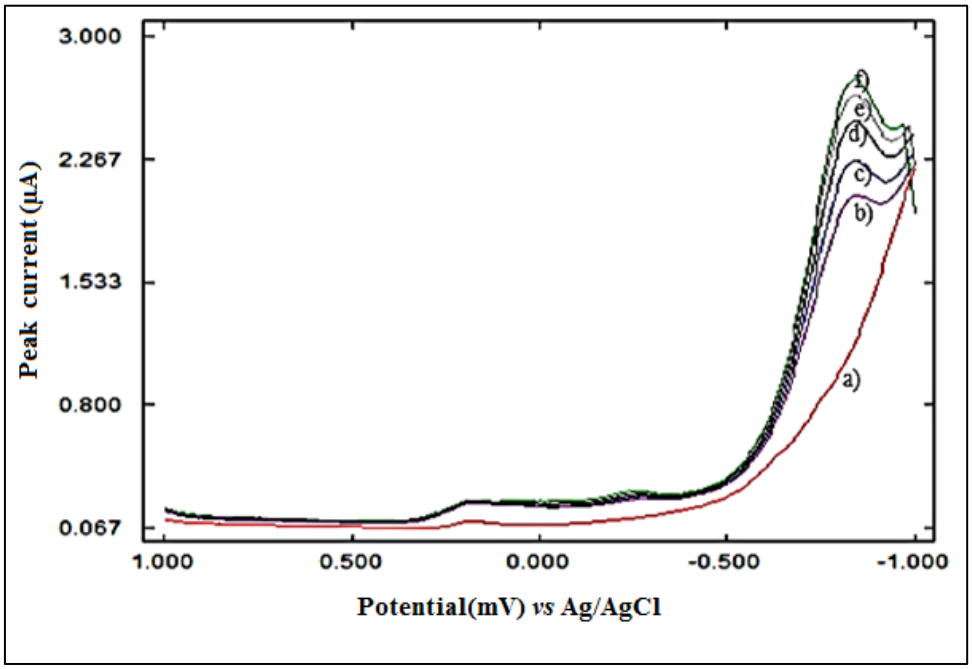

Figure 4.55. Square wave stripping voltammograms of dinobuton in spiked grape juice (a)10 mL blank- BR 7 buffer , b)$2.38x10^{-5}$ M, c)$4.74x10^{-5}$ M, d)$7.09x10^{-5}$ M, e)$9.41x10^{-5}$ M, f)$1.172x10^{-4}$ M) (pH 7, ΔEs: 5 mV, *f*: 30 hertz, ΔE: 20 mV, tacc: 50 s, Eacc: -500 mV).

In this study, 200 µL of spiked grape juice sample was transferred to 10.0 mL of BR 7 buffer in the voltammetric cell, and the 23.81 µM dinobuton was accepted as the unknown true sample. In other words, the 23.81 µM dinobuton concentration in the voltammetry cell was considered as unknown, and the % recovery values in the grape juice sample were calculated

from that content. The first measurement by SWS voltammetry when there was no dinobuton in grape juice, that is, only blank solution has exhibited no peak and the peak current height of the 23.81 μM dinobuton resulting from the addition of spiked grape juice to the cell was then measured as unknown.

Since the blank solution did not give a peak current then four identical standards were added from the stock dinobuton solution to this voltammetric cell, and the corresponding peak currents were measured and quantified after each recording. That is, the amounts in grape juice was calculated from the difference between the peak current of standard addition and the first peak arising from 23.81 μM dinobutton in the cell (Figure 4.55). The standard deviation from the four assays was calculated. Percent recovery value was determined just dividing mean value by the true value (23.81 μM). The percent recovery, RSD % and RE% values are given in the Table 4.30.

Table 4.30. Recovery values of dinobuton in spiked grape juice*.

Spiked grape juice (M)	Found (M)	Recovery %	RSD %	RE %
2.381×10^{-5} M	$(2.470 \pm 0.060) \times 10^{-5}$	103.7 ± 2.5	2.43	3.74

*n=4

In summary, recovery studies were performed on the MWCNTP electrode in real samples such as spiked apple juice, tap water, and grape juice using SWS voltammetry, and the recovery percentages were presented as percent relative standard deviation (RSD%) and percent relative error (%RE) (Table 4.31). As can be seen, the recovery values are within the tolerance limits of 10%, the relative standard deviation values vary between 0.97-2.43%, and the relative standard deviations vary between -1.65 percent and plus 5.9 percent. These values show that the accuracy and reproducibility of the proposed method is quite good.

Table 4.31. Summary of recovery studies of dinobuton in spiked samples*

Spiked Samples	Spiked amount (M)	Found (M)	Recovery (%)	RSD (%)	RE (%)
Apple juice	1.225×10^{-5}	$(1.297 \pm 0.052) \times 10^{-5}$	105.9±4.3	4.00	5.9
Tap water	1.255×10^{-5}	$(1.234 \pm 0.012) \times 10^{-5}$	98.3±0.9	0.97	-1.65
Grape juice	2.381×10^{-5}	$(2.470 \pm 0.060) \times 10^{-5}$	103.7±2.5	2.43	3.74

*n=4

4.7. Validation of the Method

Some parameters for the validation of a method was evaluated like selectivity, linearity, accuracy, precision, sensitivity, linear working range, limit of detection(LOD) and limit of quantification(LOQ) (Christian et al., 2021; 135).

4.7.1. Selectivity

Dinobuton determination was tested in different matrices to determine selectivity. Interference studies with different pesticides and ions allow us to comment on the selectivity of the proposed method. In the presence of triasulfuron, azinphos-methyl, bromoxynil octanoate, dialifos, fipronil, vinclozolin, iprodione and procymidone (when their molar ratio is 1:1), dinobuton can be determined within the 5% tolerance limit. When the mole ratio is 1:5, except for bromoxynil octanoate and dialifos, the others can be determined within the tolerance limit of 10%. When the molar ratio is 1:10, only iprodione and procymidone can be determined within the 10% tolerance limit.

4.7.2. Linearity

A calibration graphs were drawn to determine the linearity range for dinobuton in real samples or blank solutions, and a regression coefficient close to one indicated that linearity was acceptable. Calibration graph of dinobuton was constructed in an apple juice sample (r=0.9940 and linear operating range 12.25−35.38 µM), tap water sample (r=0.9989 and linear operating range 13.1 - 31.81 µM), in pH 7 BR buffer (r=0.9985 and linear operating range 3.74 − 25.8 µM). According to calibration graph of dinobuton shown in Figure 4.17, the equation of the linear line was:

I_p (μA) = (0.73 ± 0.01) C (μA/µM) – (0.78 ± 0.18) r = 0.9985

A regression coefficient close to 1 means that this graph has good linearity.

4.7.3. Accuracy

Recovery studies in apple juice, tap water and grape juice are to determine accuracy showed that detections can be made in matrix media and the method is accurate. Recovery studies of dinobuton in spiked apple juice, tap water and grape juice were 105.9±4.3%, 98.3±0.9% and103.7±2.5%, respectively. Relative errors are within the 10% tolerance limit, which indicates that the accuracy is reasonable.

4.7.4. Precision

Precision is defined as the degree to which the results are congruent and close to each other. In other words, precision is a measure of consistency and is often evaluated in terms of range or distribution of results. In practice, this means that precision is inherently correlated with the standard deviation of repeated results. Determination of dinobuton in apple juice, tap water and grape juice showed that detections can be made with a good precision since the relative standard deviations (RSD%) were 4.0%, 0.97% and 2.43%, respectively.

Intra-day

Intra-day repeatability study was carried out at different intervals in the same day. Intra-day repeability gives an idea whether same results could be obtained with same set of experimental paremeters. Relative standard deviations from data recorded intra-day indicate good intraday precision of the method. In this study, 0.0052 grams of dinobuton was weighted in analytical balance and dissolved in 10.0 mL of acetone to prepare $1.59x10^{-3}$ M dinobuton stock solution. In intra-day study, 100 µL of $1.59x10^{-3}$ M dinobuton stock solution was transfered to 10.0 mL of pH 7 BR buffer solution and recorded peak currents (µA) within the day is shown in Table 4.32.

Table 4.32. Intra-day repeatability of dinobuton ($1.59x10^{-5}$ M).

Number of observation	Peak current heights (µA)
1	8.0934
2	8.6152
3	8.7984
4	8.2216
5	8.9601
6	8.3955
7	9.0791
Mean $\bar{X}$	8.59
Standard deviation,s	0.37
Relative standard deviation(RSD%)	4.31

The relative standard deviation of 4.31% is smaller than the 5.0% tolerance limit, indicating that intraday repeatability is reasonable.

Inter-day

The inter-day reproducibility study was performed at four-day intervals. In this study, 0.0052 grams of dinobuton were weighed on an analytical balance and dissolved in 10.0 mL of acetone. 100 µL of $1.59x10^{-3}$ M dinobuton stock solution was transfered to 10.0 mL of BR buffer solution at pH 7. The peak currents recorded for inter-day studies were summarized in Table 4.33. Inter-day's determination of $1.59x10^{-5}$ M dinobuton data from the measurements of three different days and calculations for the population standart deviation was given in Table 4.34.

Table 4.33. Inter-day repeatability dinobuton(1.59x10-5 M).

The peak currents recorded for inter-say studies (µA)		
1st day	2nd days	3rd days
8.6152	9.3965	10.028
9.1432	8.9143	8.1331
9.0791	8.4413	7.5685
	Peak current heights (µA)	
Mean $\bar{X}$	8.81	
Standard deviation,s	0.81	
Relative standard deviation(RSD%)	9.19	

The population standard deviation was calculated as shown just below, and data from the measurements of three different days and calculations for the population standard deviation are shown below.

$$S_{pool}=\sqrt{\frac{\sum(x_i-\overline{x_i})^2+\sum(x_j-\overline{x_j})^2+\sum(x_k-\overline{x_k})^2}{N_1+N_2+N_3-N_t}}$$

Mean±standart deviation

Day 1- 8.94±0.29 Day 2- 8.92±0.48 Day 3- 8.58±1.29

Mean of all day measurements: 8.81

Table 4.34. Data from the measurements of three different days and calculations for the population standart deviation

x_i	$x_i-\overline{x_i}$	x_j	$x_j-\overline{x_j}$	x_k	$x_k-\overline{x_k}$
8.6152	-0.3248	9.3965	0.4765	10.0282	1.4482
9.1432	0.2032	8.9143	-0.0057	8.1331	-0.4469
9.0791	0.1391	8.4413	-0.4787	7.5685	-1.0115

$\overline{x_i}$ =8.94 $\overline{x_j}$ =8.92 $\overline{x_k}$ =8.58 $\sum(x_i-\overline{x_i})^2$= 0.1661

$\sum(x_j-\overline{x_j})^2$ = 0.4562 $\sum(x_k-\overline{x_k})^2$ = 3.3201 S_{pop}= 0.81

The relative standard deviation of 9.19% indicates that the inter-day reproducibility is slightly higher than the intra-day, but still reasonable within the 10% tolerance limit.

4.7.5. Sensitivity

Sensitivity is determined by the slope of the calibration curve and generally reflects the method's ability to distinguish between two different concentrations. In analytical chemistry, sensitivity is a term that describes how high a signal an instrument detects a change, and is usually plotted by the slope of the calibration graph. If a device has a high sensitivity, it means that it has good ability to detect a change in concentration by generating a very good

signal. For determination of sensitivity, you can measure the slope of the calibration graph and the slope of the dinobuton calibration graph, m=0.72μA/μM, indicates the sensitivity of the method.

4.7.6. Linear working range

The operating range of a method is a concentration range that can be obtained with acceptable accuracy and precision. This range often includes linearity as well. When recommending a method, it is usually specified with acceptable accuracy and precision. It was determined by plotting calibration curve on which least and highest concentrations were 3.74 and 25.8 μM between which were accepted as linear working range.

4.7.7. Limit of detection

Limit of detection is the concentration which is calculated by taking three times of standart deviation of blank signal and dividing by the slope of calibration curve. LOD has been determined to be 0.73 μM for dinobuton.

4.7.8. Limit of quantification

Limit of detection is the concentration which is calculated by taking ten times of standart deviation of blank signal and dividing by the slope of calibration curve. LOD has been determined to be 2.43 μM for dinobuton.

5. CONCLUSION

In this study, electrochemical determination of dinobuton pesticide was achieved on carbon nanotube paste electrode by square wave stripping voltammetry. In the literature, there are a few studies on the electrochemical determination of dinobuton, but there is no study using carbon nanotube electrodes and square wave stripping voltammetry method. In this study, the electrochemical behavior of the dinobuton was observed using different voltammetric techniques on the same working electrode. Optimum conditions were determined and dinobuton determination was made under these conditions. The proposed method was applied to apple juice, tap water and grape juice samples. The following conclusions can be drawn from our study.

1. The electrochemical behaviors of dinobuton was investigated by using square wave stripping voltammetry and cyclic voltammetry methods on multi-walled carbon nano tube electrode.
2. The electrochemical behaviors of dinobuton was observed in BR buffer solution at pH range of 1 and 12. The reduction peak potential switched to more negative values as pH was increased. The highest and suitable peak for electrochemical determination was observed at pH 7 which was accepted as an optimum.
3. Optimum SWSV parameters such as step potential, frequency, amplitude, deposition time and deposition potential was determined to be 5 mV, 30 Hertz, 20 mV, 50 s and -500 mV respectively.
4. A single reduction peak was observed at approximately -796 mV in cyclic voltammetry study. No peak was observed in reverse direction due to the irreversibility of the electrode reaction of dinobuton. The logarithm of the peak current (μA) vs the logarithm of the scan rate (ν) was plotted on the graph, the trendline was drawn and the slope was determined to be 0.65 which is closer to the theoretical value of diffusion controlled reactions (Laviron et al., 1980). If the slope of the Log (Ip) vs log (ν) graph is 0.5, the reaction is accepted as diffusion controlled, if it is 1, the reaction is accepted as adsoption controlled (Laviron et al., 1980). The slope determined 0.65 in the present work is close to both 0.5 and 1, the reaction can be accepted as both diffusion and adsoprtion controlled.
5. The linearity of the calibration curve or dynamic linear range was within 3.74 and 25.8 μM. Limit of detection (LOD) and limit of quantification (LOQ) was determined to be 0.73 and 2.43 μM, respectively. Because linear increase of peak current was proportional

with the concentration, it can be concluded that dinobuton can be determined by SWSV on MWCNT electrode.

6. Interfering effects of some pesticides including triasulfuron, azinphos-methyl, bromoxynil-octanoate, dialifos, fipronil, vinclozolin, iprodione and procymidone and metal ions Fe^{3+}, Mg^{2+} and Pb^{2+} on the determination of dinobuton was investigated. In 1:1 (mol/mol) interference ratio of dinobuton/interfering pesticide and dinobuton/metal ion, intereference effect was within 5% tolerance limit. In 1:5 interference ratio (mol/mol), only bromoxynil-octanoate and dialifos showed significant interference effect (higher than 5% tolerance limit). No interference effect was observed significantly when other pesticides and metal ions were used as matrix. In 1:10 interference ratio (mol/mol), no interference effect was observed when iprodione and procymidone was used as interfering species. The pesticides except iprodione and procymidone, metal ions showed intereference effect in determination of dinobuton. dinobuton can be determined by SWSV as electrochemically until matrix used is five times of dinobuton. Dinobuton can be determined until iprodione and procymidone is ten times of dinobuton as molarity.
7. The recommended method was applied to apple juice, tap water and grape juice samples. The calibration method was performed in apple juice and tap water. Linear operating range was determined between 12.25-35.38 μM in apple juice and 13.1- 31.81 μM in tap water. LOD and LOQ were determined to be 2.69 and 8.96 μM, respectively in apple juice. LOD and LOQ were determined to be 1.22 and 4.08 μM, respectivelty in tap water.
8. Recovery studies were performed in spiked apple juice, tap water and grape juice. Percent recoveries of spiked dinobuton ($1.225x10^{-5}$, $1.255x10^{-5}$ and $2.381x10^{-5}$, respectively) in apple juice, tap water and grape juice were determined to be 105.88%, 98.33% and 103.74% respectively. Low relative standart deviation (4%, 0.97% and 2.43%, respectively) and low relative errors (5.8%, -1.65% and 3.74%, respectively) indicates that the method is precise and accurate.

REFERENCES

Aktar, M. W., Sengupta, D. and Chowdhury, A. (2009). Impact of pesticides use in agriculture: their benefits and hazards. *Interdisciplinary toxicology*, 2(1), 1–12.

Alispahić, A., Krihovlavek, A. and Galić, N. (2021). Novel Preservation Methods for Inorganic Arsenic Speciation in Model and Natural Water Samples by Stripping Voltammetric Method. *Applied Sciences*, 11 (19), 8811.

Ang, K.B.A., Lee, M.A., Yu, H.M.O., Uy, M., Soriano, A.N. and Dugos, N.P. (2020). Determination of Diffusion Coefficients and Antioxidant Activities of Ascorbic Acid in Guava Juice using Cyclic Voltammetry. *IOP Conference Series*: *Materials Science and Engineering*, 778 (1).

Arancibia, J.A., Delfa, G.M., Boschetti, C.E., Escandar, G.M. And Olivieri, A.C. (2005). Application of partial least-squares spectrophotometric-multivariate calibration to the determination of 2-sec-butyl-4,6-dinitrophenol (dinoseb) and 2,6-dinitro-p-cresol in industrial and water samples containing hydrocarbons. *Analytica Chimica Acta*, 553, 141–147.

Aruna, P., Prasad, P.R., Reddy, C.N. and Sreedhar, N.Y. (2018). Nanostructured Fe2O3-ZnO modified GCE nanosensor for dinobuton pesticide determination in environmental samples. *International Journal of Scientific Research in Physics and Applied Sciences*, 6 (6), 88-93.

Baig, N., Sajid, M. and Saleh, T.A. (2019). Recent trends in nanomaterial-modified electrodes for electroanalytical applications. *Trends in Analytical Chemistry*, 111, 47-61.

Bartolomé, L., Lezamiz, J., Etxebarria, N., Zuloaga, O. and Jönsson, J.A. (2007). Determination of trace levels of dinitrophenolic compounds by microporous membrane liquid–liquid extraction in environmental water samples. *Journal of Separation Science*, 30, 2144 – 2152.

Bella, G.D., Saitta, M., Salvo, F., Nicotina, M. and Dugo, G. (2003). Gas Chromatographıc Determınatıon Of Azoxystrobın, Dınocap, Fenarımol, Penconazole And Quınoxyfen Durıng Wıne Makıng. *Italian Journal of Food* Science, 15(3), 427-432.

Bertomeu-Sánchez, J.R. (2019). Pesticides:Past and Present. *Journal of History of Science and Technology*, 13 (1), 1-27.

Betancourth, J.M., Cuellar, M., Ortiz, P.I. and Pfaffen, V. (2018). Multivariate cathodic square wave stripping voltammetry optimization for nitro group compounds determination using antimony film electrodes. *Microchemical Journal*, 139 (6), 139-149.

Boumya, W., Taofuik, N., Achak, M. and Barka, N. (2021). Chemically modified carbon-based electrodes for the determination of paracetamol in drugs and biological samples. *Journal of Pharmaceutical Analysis*, 11, 138-154

Christian, G.D., Dasgupta, P.K. and Schug, K.A. (2021). *Analytical Chemistry*, (revisor İnam, R.), (7th Edition). Ankara: Palme Pressing House. (The original work was published in 2014),100, 101, 102, 135, 136, 137, 139.

Chung, R.J., Leong, M.I. and Huang, S.D. (2012). Determination of nitrophenols using ultrahigh pressure liquid chromatography and a new manual shaking-enhanced, ultrasound-assisted emulsification microextraction method based on solidification of a floating organic droplet. *Journal of Chromatography* A, 13 (1246), 55– 61.

Cuellar, M., Betancourth, J.M., Pfaffen, V. and Ortiz, P.I. (2019). Response surface methodology for optimisation of 4,6-Dinitro-o-cresol quantification using hanging mercury drop electrode. *International Journal of Environmental Analytical Chemistry*, 99 (1), 74-86.

Deffo, G., Temgoua, C.T., Mbokou, S.F., Njanja, E., Tonlé, I.K. and Ngameni, E. (2021). A sensitive voltammetric analysis and detection of Alizarin Red S onto a glassy carbon electrode modified by an organosmectite. *Sensors International*, 2, 100126.

Demir, E. and İnam, R. (2014). Electrochemical behaviour and determination of rimsulfuron herbicide by square wave voltammetry. *International Journal of Environmental Analytical Chemistry*, 94 (13), 1330-1341.

Demir, E. and İnam, R. (2018). Voltammetric determination of phenmedipham herbicide using a multiwalled carbon nanotube paste electrode. *Turkish Journal of Chemistry*, 42, 997 – 1007.

Ding, Y. And Garcia, C.D. (2006). Pulsed amperometric detection with poly(dimethylsiloxane)-fabricated capillary electrophoresis microchips for the determination of EPA priority pollutants. *The Journal Analyst*, 131 (2), 208-214.

Drum, C. (1980). Soil Chemistry of Pesticides, *PPG Industries, Inc.*, USA.

Espinosa-Mansilla, A., Madera, A.Z. and Salinas, F. (1999). Use of a stopped-flow pneumatic mixing module to analyze dinitrophenol pesticides. Simultaneous determination of dinoseb and dinobuton. *Journal of Agricultural and Food Chemistry*, 47(5):1976-80.

Fernández-Salinero, G., Silva-Vargas, M.E., León-González, M.E., Párez-Arribas, L.V. and Polo-Dáiez, L.M. (1999). Study of nitrophenols preconcentration using quinolin-8-ol immobilized on controlled-pore glass in the presence of iron(III): Chromatographic determination of dinoseb in lemon juice. *Journal of Chromatography A.*, 839 (1-2), 227-232.

Gajdar, J., Barek, J. and Fischer, J. (2019). Electrochemical microcell based on silver solid amalgam electrode for voltammetric determination of pesticide difenzoquat. *Sensors and Actuators B* Chemical, 299, 126931.

GÃmez-Caballero, A., Unceta, N., Goicolea, M.A. and Barrio, R.J. (2008). Evaluation of the selective detection of 4,6-dinitro-o-cresol by a molecularly imprinted polymer based microsensor electrosynthesized in a semiorganic media. *Sensors and Actuators B: Chemical*, 130 (2), 713-722.

Gebrehiwot, W.H., Erkmen, C. and Uslu, B. (2020). A novel HPLC-DAD method with dilute-andshoot sample preparation technique for the determination of buprofezin, dinobuton and chlorothalonil in food, environmental and biological samples. *International Journal of Environmental Analytical Chemistry*, 101 (14), 2339-2353.

Geerdink, R.B., Kooistra-Sijpersma, A., Tiesnitsch, J., Kienhuis, P.G.M. and Brinkman, U.A.T. (1999). Determination of polar pesticides with atmospheric pressure chemical ionisation mass spectrometry–mass spectrometry using methanol and/or acetonitrile for solid-phase desorption and gradient liquid chromatography. *Journal of Chromatography A*, 863, 147-155.

Harnisch, F. and Freguia, S. (2012). A Basic Tutorial on Cyclic Voltammetry for the Investigation of Electroactive Microbial Biofilms. *Chemistry An Asian Journal*, 7 (3), 466-475.

Jain, R., Gupta, V.K., Jadon, N. and Radhapyari, K. (2010). Voltammetric determination of cefixime in pharmaceuticals and biological fluids. *Analytical Biochemistry*, 407, 79–88.

Jakubczyk, M., Michalkiewicz, S., Skorupa, A. and Slefarska, D. (2021). Voltammetric Determination of Isopropylmethylphenols in Herbal Spices. *Molecules 2021*, 26 (20), 6095.

Jarman, W.M. and Ballschmiter, K. (2012). From Coal to DDT: The History of the Development of the Pesticide DDT from Synthetic Dyes till Silent Spring. *Endeavour*, 36 (4), 131–42.

Kaur, R., Mavi, G.K., Raghav, S. and Khan, I. (2019). Pesticides Classification and its Impact on Environment. *International Journal of Current Microbiology and Applied Sciences*, 8 (3), 1889-1897.

Kościelniak, P. (2003). Caibration methods-Nomenclature and Classification. *New Horizons and Challenges In Environment,* 8, 11-128.

Kościelniak, P., Wieczorek, M., Kozak, J. and Herman, M. (2011). Generalized Calibration Strategy in Analytical Chemistry, *Analytical Letters*, 44 (1-3), 411-430.

Kumar, Y., Yadav, A.N., Saxena, R., Paul, D. and Tomar, R.S. (2020). Biodiversity of pesticides degrading microbial communities and their environmental impact. *Biocatalysis and Agricultural Biotechnology*, 31, 101883.

Laviron, E., Roullier, L. and Degrand, C. (1980). A multilayer model for the study of space distributed redox modified electrodes: Part II. Theory and application of linear potential sweep voltammetry for a simple reaction. *Journal of Electroanalytical Chemistry and Interfacial Electrochemistry*, 112 (1), 11-23.

Muro-Suñé, N., Gani, R., Bell, G. and Shirley, I. (2005). Predictive property models for use in design of controlled release of pesticides. *Fluid Phase Equilibria*, 228, 127-133.

Musa, D.E., Sha'Ato, R., Eneji, I.S. And Itodo, A.U. (2018). Electrogravimetric Determination of Copper Using a Constructed Compact Electrolytic Cell. *Open Access Library Journal*, 5 (3), 1-14.

Ober, E.S. and Sharp, R.E. (1996). A microsensor for direct measurement of 0 2 partial pressure within plant tissues. *Journal of Experimental Botany*, 47 (296), 447-454.

Ohfuji, M., Chikamoto, T., Kamada, I. and Komatsu, M. (1997). A gas chromatographic method for determination of dinoseb, dinoterb and 4, 6-dinitro-0-cresol (DNOC) in citrus fruits by methylation using trimethylsilyldiazomethane. *Journal of the Food Hygienic Society of Japan*, 38 (2), 85-91

Opeolu, B.O., Fatoki, O.S. and Odendaal, J. (2010). Development of a solid-phase extraction method followed by HPLC-UV detection for the determination of phenols in water. *International Journal of the Physical Sciences*, 5(5), 576-581.

Pedrero, M., Casado, B., Villena, F.J.M and Pingarrón, J.M. (1994). Determination of dinoseb by adsorptive stripping voltammetry using a mercury film electrode. *Fresenius' Journal of Analytical Chemistry*, 349, 546-551

Pınar, P. T., Allahverdiyeva, S., Yardım, Y. and Şentürk, Z. (2020). Voltammetric sensing of dinitrophenolic herbicide dinoterb on cathodically pretreated boron-doped diamond electrode in the presence of cationic surfactant. *Microchemical Journal*, 155, 104772.

Reddy, C.N., Prasad, P.R. and Sreedhar, N.Y. (2016). ZnO/MWCNTs Nanosensor for Differential Pulse Voltammetric Determinations of Dinosulfon in Water Samples. *Journal of Chemistry and Chemical Sciences*, 6(11), 997-1005.

Roberts, T.R., Hutson, D.H., Jewess, P.J., Lee, P. and Nicholls, P.H.(1999). *Metabolic Pathways of Agrochemicals*, (editor Plimmer, J.) Cambridge:The Royal Society of Chemistry, 1189, 1192

Roja, K., Prasad, P.R., Sandhya, P. and Sreedhar, N.Y. (2016). Preparation of NiO-graphene oxide nanosensor for adsorptive stripping voltammetric determination of dinoterbon in food samples. *Journal of Electrochemical Science and Engineering*, 6(3), 253-263.

Rouessac, F. And Rouessac A., (2007). *Chemical Analysis Modern Instrumentation Methods and Techniques*.(translator Rouessac, F., Rouessac, A. and Brooks, S.), (2nd Edition). Chichester: John Wiley & Sons, Ltd., 453, 454, 465, 466, 470, 471, 478, 479.

Samsidar, A., Siddiquee, S. and Shaarani, S.M. (2018). A review of extraction, analytical and advanced methods for determination of pesticides in environment and foodstuffs. *Trends in Food Science&Technology*, 71, 188-201.

Santana, C.M., Ferrera, Z.S. And Rodríguez, J.J.S. (2004). Extraction and Determination of Phenolic Derivatives inWater Samples by Using Polyoxyethylene Surfactants and Liquid Chromatography with Photodiode Array Detection. *Journal of AOAC International*, 87 (1), 166-171.

Skoog, D.A., West, D.M., Holler, F.J. and Crouch, S.R. (2011). *Fundamentals of Analytical Chemistry*.(revisor Kılıç, E. and Yılmaz, H)., (8th Edition). Ankara: Bilim Publishing. (The original work was published in 2004), 124, 192, 667, 634, 665, 673, 681, 589, 633, 667, 702, 700, 588, 196, 204, 205, 689, 717, 628, 665.

Sreedhar, M., Reddy, T.M., Sirisha, K.R., Reddy, S. and Reddy, J. (2003). Differential Pulse Adsorptive Stripping Voltammetric Determination of Dinoseb and Dinoterb at a Modified Electrode. *Analytical Sciences*, 19 (4), 511-6.

Sreedhar, N.Y., Samatha, K. and Sujatha, D. (2000). An electrochemical approach to the determination dinobuton: a study of water samples. *The Royal Society of Chemistry*, Analyst, 125 (9), 1645-1648.

Szeto, S.Y. And Price, P.M. (1991). High-performance liquid chromatography method for the determination of dinoseb: application to the analysis of residues in raspberries. *Journal of Agricultural and Food Chemistry*, 39 (9), 1614–1617

Takahashi, K., Ishii, R., Nemoto, S. and Matsuda, R. (2013). Analytical Method of Dinoseb and Dinoterb in Agricultural Products, Livestock Products and Seafood by LC-MS/MS. Shokuhin Eiseigaku Zasshi, 54(1), 1-6.

Terziev, V. And Petkova-Georgieva, S. (2019). The Pesticides Toxic Impact on the Human Health Condition and the Ecosystem. *International E-Journal of Advances in Social Sciences*, 5 (15), 1314-1320.

Uzer, A., Ercag E., Parlar, H., Apak, R. and Filik, H. (2006). Spectrophotometric determination of 4,6-dinitro-o-cresol (DNOC) in soil and lemon juice. *Analytica Chimica Acta*, 580 (1), 83-90.

Védrine, C., Leclerc, J.C., Durrieu, C. and Tran-Minh, C. (2003). Optical whole-cell biosensor using Chlorella vulgaris designed for monitoring herbicides. *Biosensors and Bioelectronics*, 18 (4), 457-463.

Wang, J. (2006). *Analytical Electrochemistry*, (3rd Edition). New York: A John Wiley & Sons, Inc., Publication, 1, 115, 116, 123, 124, 127, 136, 149, 2, 29

Yadav, I.C. and Devi, N.L. (2017). Pesticides Classification and Its Impact on Human Environment. *Environmental Science and Engineering*, 6, 140-158.

Zhao, R.S., Wang, X., Yuan, J.P. and Wang, X.D. (2009). Sensitive determination of phenols in environmental water samples with SPE packed withbamboo carbon prior to HPLC. *Journal of Separation Science*, 32 (4), 630–6.

GAZİ GELECEKTİR…